

博士論文

**Physiological function of
type II PAF-acetylhydrolase-derived ω 3-epoxides**

(酸化リン脂質選択的ホスホリパーゼを介した
エポキシ化 ω 3脂肪酸の産生とその生理的意義)

嶋中 雄太

Table of contents

Abstract	3
Introduction	4
Results	7
Discussion	18
Figures	25
Material and methods	63
References	74
Acknowledgements	84

Abstract

Mast cells are key effector cells involved in many pathological conditions such as atopic dermatitis, allergic rhinitis and asthma. However, therapeutic target for inhibiting mast cell activation has not been fully established. Here I report that suppression of type II PAF-acetylhydrolase (PAF-AH (II)), an oxidized phospholipid-selective phospholipase A₂, impairs mast cell activation. Mice lacking PAF-AH (II) impaired IgE-dependent anaphylaxis. Lipidomics analysis of mast cells revealed dramatic reduction of ω 3 fatty acid epoxides such as 17,18-EpETE in PAF-AH (II)-deficient mast cells, suggesting PAF-AH (II) as an ω 3 fatty acid epoxide-producing enzyme. Treatment of PAF-AH (II)-null mice with 17,18-EpETE restored IgE-dependent-mast cell activation. Finally, selective PAF-AH (II) inhibitor impaired IgE-dependent anaphylaxis in wild-type mice. Thus, ω 3 fatty acid epoxides are new lipid mediators of mast cell activation, and PAF-AH (II) is a druggable target to combat allergic diseases.

Introduction

Allergic diseases such as atopic dermatitis and asthma are very common disease in developed countries. The prevalence has increased two- to threefold during the past two decades, and approaching 15%~30% of children and approximately 5% of adults¹. Patients with allergy show inflammation characterized by increased serum-immunoglobulin E (IgE) levels and mast cell degranulation.

Mast cells are key effector cells in IgE-associated immune responses, including allergic disorders. When IgE-bound mast cells are exposed to antigens, they degranulate and secrete various proinflammatory substances such as histamine, lipid mediators, growth factors, cytokines and chemokines². Various drugs have been developed to combat allergic diseases. H1-receptor antagonists and leukotriene receptor antagonists have been used to allergies for many years³. Omalizumab, a humanized monoclonal antibody against IgE have been developed to lower the plasma IgE level⁴. The drugs that target mast cells have also been developed. Cromoglicate inhibits the release of inflammatory mediators by stabilizing mast cell membranes, although the precise mechanisms of the action are unknown^{5,6}. Steroids, which suppress cytokine production by inhibiting the NF-kB pathway, are also prescribed for allergic disease⁷. However, these drugs are sometimes ineffective and have side effects. Identification of a new therapeutic target based on detailed understanding of the molecular mechanisms underlying mast cell activation is definitely required in order to improve allergic symptoms.

Activated mast cells release prostaglandins and leukotrienes, which are produced via cyclooxygenase (COX) and lipoxygenase (LOX) pathways, respectively from arachidonic acid. Recent studies revealed that these lipid mediators released from mast cells affect mast cell function. For example, PGD₂ inhibit mast cell migration into the colon in food allergy, and LTB₄ and PGE₂ are the potent chemoattractants for mast cells⁸⁻¹⁰.

Besides these bioactive lipids, polyunsaturated fatty acids (PUFAs) are also converted via cytochrome P450 (CYP) epoxygenase pathway to epoxidized fatty acids including epoxyeicosatrienoic acids (EETs) from AA, epoxyeicosatetraenoic acids (EpETE) from EPA and epoxydocosapentaenoic acids (EpDPE) from DHA¹¹. Among the epoxidized fatty acids, 17,18-EpETE and 19,20-EpDPE, both of which are derived from ω 3 PUFAs, are shown to exhibit vasodilatory and cardioprotective effects¹²⁻¹⁴. Very recently, both epoxides have been reported to exert beneficial actions in counteracting metabolic disorders associated with obesity¹⁵. Furthermore, EpDPEs have attracted much attention because they inhibit angiogenesis, tumor growth and metastasis¹⁶. Although some of ω 3-epoxides are now considered to be bioactive lipid mediators, the association of ω 3-epoxides with mast cell function is unknown.

Recent studies revealed that the phospholipases A₂ family, key enzymes for the production of lipid mediators, plays important roles in mast cell function. Cytosolic PLA₂ α (cPLA₂ α), also called PLA2G4A, participates in PGD₂ and LTC₄ production in activated mast cells¹⁷. PLA2G3, one of the secretory PLA₂s, is critical for mast cell maturation through producing PGD₂¹⁸. Platelet-activating factor-acetylhydrolase

(PAF-AH) was originally identified as an enzyme that hydrolyzes the acetyl group attached to the *sn*-2 position of PAF (1-*O*alkyl-2-acetyl-*sn*-glycero-3-phosphocholine). Three types of PAF-AH have been identified in mammals, namely the intracellular types I and II and a plasma type^{19 20 21}. Intracellular type II PAF-AH (PAF-AH (II)) and plasma type PAF-AH show similarity in amino acid sequence and substrate specificity. Unlike other intracellular phospholipase A₂, they cannot hydrolyze long fatty acyl chains but can hydrolyze oxidized fatty acyl chains attached to phospholipids. The PAF-AH (II) null mice are born normally and survive to adulthood with no apparent abnormalities in various organs. The mice show some susceptibility to oxidative stress-induced hepatic injury²². We found in this study that PAF-AH (II) is expressed at high levels in dermal mast cells.

In this study, I show that mast cells produce bioactive ω 3-epoxides, 17,18-EpETE and 19,20-EpDPE in a PAF-AH (II) dependent manner and PAF-AH (II)-derived ω 3-epoxides facilitates IgE-dependent mast cell activation. Furthermore, PAF-AH (II) selective inhibitor suppresses anaphylaxis *in vivo*. Thus, ω 3 fatty acid epoxides are new lipid mediators of mast cell activation, and PAF-AH (II) is a druggable target to combat allergic diseases.

Results

PAF-AH (II) depletion suppresses release of oxidized ω 3 fatty acids

I first performed LC-MS/MS-based lipidomics analysis of oxidized metabolites of AA, EPA and DHA in the supernatant from bone marrow-derived mast cells (BMMCs) stimulated with IgE-antigen²³. As reported before^{17 9 24}, mast cells release oxidized metabolites of AA such as PGD₂, LTB₄, TxB₂, 12-HHT and 5-HETE (Fig. 1). In this condition, we could not detect any oxidized metabolite of EPA and DHA. I also examined oxidized metabolites of AA, EPA and DHA in the conditioned media of BMMCs. As shown in Fig. 2, many monooxygenated and dioxygenated metabolites of AA, EPA and DHA were unexpectedly detected in the conditioned media of BMMCs, while prostaglandins and thromboxanes were not detectable.

Since PLA₂s are key enzymes for the generation of oxidized fatty acid metabolites, I then examined the expression levels of the PLA₂ family by DNA microarray analysis and found that cPLA₂ α (*pla2g4*), iPLA₂ γ (*pnpla8*) and PAF-AH (II) (*pafah2*) were expressed at high levels in mast cells. Quantitative RT-PCR confirmed that these three enzymes were the major PLA₂ enzyme expressed in BMMCs (Fig. 3a). I then cultured BMMCs obtained from wild-type mice, *pafah2*^{-/-} mice, *pla2g4*^{-/-} mice or *pnpla8*^{-/-} mice to get the conditioned media of BMMCs and performed LC-MS/MS-based lipidomics analysis. As shown in Fig. 3b, cPLA₂ α depletion and iPLA₂ γ depletion had no effect on the release of oxidized metabolite of AA, EPA and DHA from BMMCs. On the other hand, PAF-AH (II) depletion had marked effect on the production of

oxygenated fatty acids. Among the metabolites, the levels of monooxygenated metabolites of AA (19-HETE, 18-HETE, 17-HETE, 14,15-EET, 11,12-EET, 8,9-EET and 5,6-EET), monooxygenated metabolites of EPA (20-HEPE, 19-HEPE, 18-HEPE and 17,18-EpETE), and monooxygenated metabolites of DHA (22-HDoHE, 21-HDoHE, 20-HDoHE, 16-HDoHE, 19,20-EpDPE and 16,17-EpDPE) were much lower in the conditioned media obtained from *pafah2*^{-/-} BMMCs than those from wild-type PAF-AH (II)-expressed BMMCs, suggesting that these metabolites are synthesized via PAF-AH (II).

PAF-AH (II) depletion suppresses IgE-dependent anaphylaxis

Next, I examined the expression levels of PAF-AH (II) in various immune cells. In bone marrow-derived cell populations, *Pafah2* mRNA was more highly enriched in BMMCs and thymic stromal lysophopietin (TSLP)-driven bone marrow derived basophils (BMbasophils) than in IL-5-driven bone marrow-derived eosinophils (BMEos), GM-CSF-driven bone marrow-derived dendritic cells (BMDCs) and M-CSF-driven bone marrow-derived macrophages (Fig. 4a). *Pafah2* mRNA was also more highly enriched in BMMCs than in lymphocytes isolated from spleen (Fig. 4b). Immunohistochemistry analysis revealed that PAF-AH (II) localized with toluidine blue-stained dermal mast cells in wild-type mice but not in *pafah2*^{-/-} mice (Fig. 4c).

In order to examine the function of mast cells in *pafah2*^{-/-} mice, I then carried out passive cutaneous anaphylaxis (PCA) assay and passive systemic anaphylaxis (PSA) assay using *pafah2*^{-/-} mice. IgE-Ag induced ear edema (Fig. 5a-c) and temporary

decrease in rectal temperature after systemic antigen challenge (Fig. 6) was markedly suppressed in *pafah2*^{-/-} mice on a C57BL/6J background. The number of toluidine blue-positive mast cells in the ear skin of wild-type and *pafah2*^{-/-} mice were almost same, the number of degranulated mast cells were fewer in *pafah2*^{-/-} mice than wild-type mice upon IgE-Ag mediated PCA (Fig. 7a-c). IgE-independent secretagogue compound 48/80-induced PCA was comparable between wild-type and *pafah2*^{-/-} mice (Fig. 8a-c). Gene expression level of mast cells markers in the ear, stomach and small intestine were also comparable between both phenotypes, which indicates proliferation and maturation of mast cells are normal in *pafah2*^{-/-} mice (Fig. 9a-c). IgE-Ag-induced ear edema was also suppressed in *pafah2*^{-/-} mice on a BALB/c background (Fig.10 a-c).

PAF-AH (II) expressed in mast cell is essential for anaphylaxis

To assess whether PAF-AH (II) expressed in mast cells are responsible for IgE-Ag mediated PCA reduction in *pafah2*^{-/-} mice *in vivo*, I engrafted wild-type or *pafah2*^{-/-} BMNCs intradermally into the ears of mast cell deficient mice, *Kit*^{W^{-sh}/W^{-sh} mice and performed IgE-dependent PCA assay. PAF-AH (II) expression was observed in BMNCs obtained from wild-type mice but not from *pafah2*^{-/-} mice (Fig. 11a). Both BMNCs expressed comparable amount of mast cell markers FcεRI and c-kit, and matured normally (Fig. 11b, c). Four weeks after reconstitution, the distribution of mast cells in the ear was comparable between mice reconstituted with wild-type BMNCs and with *pafah2*^{-/-} BMNCs (Fig. 12a, b) and matured normally (Fig. 12c). Mast cell-deficient mice exhibited no dye extravasation and ear swelling (Fig. 12d-f). When}

wild-type BMMCs were introduced into the mice, IgE-dependent anaphylaxis was restored. On the other hand, when *pafah2*^{-/-} BMMCs were introduced, the anaphylaxis was not restored. These results suggest that PAF-AH (II) expressed in the mast cells is essential for IgE-dependent anaphylaxis *in vivo*.

Enzymatic activity of PAF-AH (II) is required for IgE-dependent mast cell activation

Next, the effect of PAF-AH (II) depletion on the Ag-induced and Ag-independent activation of BMMCs was examined. IgE-Ag-induced degranulation, which was assessed by the amount of β -hexosaminidase released from BMMCs, was greatly reduced in *pafah2*^{-/-} BMMCs compared with wild-type BMMCs (Fig. 13a). In contrast, A23187 calcium ionophore-induced degranulation was comparable between wild-type and *pafah2*^{-/-} BMMCs. IgE-Ag-induced production of eicosanoids (PGD₂ and LTC₄) and cytokines (IL-6 and TNF α) were also impaired in *pafah2*^{-/-} BMMCs (Fig. 13b-e). IgE-Ag-induced crosslinking of cell surface Fc ϵ RI triggers activation of the kinase Lyn, which phosphorylates Fc ϵ RI and activates the kinase Syk²⁵. Fc ϵ RI aggregation also activates a kinase, Fyn, that phosphorylates the adaptor Gab2²⁶. IgE-Ag-induced phosphorylation of Fc ϵ RI, Syk and Gab2 were all suppressed in *pafah2*^{-/-} BMMCs (Fig. 14a-c).

I then tested if enzymatic activity of PAF-AH (II) is required for the mast cell activation. Wild-type PAF-AH (II) or its catalytic inactive mutant S234C, in which a catalytic center Ser234 was substituted to Cys²⁰, was retrovirally expressed in *pafah2*^{-/-} BMMCs (Fig. 15a). Wild-type PAF-AH (II) expression restored IgE-dependent

degranulation of *pafah2*^{-/-} BMMCs, whereas catalytic inactive S234C did not restore the degranulation (Fig. 15b). Impaired phosphorylation of Syk and Gab2 in *pafah2*^{-/-} BMMCs was also restored in a PAF-AH (II) enzymatic activity-dependent manner (Fig. 15c).

PAF-AH (II)-produced ω 3-epoxides restore IgE-mediated degranulation in *pafah2*^{-/-} BMMCs

Because PAF-AH (II) depletion suppressed the production of oxygenated fatty acids in the conditioned media of BMMCs and the catalytic activity of PAF-AH (II) was required for mast cell activation, I hypothesized that lipid product(s) of PAF-AH (II) participates in the mast cell activation. To test this, free fatty acid fractions were extracted from the conditioned media of *pafah2*^{-/-} BMMCs, and *pafah2*^{-/-} BMMCs overexpressed with wild-type PAF-AH (II) or the catalytic inactive PAF-AH (II) by solid phase extraction. Then extracted free fatty acid fractions were added to the cultured *pafah2*^{-/-} BMMCs, and IgE-Ag-dependent degranulation was assessed (Fig. 16a). As shown in Fig. 16b, the free fatty acid fraction obtained from the conditioned media of PAF-AH (II)-overexpressed BMMCs could restore impaired IgE-mediated degranulation in *pafah2*^{-/-} BMMCs. However, the free fatty acid fractions obtained from the conditioned media of *pafah2*^{-/-} BMMCs or the catalytic inactive PAF-AH (II)-overexpressed BMMCs could not restore the IgE-mediated degranulation (Fig. 16b). These results suggest that the free fatty acid(s) released by PAF-AH (II) promotes IgE-dependent mast cell activation. The phospholipid and neutral lipid fractions

obtained from the conditioned media of PAF-AH (II)-overexpressed BMMCs had no effect on IgE-mediated degranulation of *pafah2*^{-/-} BMMCs (data not shown).

As shown in Fig. 3b, the levels of monooxygenated metabolites of AA, EPA and DHA were much lower in the conditioned media obtained from *pafah2*^{-/-} BMMCs than those from wild-type PAF-AH (II)-expressed BMMCs, suggesting that these metabolites are responsible for the restoration of IgE-mediated degranulation of *pafah2*^{-/-} BMMCs. Among the oxygenated fatty acids, the levels of which were decreased in the conditioned media obtained from *pafah2*^{-/-} BMMCs, I focused on monooxygenated metabolites of EPA and DHA, because the levels of these metabolites were much higher than those of monooxygenated metabolites of AA. Omega3-monooxygenated metabolites consisted of ω 3-monohydroxides (20-HEPE, 19-HEPE, 18-HEPE, 22-HDoHE, 21-HDoHE and 20-HDoHE) and ω 3-epoxides (17,18-EpETE and 19,20-EpDPE) (Fig. 16c). Then, a mixture of the ω 3-monohydroxides and a mixture of the ω 3-epoxides were added to the culture of *pafah2*^{-/-} BMMCs twice in three days, and IgE-mediated degranulation was evaluated a day after last treatment (Fig. 16d). The compositions of ω 3-monohydroxides and ω 3-epoxides mimicked the composition of the oxygenated metabolites detected in the conditioned media from PAF-AH (II)-expressed BMMCs. I found that only the mixture of ω 3-epoxides, which include 17,18-EpETE and 19,20-EpDPE, could restore the IgE-mediated degranulation of *pafah2*^{-/-} BMMCs. I also found that both epoxides have a comparable activity (Fig. 17a); Three hundred nM of 17,18-EpETE or 19,20-EpDPE was enough for full recovery of IgE-mediated degranulation of *pafah2*^{-/-} BMMCs. Phosphorylation of Fc ϵ RI, Syk

and Gab2 were also recovered by these ω 3-epoxides (Fig. 17b, c). These epoxides did not further enhance the IgE-mediated degranulation of wild-type BMMCs (data not shown). Fatty acid epoxides are converted to dihydrodiols (Fig. 16c) by soluble epoxy hydrolase (sEH)^{27 28}. Hydrolyzed products, 17,18-diHETE and 19,20-diHDoPE had no activity to restore the IgE-mediated degranulation of *pafah2*^{-/-} BMMCs (Fig. 17a).

ω 3-epoxides restore anaphylaxis in PAF-AH (II) knockout mice

I then examined whether administration of these ω 3-epoxides could restore the impaired IgE-dependent anaphylaxis in *pafah2*^{-/-} mice. Either 17,18-EpETE or 19,20-EpDPE was injected into the ears of *pafah2*^{-/-} mice twice in three days, and PCA assay was performed a day after last treatment. As shown in Fig. 18a-c, both epoxides could restore the IgE-mediated anaphylaxis *in vivo*. The number of degranulated mast cells in the ear was also restored by these ω 3-epoxides (Fig. 19a, b). On the other hand, 17,18-diHETE and 19,20-diHDoPE had no effect on anaphylaxis (Fig. 18b, c). ω 3-epoxides treatment had no effect on the total number of mast cells in the dermis (Fig. 19a, b).

Ability of PAF-AH (II) to release ω 3-epoxides from membrane phospholipids

If PAF-AH (II) releases ω 3-epoxides from phospholipids, phospholipid-esterified ω 3-epoxides must exist in mast cells. To test this possibility, I performed multiple reaction monitoring (MRM) using m/z 317 for 17,18-EpETE or 343 for 19,20-EpDPE as daughter ion for high sensitive detection of ω 3-epoxide-containing phospholipids

(Fig. 20, 21). Phosphatidylcholine (PC) containing 16:0 and monooxygenated EPA, which was detected MRM with transition of m/z 854→317, was observed with several peaks in BMMCs (Fig. 20a). Among the peaks, a peak at 11.5min was greatly elevated when BMMCs was incubated with 17,18-EpETE (Fig. 20b), suggesting that this peak represents PC containing 17,18-EpETE. EPI spectra of m/z 854.5 acquired in this time window demonstrated daughter ions characteristic for PC containing 16:0 and 17,18-EpETE (16:0/17,18-EpETE-PC) (Fig. 20c, d). Similarly, 16:0/19,20-EpDPE-PC was also detected in BMMCs (Fig. 21a-d). All the ω 3 epoxide-containing phospholipids that could be detected in BMMCs were listed on Table 1.

The amount of ω 3 epoxides in the phospholipid fraction was estimated after the chemical hydrolysis of lipids obtained from BMMCs. 17,18-EpETE and 19,20-EpDPE amount to ~50 ng and ~200 pg, respectively in the phospholipid fraction from 10^7 BMMCs. These amounts appear to be sufficient to account for the ω 3 epoxides released into the conditioned media of BMMCs.

I next investigated phospholipase activities of PAF-AH (II) that could release ω 3-epoxides from esterified precursors. Wild-type PAF-AH (II) and its catalytically inactive S234C mutant were prepared from HEK293T cells by transfecting their cDNAs (Fig. 22a). 17,18-EpETE-esterified phospholipids were prepared by incubating *pafah2*^{-/-} BMMCs with 17,18-EpETE as described in Material and Methods. When the membrane fraction containing 17,18-EpETE-esterified phospholipids was incubated with the cytosol fraction obtained from HEK293T cells transfected with wild-type PAF-AH (II), free 17,18-EpETE was produced time-dependently, and ω 3

epoxide-esterified phospholipids such as 16:0/17,18-EpETE-PC and 18:1/17,18-EpETE-PC were diminished concomitantly (Fig 22b). On the other hand, the cytosol fractions obtained from cells transfected with empty vector or S234C mutant had much lower effect on the amounts of free ω 3-epoxide and esterified precursors. These results demonstrate that PAF-AH (II) could hydrolyze ω 3 epoxide-esterified phospholipids to release free ω 3 epoxide.

Selective PAF-AH (II) inhibitor reduces IgE-mediated mast cell activation both in vitro and in vivo

Having found that the enzymatic activity of PAF-AH (II) is required for IgE-mediated mast cell activation, I next examined the effect of PAF-AH (II) inhibitor on mast cell activation. AA39-2 shows remarkable selectivity for inhibiting PAF-AH (II) among serine esterases (Fig. 23a) ²⁹. As shown in Fig. 23b, AA39-2 inhibited activity of PAF-AH (II) to release 17,18-EpETE from esterified precursors. Wild-type or *pafah2*^{-/-} BMMCs were treated with AA39-2 twice in three days and evaluated degranulation a day after last treatment (Fig. 24a). AA39-2 at 3 μ M significantly reduced IgE-mediated degranulation of wild-type BMMCs, but had no effect on A23187-induced degranulation. AA39-2 failed to suppress further IgE-mediated degranulation of *pafah2*^{-/-} BMMCs. These results indicated that suppression of IgE-mediated activation of wild-type BMMCs by AA39-2 was through the inhibition of PAF-AH (II). AA39-2 also inhibited the phosphorylation of Fc ϵ RI, Syk and Gab2 (Fig. 24b,c).

I then tested the effect of AA39-2 *in vivo* (Fig. 25a,b). Injection of AA39-2 into the ears of wild-type mice resulted in reduced IgE-dependent anaphylaxis. AA39-2 could not further impair anaphylaxis of *pafah2*^{-/-} mice. Thus, treatment with a PAF-AH (II) inhibitor could suppress IgE-mediated mast cell activation and anaphylaxis.

PPAR γ antagonist restores the IgE-mediated degranulation of *pafah2*^{-/-} BMMCs and anaphylaxis in *pafah2*^{-/-} mice

IgE-mediated degranulation of *pafah2*^{-/-} BMMCs was restored by the treatment with ω 3-epoxides for three days before IgE-Ag stimulation. I found that treatment with ω 3-epoxides for one day before the stimulation restored partly the BMMCs degranulation, but treatment for a shorter time such as four hours could not (Fig. 26). This result implied that ω 3-epoxides augmented the IgE-Ag sensitivity of *pafah2*^{-/-} BMMCs through gene expression.

Peroxisome proliferator-activated receptor-gamma (PPAR γ), which plays a central role in adipocyte differentiation, is expressed in mouse BMMCs, and treatment with PPAR γ agonist modulates the function and maturation of mast cells^{30,31}. On the other hand, ω 6 epoxides such as AA-derived 8,9-EET are shown to directly activate PPAR γ by using a reporter gene assay³². I then examined the effect of the agonist and antagonist of PPAR γ and found that treatment of *pafah2*^{-/-} BMMCs with PPAR γ antagonist GW9662 for 3 days fully restored the degranulation (Fig. 27). GW9662 had no effect on wild-type BMMCs. GW9662 treatment on *pafah2*^{-/-} mice also restored IgE-mediated anaphylaxis *in vivo* (Fig. 28a-c). These results indicated that PPAR γ

antagonist mimicked the action of ω 3-epoxides on BMMCs.

I then tested whether ω 3-epoxides functions directly as an PPAR γ antagonist by using a reporter gene assay (Fig. 29) ³³. As positive controls, established PPAR γ agonists, 15d- Δ ^{12,14}-PGJ2 or Rosiglitazone activated PPAR γ and, a PPAR γ antagonist GW9662, abolished the 15d- Δ ^{12,14}-PGJ2 or Rosiglitazone-induced PPAR γ activation. However, ω 3-epoxides (17,18-EpETE or 19,20-EpDPE) had no effect on the agonist-induced PPAR γ activation. Thus, I could not show that these ω 3-epoxides play as an antagonist of PPAR γ under the present assay conditions (Fig. 30).

Contribution of PAF-AH (II) and ω 3-epoxides to the activation of human mast cells.

Finally, I investigated whether PAF-AH (II)/ ω 3-epoxides are also involved in the IgE-stimulated human mast cells. High expression of *PAFAH2* mRNA in mast cells obtained from skin, lung, cord blood, peripheral blood and synovium (Fig. 31a). Human mast cells obtained from synovium, were treated with PAF-AH (II) inhibitor AA39-2 for three days, and IgE-dependent histamine release was examined. As shown in (Fig. 31b), degranulation was suppressed considerably by the treatment with AA39-2, whereas degranulation was not affected when the mast cells were treated with AA39-2 and ω 3-epoxides (a mixture of 17,18-EpETE or 19,20-EpDPE). Thus, PAF-AH (II)-produced ω 3-epoxides may also contribute to the function of human mast cells.

Discussion

Here I showed that PAF-AH (II), the major PLA₂ enzyme expressed in mast cells, contributed to anaphylaxis by facilitating IgE-Ag dependent activation of mast cells through producing ω 3-epoxides from esterified precursors. PAF-AH (II) releases ω 3-epoxides, 17,18-EpETE and 19,20-EpDPE from esterified precursors. Released ω 3-epoxides facilitate IgE-Ag induced phosphorylation of Fc ϵ RI via indirectly inhibiting PPAR γ activity.

Lipid mediators, such as prostaglandins and leukotriens play important roles in physiological and pathological processes. Eicosanoid biosynthesis is initiated by release of arachidonic acid from phospholipid by phospholipase A₂. Released free arachidonic acid is oxidized by cyclooxygenase, lipoxygenase and cytochrome P450, and then converted to prostaglandins, leukotriens and other bioactive oxidized fatty acids. Cytosolic PLA₂ (cPLA₂ α) has an essential role in release of arachidonic acid from phospholipid in various cells. New bioactive oxygenated product of ω 3 fatty acids, primarily eicosapentanoic acid (EPA) and docosahexaenoic acid (DHA) are also highlighted in recent years. For example, resolvin E1 and protectin D1 reduce immune cell infiltration and 18-HEPE inhibits proinflammatory activation of cardiac fibroblasts^{43,44}. However, how production of these oxygenated ω 3 fatty acids is regulated remains unclear.

In the present study, I suggest previously unidentified production pathway of lipid mediators, in which PAF-AH (II) directly releases bioactive ω 3-epoxides such as

17,18-EpETE and 19,20-EpDPE, from esterified precursors (Fig. 32). What is the advantage of this pathway? Fatty acid epoxides are converted to nonfunctional dihydrodiols (Fig. 16c) by soluble epoxy hydrolase (sEH) ^{27,28}. It is possible that esterified forms protect ω 3-epoxides from hydrolyzing its epoxy group. It has been also reported that once lipid mediators such as PGD₂ are generated, they are immediately acylated into phospholipids presumably by acyltransferases ⁴⁵. Unlike conventional lipid mediators which exert their functions through extracellular G-protein-coupled receptors (GPCRs), ω 3-epoxides regulate mast cell function through intracellular PPAR γ . Thus PAF-AH (II) may protect free ω 3-epoxides from incorporation into phospholipids by its oxidized phospholipid-selective hydrolase activity to promote interaction with their intracellular targets.

I found that treatment of *pafah2*^{-/-} BMDCs with ω 3-epoxides restored the IgE-mediated mast cell signaling via inhibiting PPAR γ pathway, but how PPAR γ regulate phosphorylation of Fc ϵ RI expressed on the mast cell surface, remains to be elucidated. Although mast cell signaling has been extensively studied and the Fc ϵ RI-proximal pathways involved in mast cell activation by IgE-Ag are largely well defined ², there remains some confusion about the precise function of src family members that are crucial for signaling ⁴⁶.

Fc ϵ RI is a tetrameric complex consisting of an IgE-binding α subunit, a signal-transducing β subunit and dimer of the signal-generating γ subunit (Fig. 33a). The multivalent binding of antigen to IgE-bound Fc ϵ RI induces aggregation. After Fc ϵ RI aggregation, Fc ϵ RI complex is translocated to sphingolipid- and cholesterol-rich

plasma membrane microdomains, called “lipid rafts” where it is associated with Lyn, a Src family kinase⁴⁷. Lyn phosphorylates tyrosine residues within the immunoreceptor tyrosine-based activation motifs (ITAMs) in the cytoplasmic regions of the β and γ subunits, which serves as binding sites for additional Lyn to the β chain, Syk, to the γ chains, and other signaling and adaptor molecules to the activated Fc ϵ RI complex. However, the role of Lyn in Fc ϵ RI activation has been controversial. Recent studies suggest that Lyn has both positive and negative regulatory roles in cultured mast cells⁴⁸ and Lyn-deficient mice exhibit suppressed⁴⁹, normal⁵⁰ or enhanced⁵¹⁻⁵² anaphylactic responses. It is also reported that two alternatively spliced variants Lyn A and B play different roles in IgE-Ag dependent mast cell activation⁵³. Fyn, a member of src family kinases, is also known to associate with Fc ϵ RI and to phosphorylate Gab2, which is essential for recruitment of phosphatidylinositol 3-kinase (PI3K) to the plasma membrane and microtubule-dependent granule translocation²⁶ (Fig. 33b). In addition to Lyn and Fyn, Fgr and Hck, members of src family kinases, are also regulate IgE-Ag dependent mast cell activation in a Syk-or Lyn-dependent manner, though their substrates remain to be determined⁵⁴⁻⁵⁵. It is reported that depletion of either Lyn or Fyn results in disturbed phosphorylation of Syk and Gab2. Although phosphorylation of Fc ϵ RI, Syk and Gab2 is suppressed in *pafah2*^{-/-} BMMCs, the expression of Lyn and Fyn were comparable between *pafah2*^{-/-} and wild-type cells (data not shown).

Phosphatases are also play important roles in IgE-Ag dependent mast cell activation. It is reported that depletion of phosphatidylinositol 3,4,5-trisphosphate 5-phosphatase 1 (SHIP) which is known to suppress downstream event of PI3K⁵⁶⁻⁵⁷, or protein tyrosine

phosphatase non-receptor type 6 (SHP1), which is known to regulate activity of Lyn, enhances mast cell activation⁵⁸. However, the expression of SHIP and SHP1 were comparable between *pafah2*^{-/-} and wild-type cells (Fig. 34). The key molecule responsible for suppressed phosphorylation of FcεRI in *pafah2*^{-/-} mast cells can be identified using microarray analysis or chromatin immunoprecipitation on ω 3-epoxide- or PPAR γ antagonist-treated BMMCs. Further studies are needed to unravel the mechanism how PPARγ regulate phosphorylation of FcεRI.

Mammalian genomes encode genes for more than 30 phospholipase A₂s (PLA₂s) or related enzymes, which are subdivided into several classes including low-molecular-weight secreted PLA₂s (sPLA₂s), Ca²⁺-dependent cytosolic PLA₂s (cPLA₂s), Ca²⁺-independent PLA₂s (iPLA₂s), platelet-activating factor acetylhydrolases (PAF-AHs), lysosomal PLA₂s, and a recently identified adipose-specific PLA⁵⁹. Recent works revealed that PLA₂s play important roles in mast cell function. PLA2G4A is essential for eicosanoid production of activated mast cells and PLA2G3 provides PGD₂ which is essential for mast cell maturation^{17,18}. However, among the PLA₂s, PAF-AH (II) is the only PLA₂ which facilitates IgE-Ag dependent mast cell activation. PAF-AH (II) exhibits 41% amino acid identity to plasma PAF-AH (PLA2G7) and both enzymes show similar substrate selectivity⁶¹. Though plasma PAF-AH is secretory enzyme, plasma PAF-AH is also expressed in BMMCs⁶⁰. In order to examine the involvement of plasma PAF-AH in IgE-mediated anaphylaxis, plasma PAF-AH/ PAF-AH (II) double knockout mice were subjected to anaphylaxis. Plasma PAF-AH depletion from *pafah2*^{-/-} mice did nothing on IgE-Ag induced anaphylaxis (Fig. 35a-c). This indicates

that PAF-AH (II) substrates localize intracellular compartment such as endoplasmic reticulum (ER) and ω 3-epoxides from esterified precursors access to their intracellular targets very efficiently.

I found that PPAR γ antagonist mimicked the action of ω 3-epoxides on BMMCs, although I could not show that these ω 3-epoxides inhibit agonist-induced PPAR γ activation using a reporter gene assay (Fig. 27-29). Although the structure of PPAR γ has been extensively studied, the precise mechanisms modulating PPAR γ activity remains unclear. PPAR γ forms a heterodimer with retinoid X receptor α (RXR α) and binds to PPAR response element (PPRE) in the nucleus. Agonist bindings to ligand binding pocket (LBP) of PPAR γ , stabilizing PPAR γ conformation which induces coactivator assembly. PPAR γ is also regulated by post-translational modifications. Recently it was found that Cdk5 phosphorylates PPAR γ within the LBD at Ser273⁶². Phosphorylation of PPAR γ does not alter its adipogenic capacity, but leads to a reduction in the expression of genes whose expression is altered in obesity including adiponectin. Recently a new PPAR γ agonist SR1664 was identified⁶³. Although SR1664 showed weak transcriptional activity compared to rosiglitazone, this compound very effectively block the Cdk5-mediated phosphorylation of PPAR γ . It is possible that ω 3-epoxides could not inhibit agonist-induced PPAR γ activation using a reporter gene assay because they inhibit PPAR γ activity by enhancing phosphorylation of PPAR γ .

The identity of the bona-fide ligand of PPAR γ is also still not clear⁶⁴. The oxidized fatty acids such as 15-deoxy- Δ ^{12,14}-PGJ2, 15-keto-PGE2 and 5-oxo-eicosatetraenoic acid (5-oxo-EETE) has been reported as potent agonists^{33,65,66}. These oxidized fatty acids

can covalently bind to PPAR γ through a Michael addition reaction between an α,β -unsaturated ketone of oxidized fatty acids and a cysteine residue in the PPAR γ ligand binding pocket. Omega3-epoxides also have nucleophilic epoxy groups which can form covalent bond with cysteine. Thus ω 3-epoxides possibly bind PPAR γ directly and induce conformational change. I could detect 20000 pg of 17,18-EpETE in the cytosol fraction from 10^7 cells of wild-type BMMCs, which is sufficient to affect the function of PPAR γ because the concentration of 17,18-EpETE can be estimated to 1.5 mM. Thus ω 3-epoxides might be the first reported natural PPAR γ antagonist.

How ω 3 fatty acids or ω 3 fatty acid-containing phospholipids are epoxygenated? PUFAs are converted via cytochrome P450 pathway to epoxygenated fatty acids. EETs (ω 6-epoxides) are mainly generated by P450 enzymes belonging to CYP2 family⁶⁷. On the other hand, *in vitro* studies have demonstrated that ω 3-epoxides are mainly generated by CYP4⁶⁸⁻⁷¹. I found that some P450 enzymes belonging to CYP4 family are expressed at high levels in BMMCs (data not shown). Thus these enzymes are probably responsible for ω 3-epoxides production in mast cells. In addition to mast cells, PAF-AH (II) and CYP4 isozymes are also expressed at high levels in livers and kidneys. Thus CYP4/epoxygenated phospholipids/PAF-AH (II)/ ω 3-epoxides/PPAR γ axis may exist in these tissues and physiological function of PAF-AH (II) in these tissues remains to be elucidated.

Some epidemiological studies showed beneficial associations between dietary intake of ω 3 fatty acids, and asthma and allergic diseases^{34 35 36 37}. However, others have not been able to replicate this, and some studies have shown the contrary^{38 39 40 41}

⁴². The ω 3 fatty acids may suppress mast cell function by competing with arachidonic acid and reducing pro-inflammatory eicosanoids production ⁷². On the other hand, ω 3-epoxides facilitate IgE-Ag dependent activation of mast cells. The allergenic ω 3 fatty acids-derived epoxides might provide a explanation for the contradiction.

Treatment with selective PAF-AH (II) inhibitor suppressed IgE-mediated mast cell activation and anaphylaxis (Fig. 24, 25). Furthermore, I demonstrated that PAF-AH (II) and ω 3-epoxides are also involved in the IgE-stimulated activation of human mast cells (Fig. 31). It has been previously reported that high expression of *PAFAH2* mRNA in BMMCs from patients with systemic mastocytosis though its association with the disease has not been mentioned ⁷³. Mast cells are involved in various disease including atopic dermatitis, rheumatoid, asthma, food allergy and so on. Thus, PAF-AH (II)-produced ω 3-epoxides may also contribute to the severity of human diseases and PAF-AH (II) can be a good druggable target to combat these diseases.

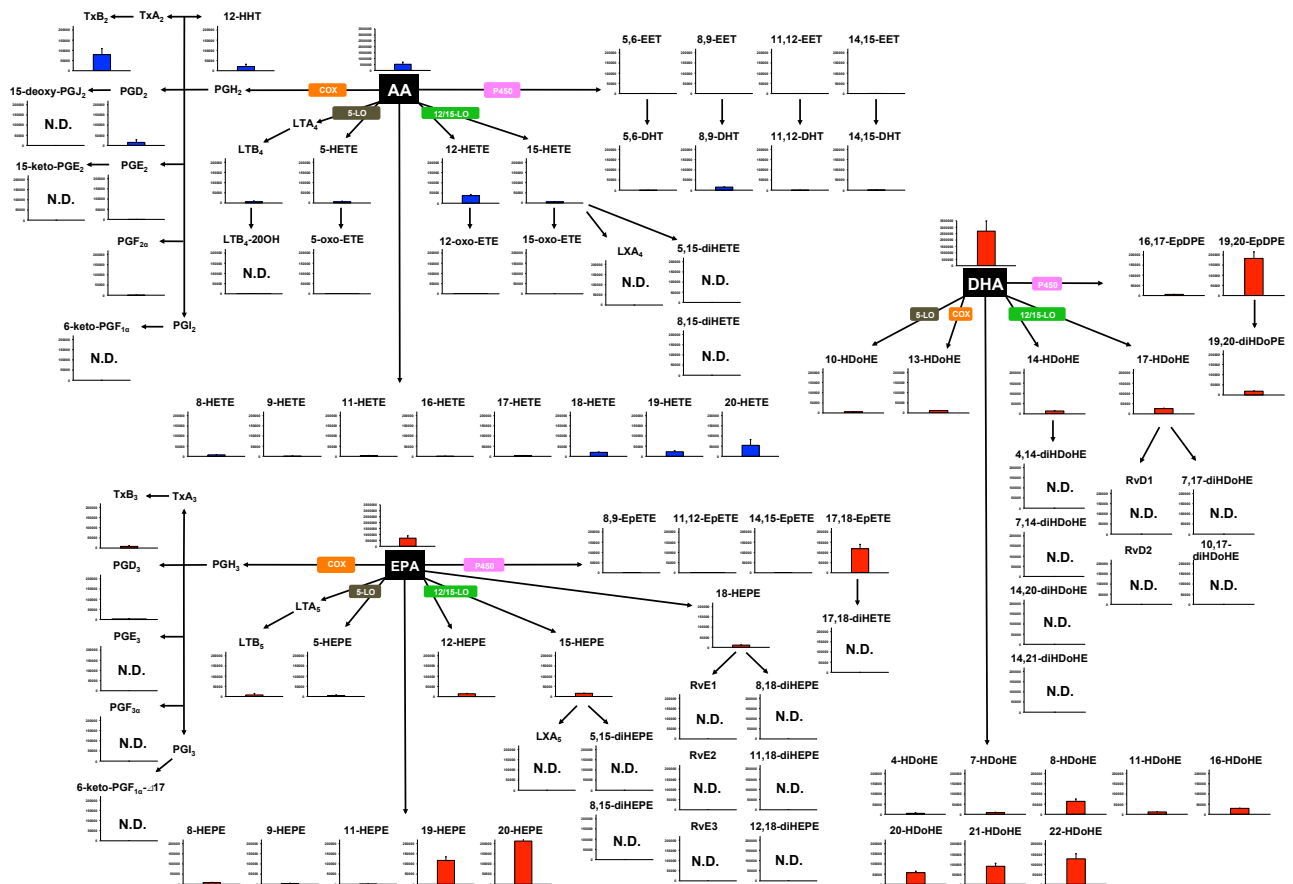


Figure 2. Oxidized ω 3 fatty acids are more abundant than oxidized ω 6 fatty acids in BMMCs-conditioned medium
 LC-MS/MS-based lipidomics analysis of conditioned medium from unstimulated BMMCs for four days (n=3). (mean \pm s.e.m.; N.D., not detectable)

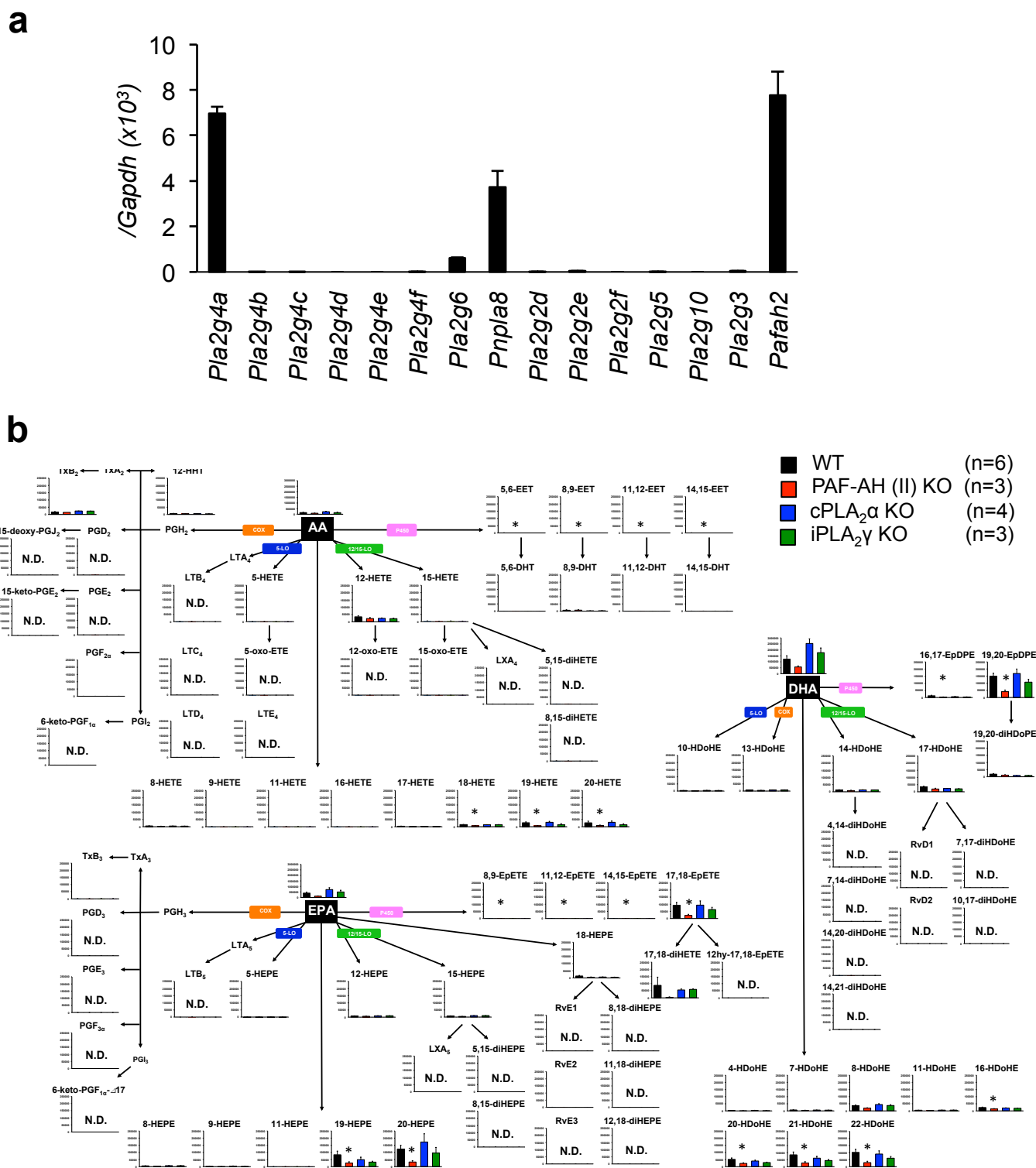


Figure 3. Impaired production of monooxygenated metabolites of EPA and DHA in PAF-AH (II) knockout BMMCs

(a) Real-time PCR of various PLA₂s relative to *Gapdh* in C57BL/6-derived BMMCs (n=3).

(b) LC-MS/MS-based lipidomics analysis of wild-type, *pla2g4a*^{-/-}, *pnpla8*^{-/-} or *pafah2*^{-/-} BMMCs-conditioned medium.

(mean ± s.e.m., **p*<0.05; N.D., not detectable).

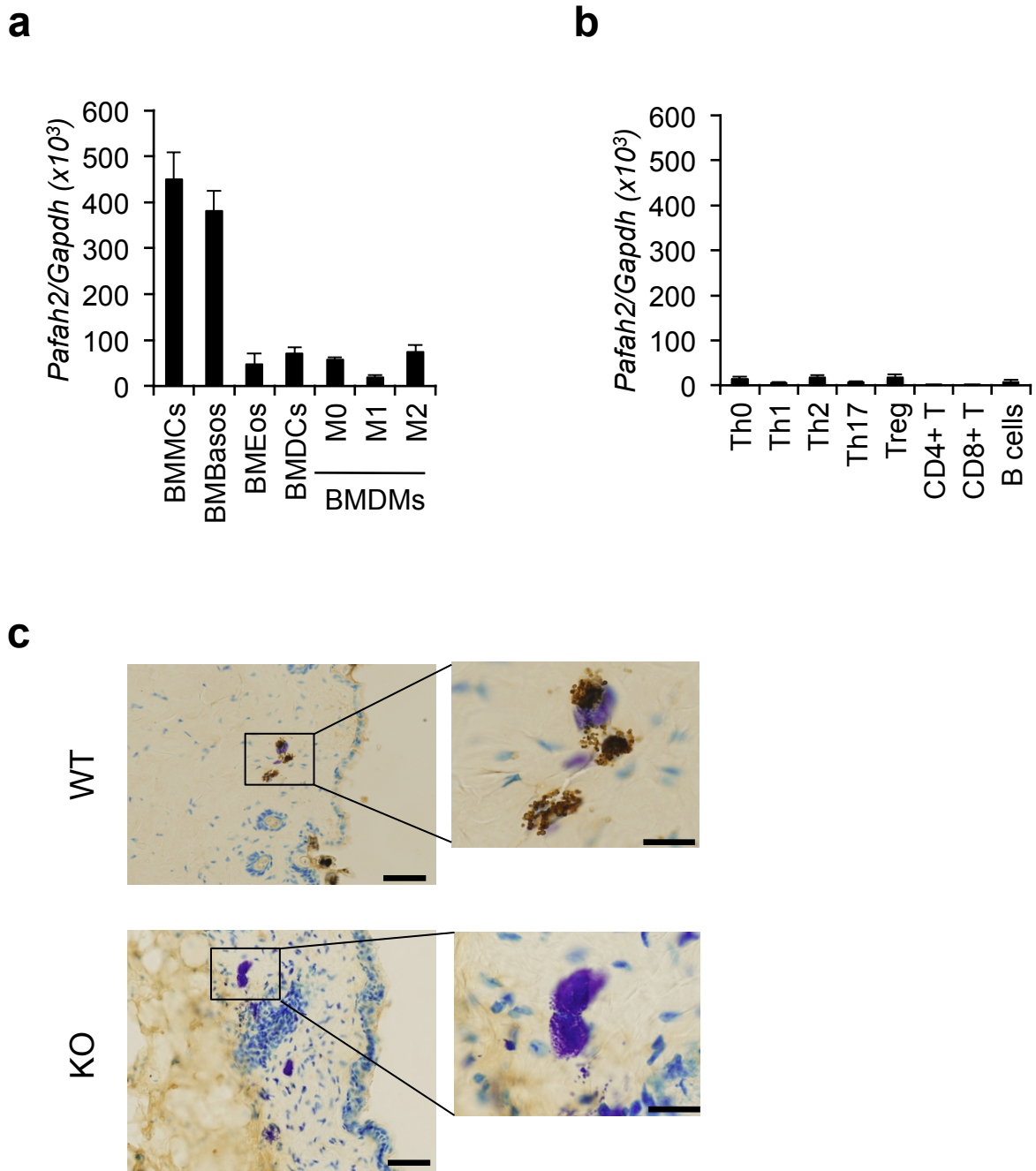


Figure 4. PAF-AH (II) is expressed at high level in mast cells

(a) Real-time PCR of *Pafah2* relative to *Gapdh* in indicated bone marrow-derived cells (n=3).

(b) Real-time PCR of *Pafah2* relative to *Gapdh* in indicated lymphocytes (n=3).

(c) Immunohistochemistry analysis of PAF-AH (II) expression in the skin. Dorsal skin sections from wild-type (WT) or *pafah2*^{-/-} (KO) mice were stained with PAF-AH (II) antibody, followed by counterstaining with toluidine blue (scale bars, 50µm).

(mean ± s.e.m.)

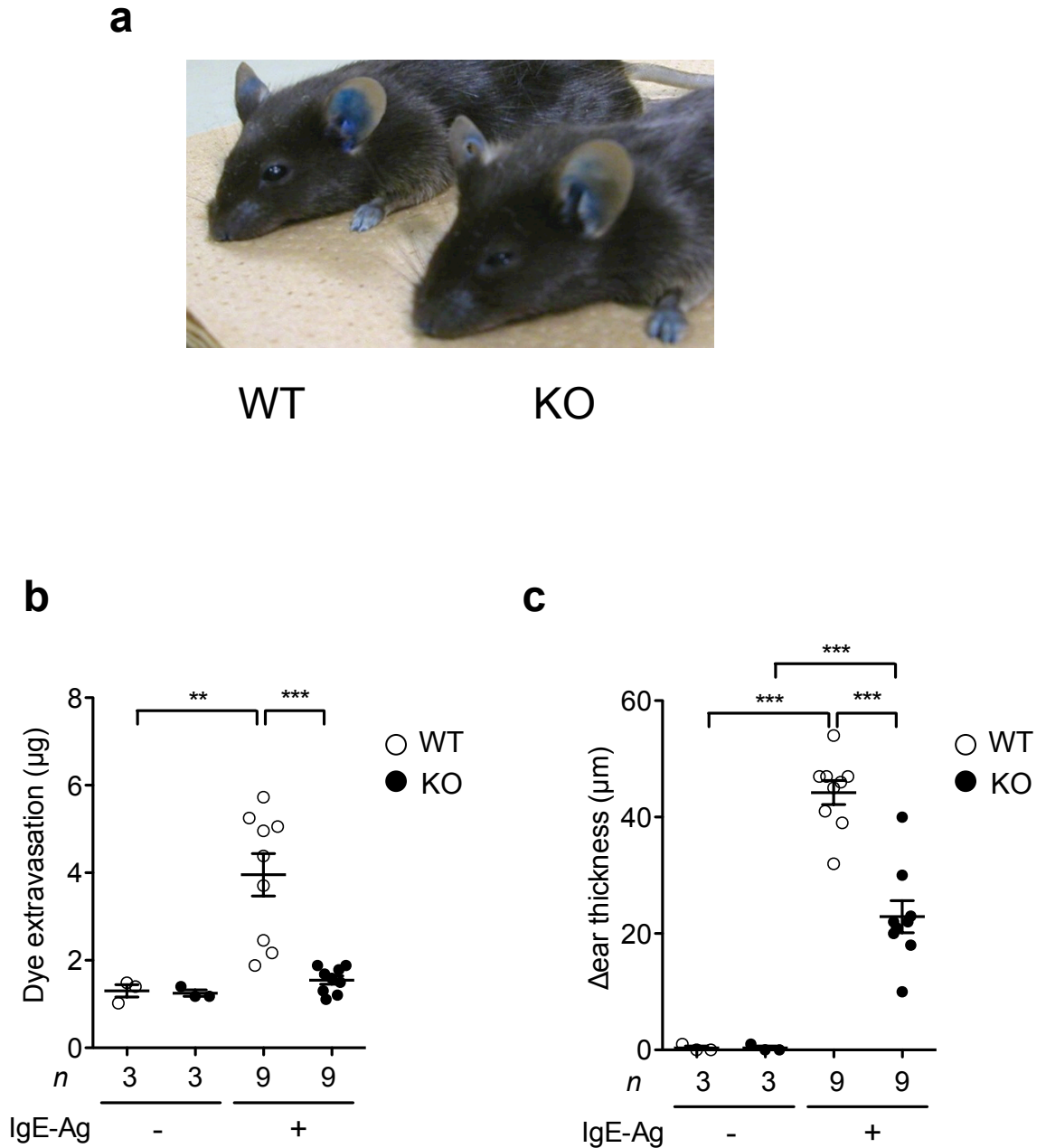


Figure 5. PAF-AH (II) knockout mice impair IgE-dependent passive cutaneous anaphylaxis

(a-c) Analysis of ear edema in IgE-Ag dependent PCA in wild-type (WT) and *pafah2*^{-/-} (KO) mice on a C57BL/6J back ground. (a) Representative photo of wild-type (WT) and *pafah2*^{-/-} (KO) mice after IgE-Ag mediated PCA. (b) Extravasation of Evans blue in the ears. (c) Changes in ear thickness after antigen challenge.

Experiments were repeated twice and the data were pooled. (mean ± s.e.m., ***p*<0.01; ****p*<0.001).

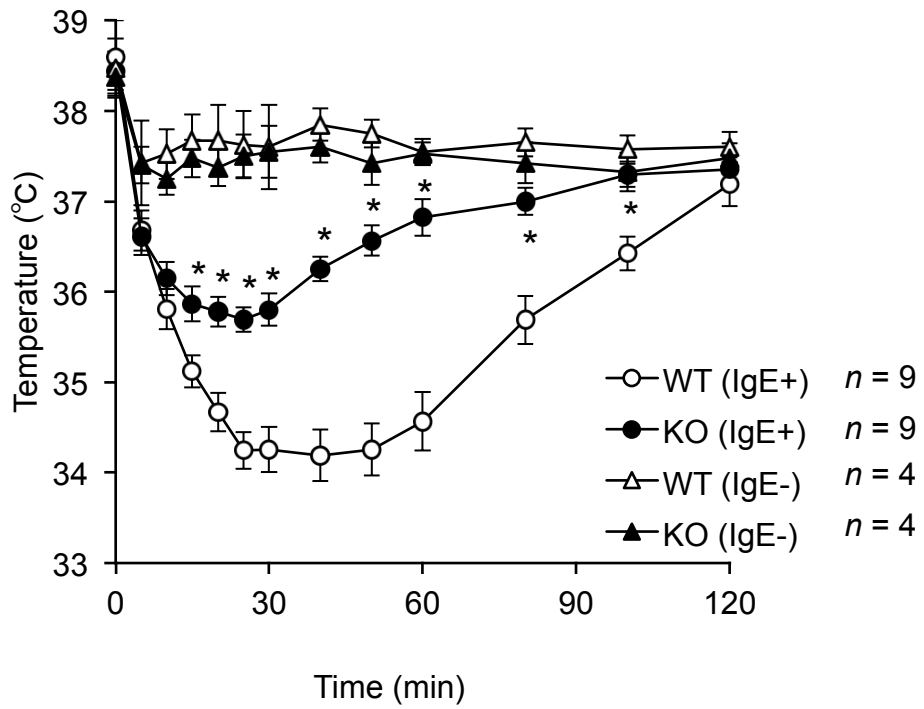


Figure 6. PAF-AH (II) knockout mice impair IgE-dependent passive systemic anaphylaxis
 Rectal temperatures in IgE-dependent PSA in wild-type (WT) and *pafah2*^{-/-} (KO) mice after challenge with 500 µg of antigen (Ag).
 (mean ± s.e.m., **p*<0.05 vs WT (IgE+)).

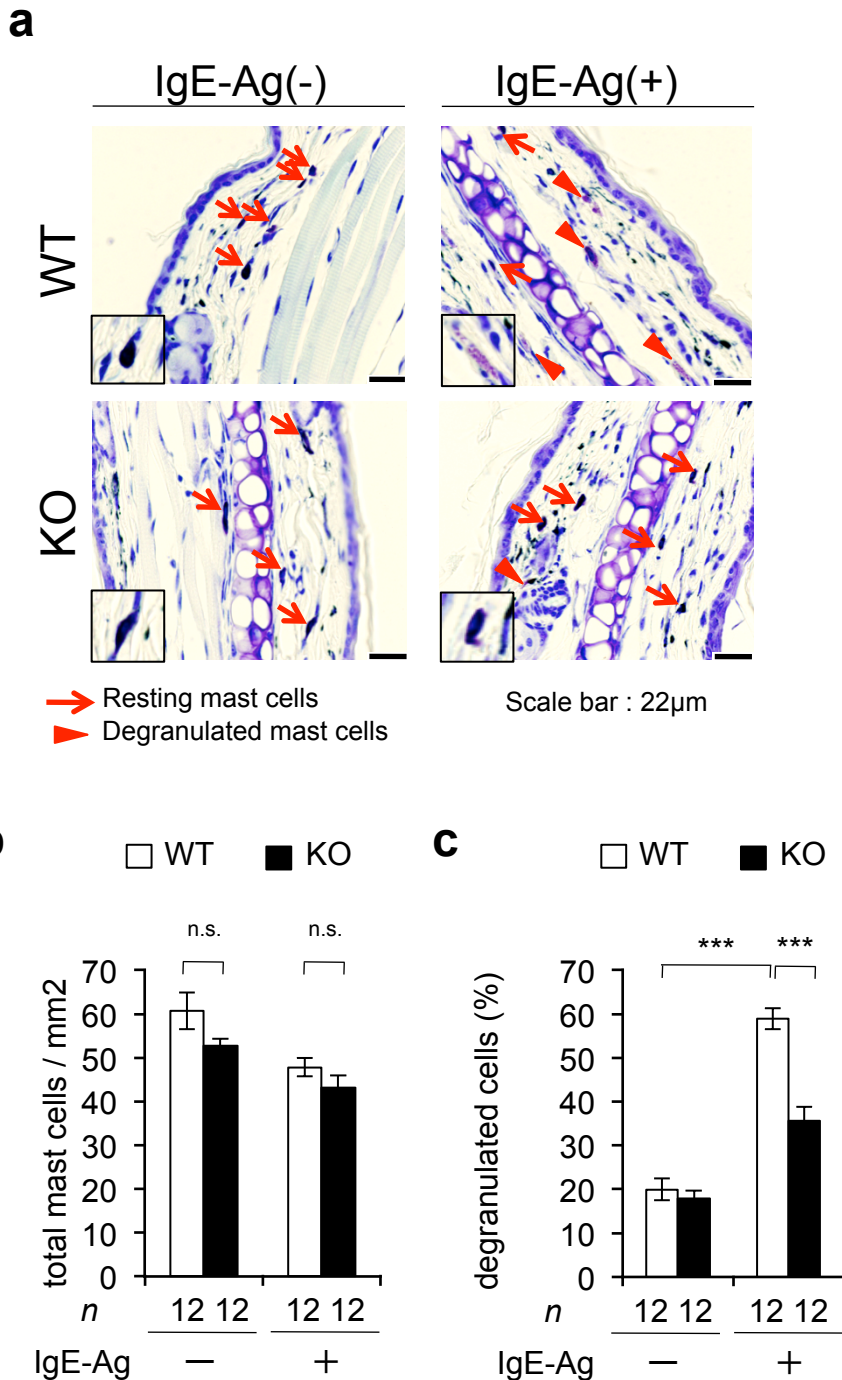


Figure 7. IgE-dependent mast cell degranulation is repressed in PAF-AH (II) knockout mice

(a-c) Wild-type (WT) and *pafah2*^{-/-} (KO) mice were subjected to IgE-mediated PCA. Before and 2 min after antigen challenge, the ear sections were stained with toluidine blue to quantify degranulated mast cells by light microscopy.

(a) Representative photographs of tissue sections of each genotypes before and after antigen challenge. Arrows and arrow heads indicate intact and degranulated tissue mast cells, respectively.

(b) The number of total mast cells per 1 mm² tissue section.

(c) The amount of degranulated mast cells in the tissue sections.

(mean ± s.e.m., ****p*, <0.001; n.s., not significant).

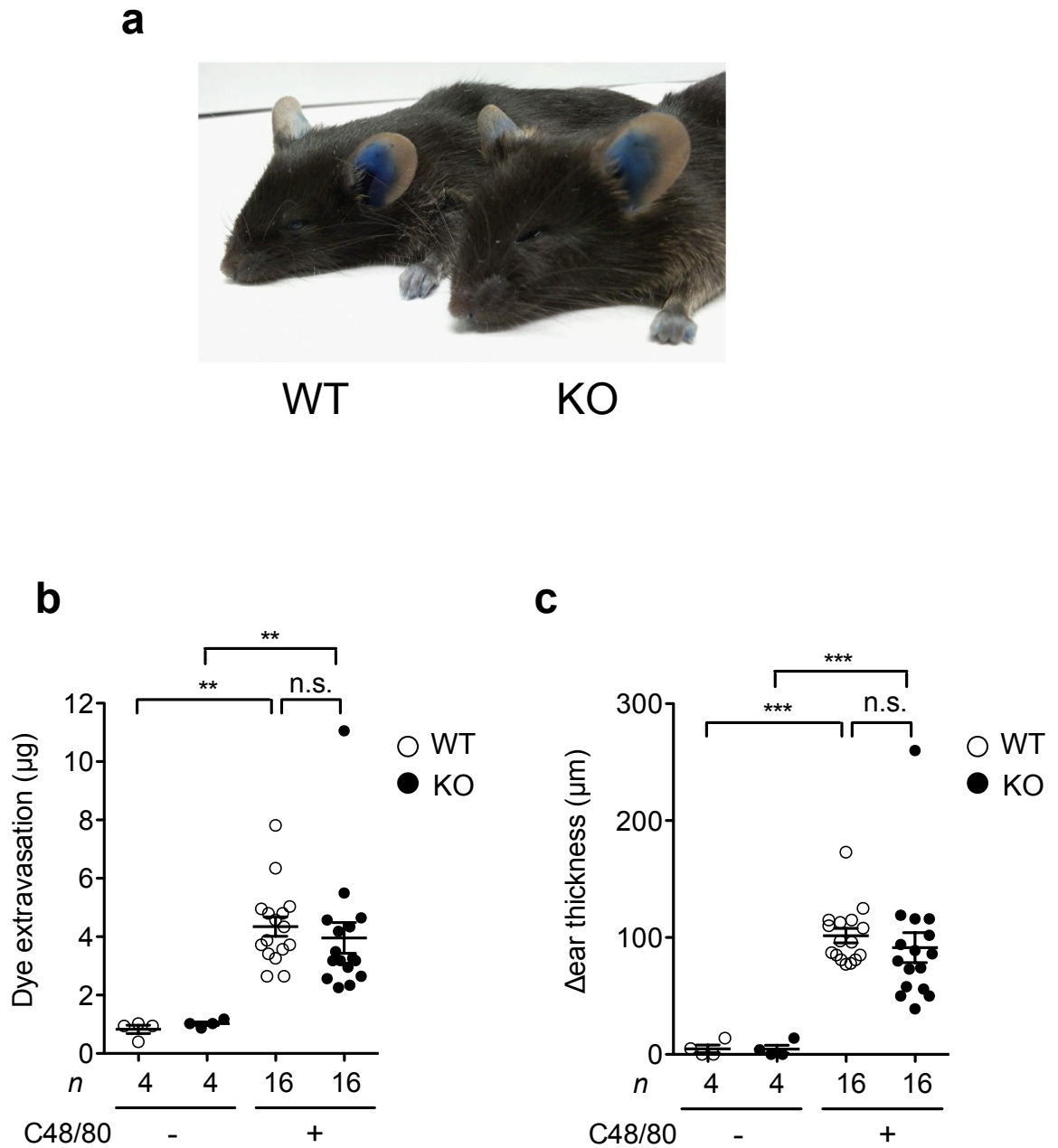


Figure 8. IgE-independent anaphylaxis is comparable between wild-type and PAF-AH (II) knockout mice

(a-c) Analysis of ear edema in C48/80-induced PCA in wild-type (WT) and *pafah2*^{-/-} (KO) mice.

(a) Representative photo of compound 48/80 treated mice.

(b) Extravasation of Evans blue in the ears.

(c) Changes in ear thickness after compound 48/80 challenge.

(mean \pm s.e.m., ** p <0.01; *** p <0.001; n.s., not significant).

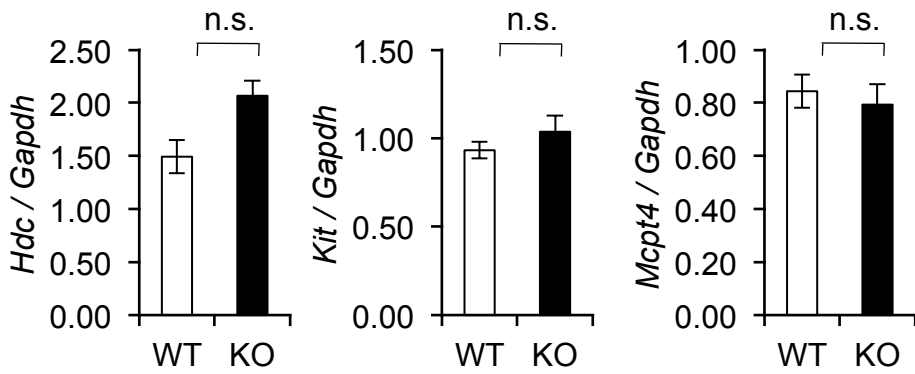
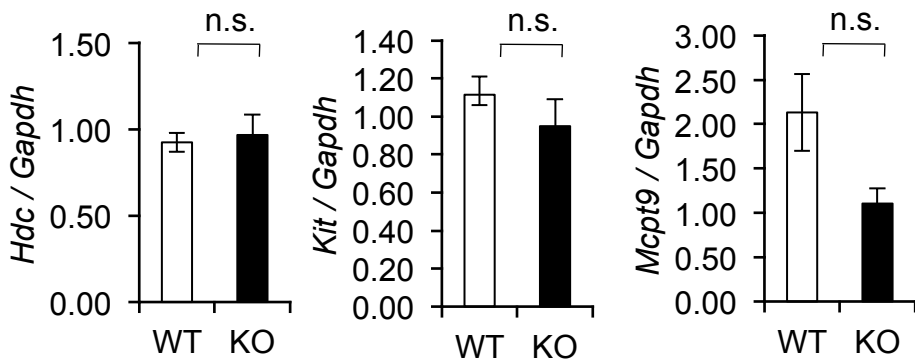
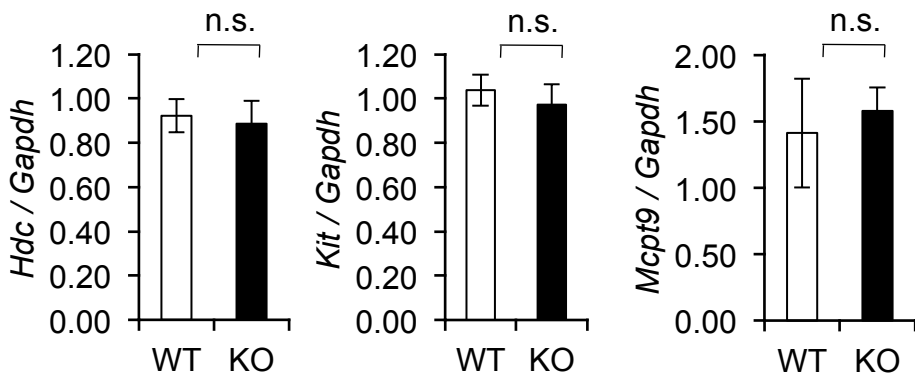
a**Ear****b****Stomach****c****Small intestine**

Figure 9. Normal maturation and proliferation of mast cells in PAF-AH (II) KO mice
 (a-c) mRNA expression of mast cell markers in ears (a), stomachs (b) and small intestines (c) obtained from wild-type (WT) and *paiah2*^{-/-} (KO) mice (n=5).
 (mean ± s.e.m., not significant).

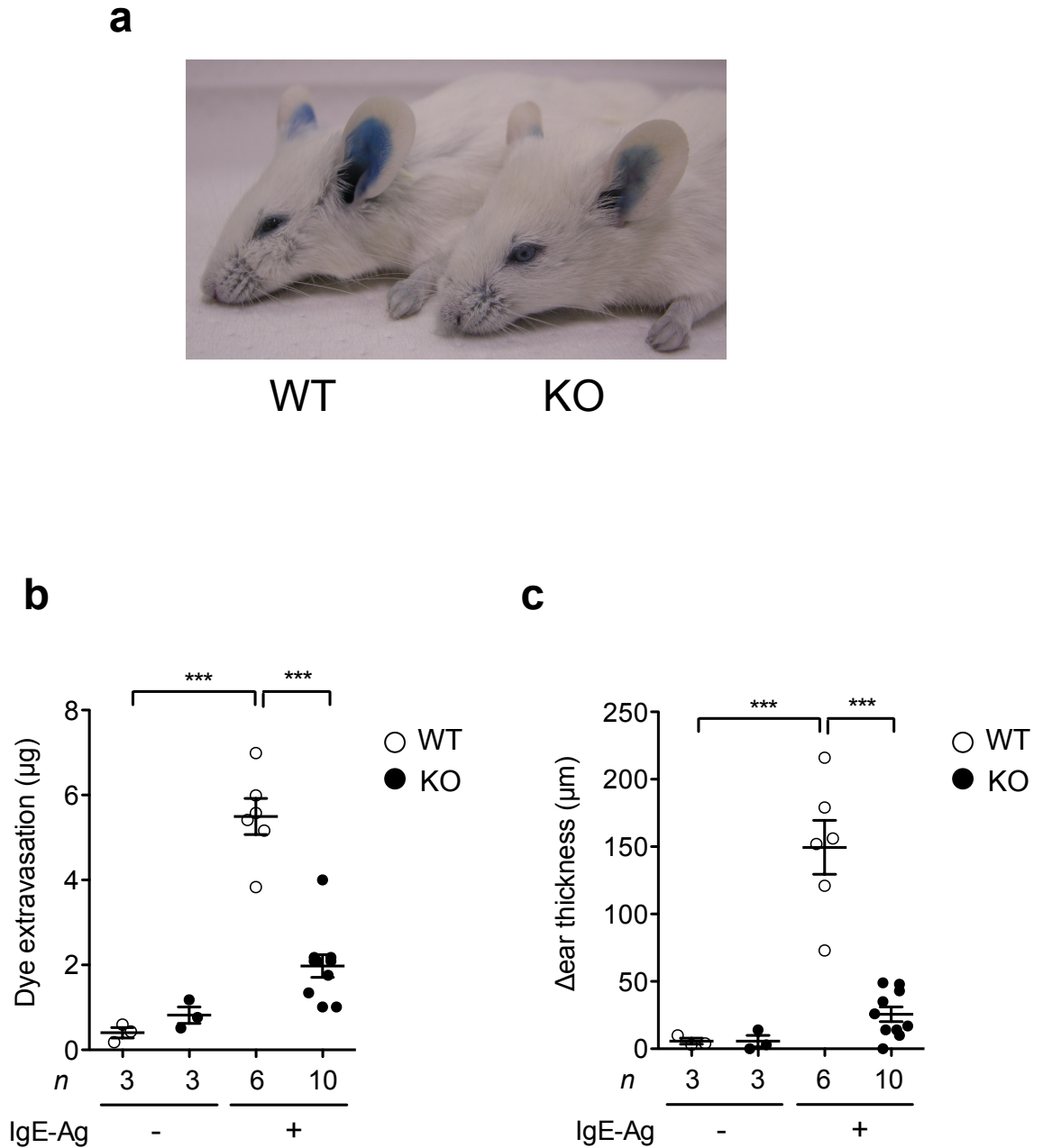


Figure 10. PAF-AH (II) knockout mice on a BALB/c background impair IgE-dependent passive cutaneous anaphylaxis

(a-c) Analysis of ear edema in IgE-Ag dependent PCA in wild-type (WT) and *pafah2*^{-/-} (KO) mice on a BALB/c background.

(a) Representative photo of wild type and *paf-ah2*^{-/-} mice after IgE-Ag mediated PCA.

(b) Extravasation of Evans blue in the ears.

(c) Changes in ear thickness after antigen challenge.

(mean ± s.e.m., ****p*, <0.001).

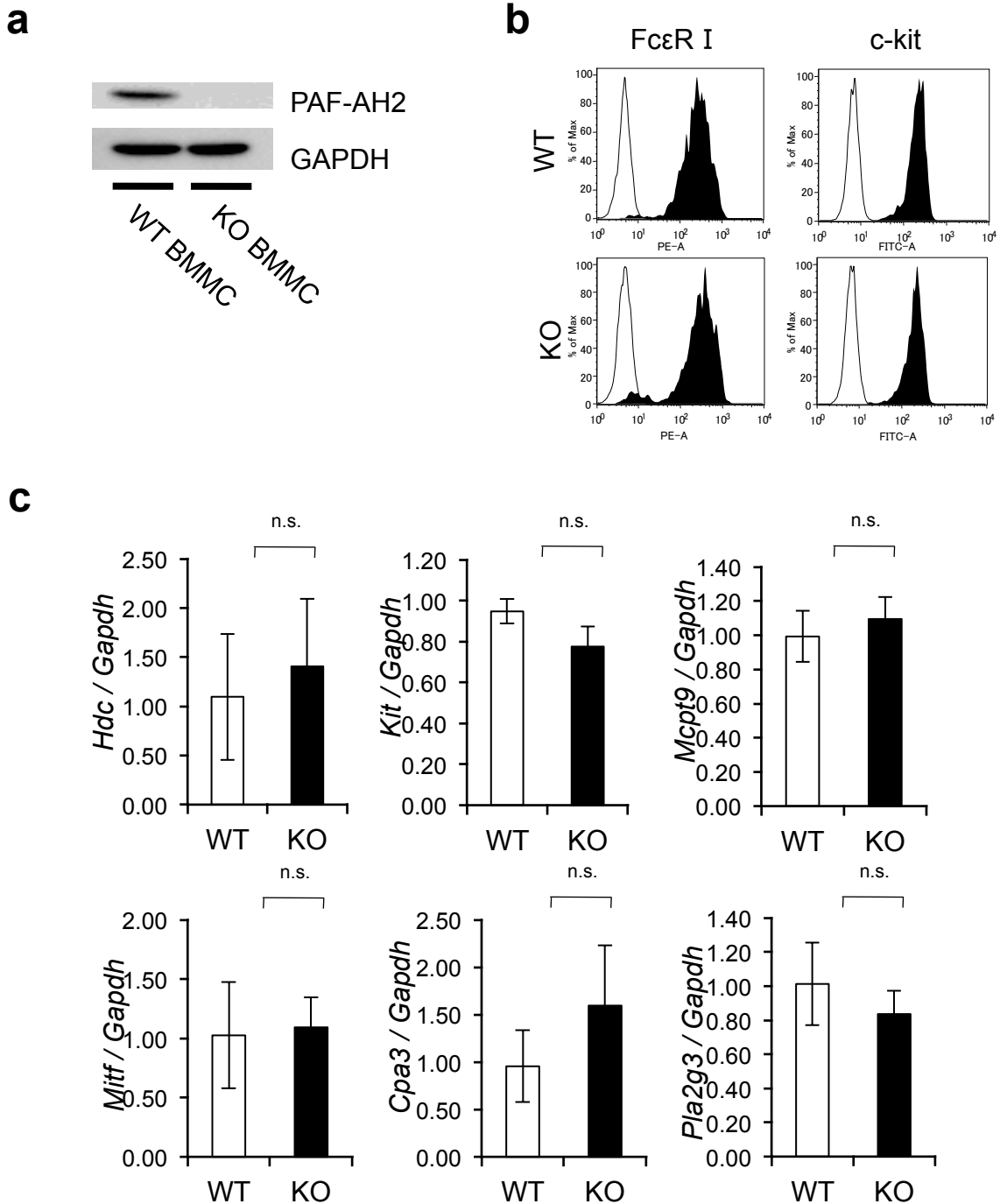


Figure 11. BMMCs obtained from PAF-AH (II) knockout mice mature normally
 (a) Immunoblotting of PAF-AH (II) in BMMCs obtained from wild-type (WT) and *pafah2*^{-/-} (KO) mice.
 (b) Flow cytometry of surface FcεR1α and c-kit expression on wild-type (WT) and *pafah2*^{-/-} (KO) BMMCs.
 (c) Real-time PCR of various mast cell maturation markers relative to *Gapdh* in BMMCs obtained from wild-type (WT) and *pafah2*^{-/-} (KO) mice (n=3).
 (mean ± s.e.m., n.s., not significant).

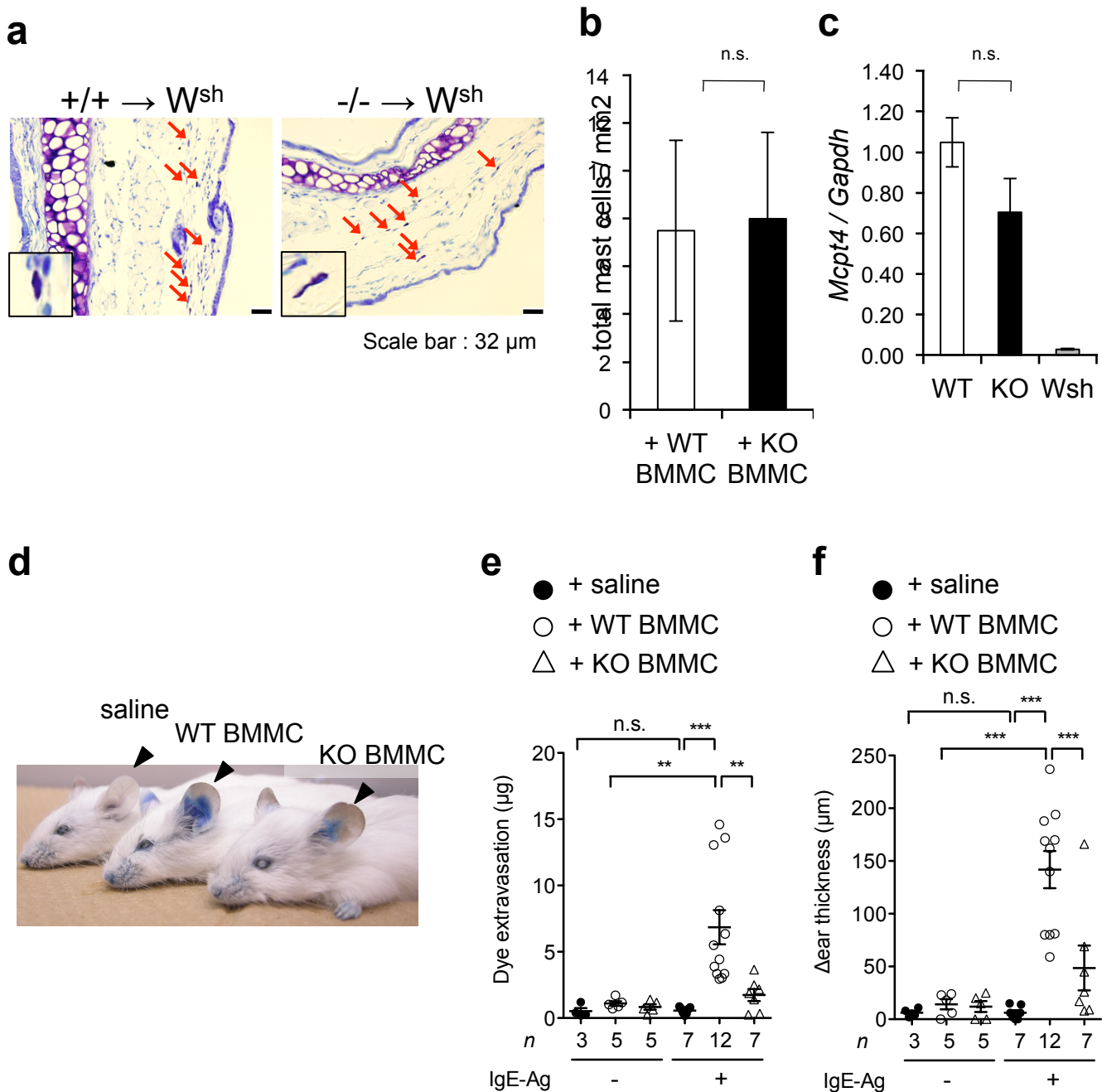


Figure 12 PAF-AH (II) expressed in mast cell is essential for anaphylaxis

(a-c) Wild-type and *pafah2*^{-/-} BMMCs were intradermally transferred into *Kit*^{W-sh/W-sh} mice. After 40 days of reconstitution, toluidine blue⁺ mast cells (red arrows) in skin sections were counted (a, b). Scale bars, 32 μm. Magnified views of representative mast cells are shown in box (n=4). (c) *Mcpt4* expression in each mouse after 40 days of reconstitution (n=3).

(d) Representative photo of ear edema in IgE-Ag dependent PCA in wild-type and *pafah2*^{-/-} BMMC-reconstituted or nonreconstituted *Kit*^{W-sh/W-sh} mice.

(e, f) Extravasation of Evans blue (e) and changes in ear thickness (f) after antigen challenge of wild-type (WT) and *pafah2*^{-/-} (KO) BMMC-reconstituted or nonreconstituted *Kit*^{W-sh/W-sh} mice after IgE-Ag mediated PCA.

(mean ± s.e.m., ***p*<0.01; ****p*<0.001; n.s., not significant).

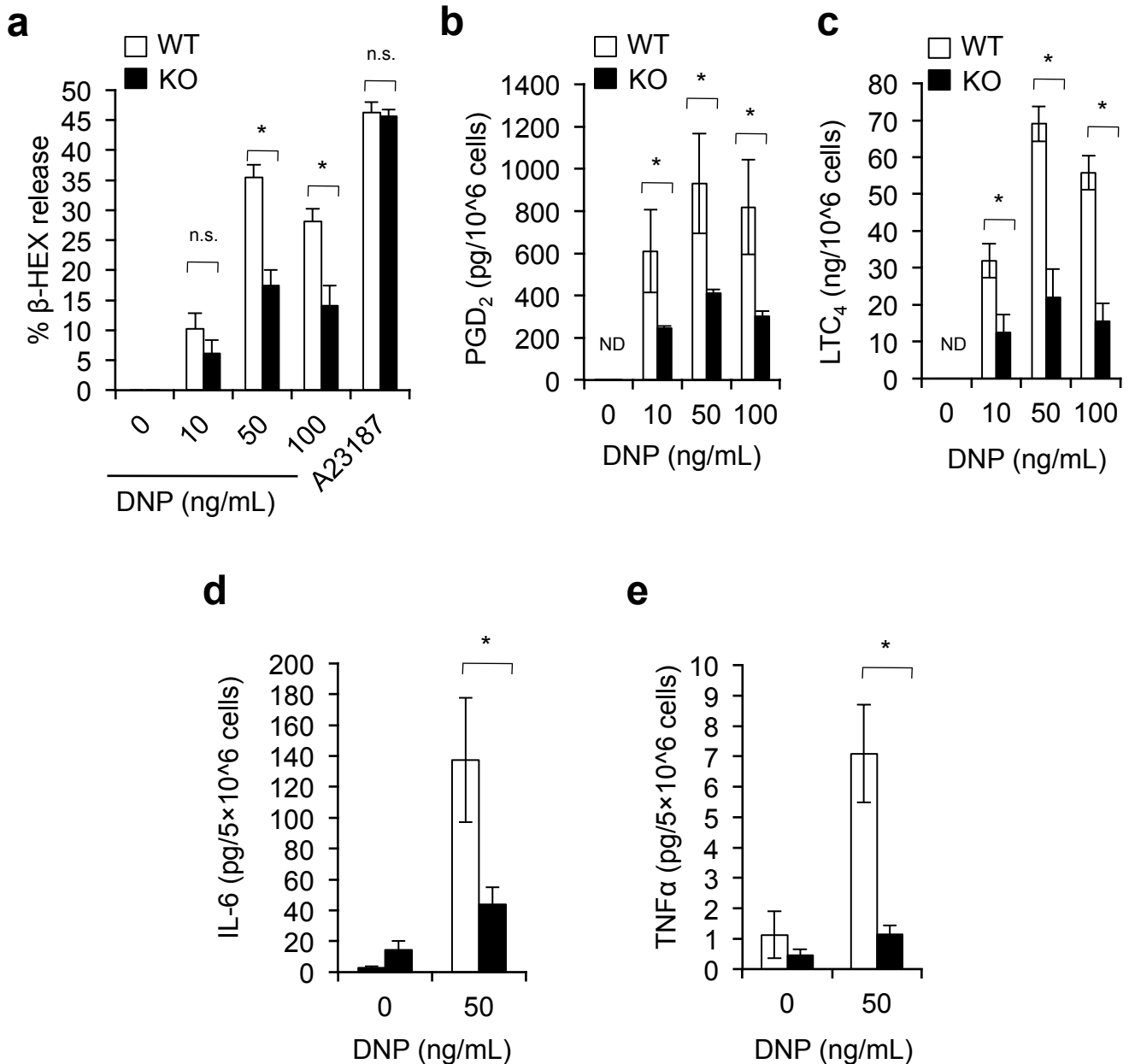


Figure 13. PAF-AH (II) is required for IgE-dependent secretion of inflammatory mediators from mast cells

(a) The percentage of degranulation of wild-type (WT) and *pafah2*^{-/-} (KO) BMMCs. BMMCs sensitized with the anti-DNP IgE were challenged with the indicated concentrations of DNP-HAS or A23187. β -Hexosaminidase released in the supernatants was measured by an enzymatic assay using 4-nitrophenyl *N*-acetyl- β -glucosaminide (n=8).

(b, c) Quantification of IgE-Ag induced PGD₂ (b) and LTC₄ (c) from wild-type (WT) and *pafah2*^{-/-} (KO) BMMCs (n=6).

(d, e) Quantification of IgE-Ag induced IL-6 (d) and TNF α (e) from wild-type (WT) and *pafah2*^{-/-} (KO) BMMCs.

Experiments were repeated at least twice and the data were pooled.

(mean \pm s.e.m., **p*<0.05; n.s., not significant).

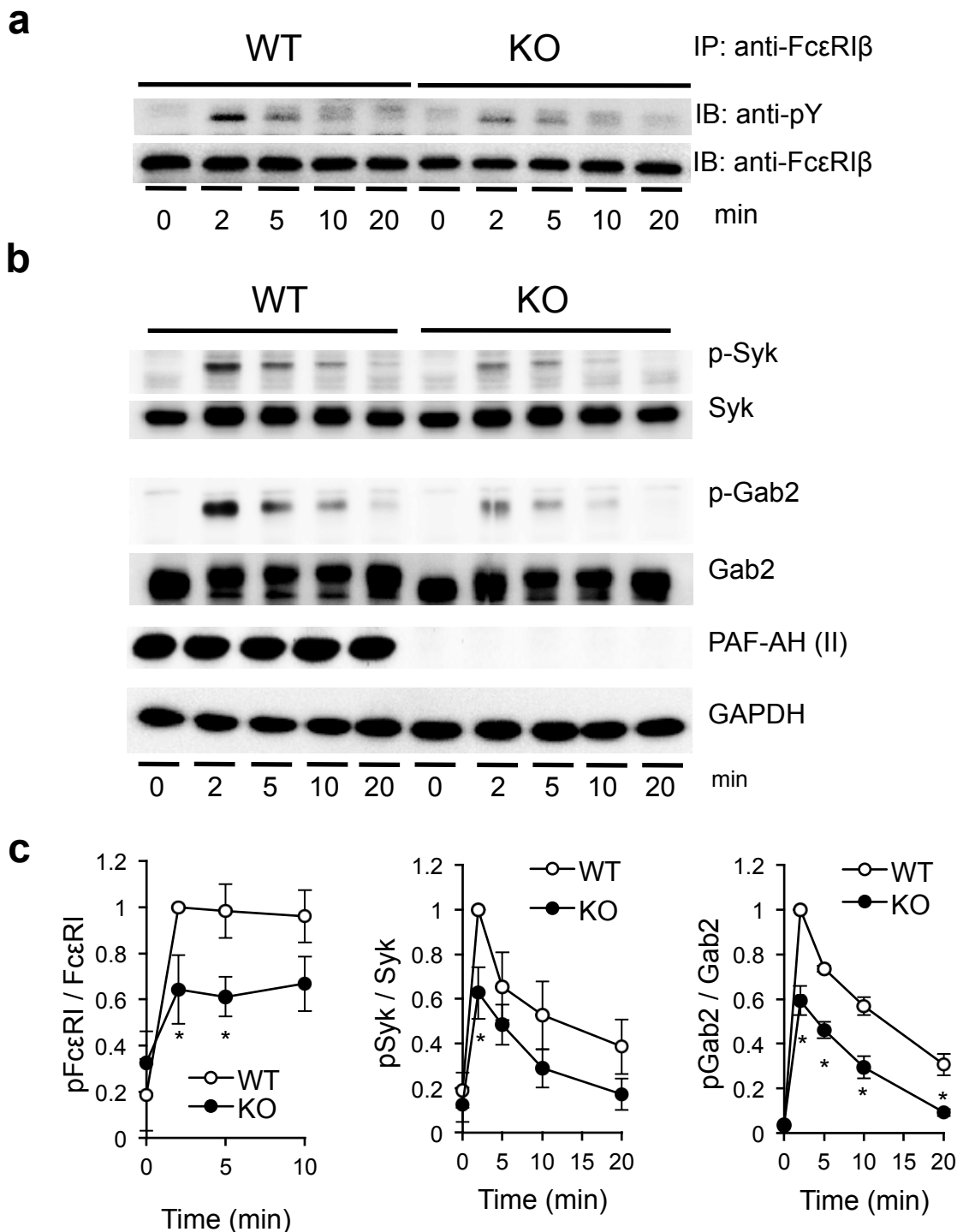


Figure 14. PAF-AH (II) is required for IgE-dependent activation of FcεRI and downstream signals

(a-c) IgE-sensitized wild-type (WT) and *pafah2*^{-/-} (KO) BMMCs were stimulated with 50 ng/mL of the antigen DNP-HAS for the indicated times. Immunoprecipitates of FcεRIβ were probed with antibodies to FcεRIβ or phosphotyrosine (a). Whole cell lysates of BMMCs stimulated as in (a) were probed with antibodies to Syk, phospho-Syk, Gab2, phospho-Gab2, PAF-AH (II) and GAPDH (b). Blots were representative of three separate experiments with three individual BMMC cultures. Fold induction of phosphorylated protein normalized to the amount of each individual protein in a given lane was determined by the relative ratio of signal intensity and compared with wild-type BMMCs stimulated for 2 min (arbitrarily set to 1) (c). Experiments were repeated at least twice and the data were pooled. (mean ± s.e.m., **p*<0.05).

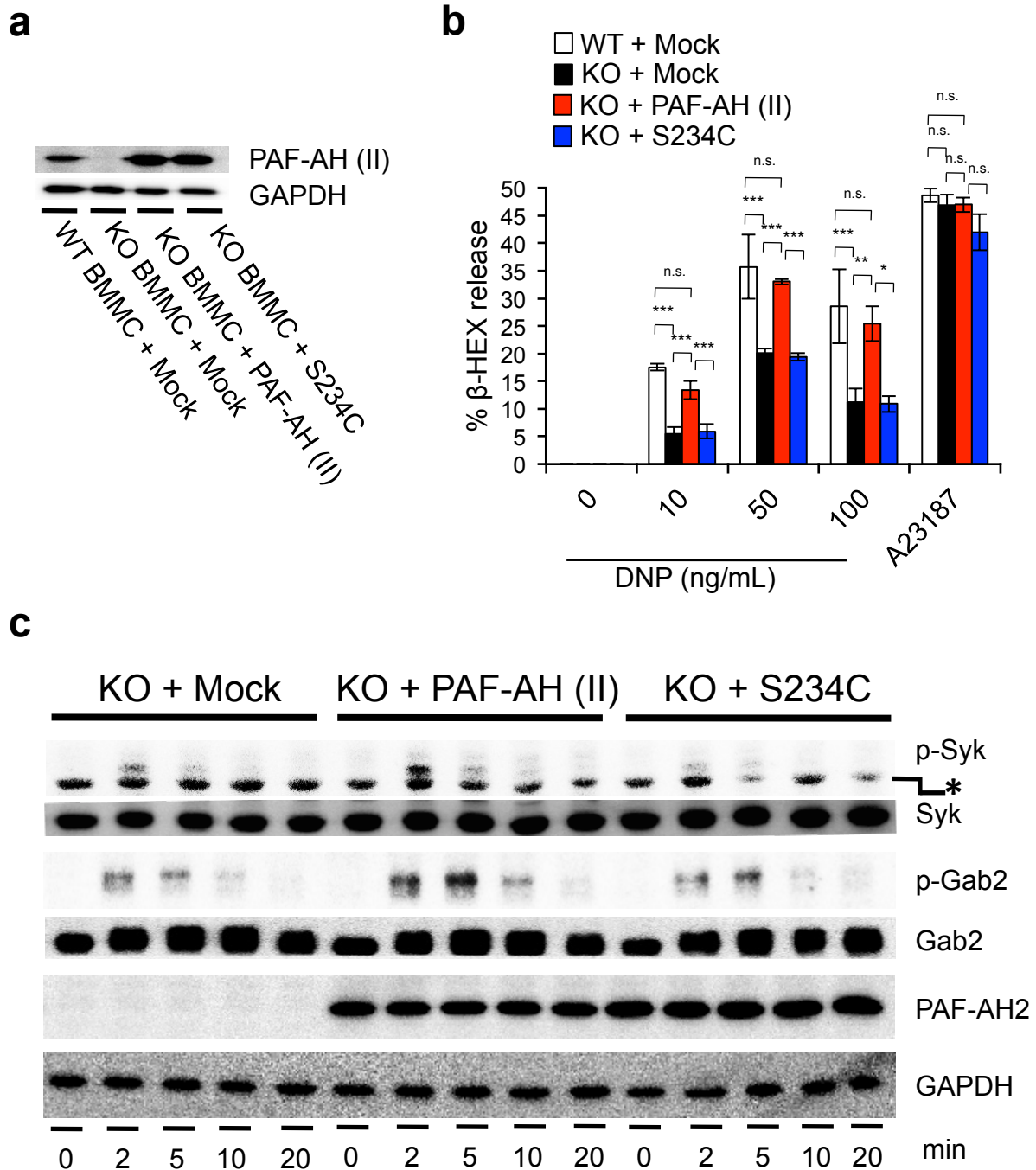


Figure 15. Enzymatic activity of PAF-AH (II) is required for IgE-dependent mast cell activation

(a-c) Wild-type PAF-AH (II) and catalytic inactive mutants S234C were retrovirally expressed in *pafah2*^{-/-} (KO) BMMCs.

(a) Expression of PAF-AH (II) in BMMCs (western blotting).

(b) The percentage of degranulation of IgE-sensitized *pafah2*^{-/-} (KO) BMMCs that had been infected with retrovirus bearing an empty vector, a PAF-AH2 expression vector or S234C expression vector (n=6).

(c) Phosphorylation of Syk or Gab2 after antigen stimulation (western blotting).

Experiments were repeated at least twice and the data were pooled.

(mean \pm s.e.m., * p <0.05; ** p <0.01; *** p ,<0.001; n.s., not significant).

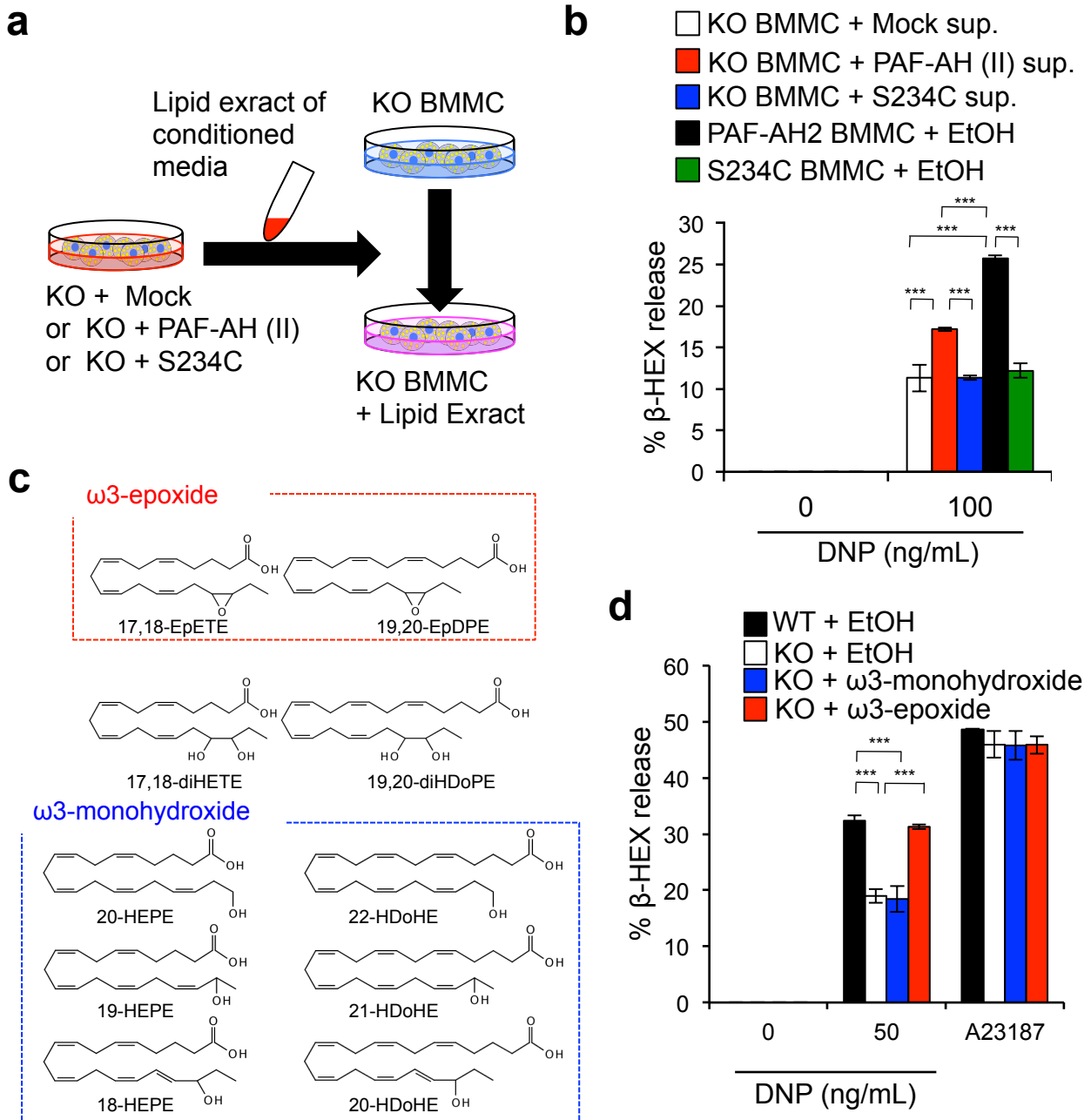


Figure 16. Conditioned media from PAF-AH (II) expressed BMMCs restore IgE-mediated degranulation of *pafah2*^{-/-} BMMCs

(a) Schematic protocol of exogenous lipid addition to cultured BMMCs. Lipid extracts from conditioned media were dissolved in ethanol and added to *pafah2*^{-/-} (KO) BMMCs twice in three days and β -HEX assay was performed a day after last lipid treatment.

(b) Free fatty acid fractions extracted from conditioned media of *pafah2*^{-/-} (KO) BMMCs that had been infected with retrovirus bearing an empty vector, a PAF-AH (II) expression vector or S234C expression vector were added to the cultured *pafah2*^{-/-} BMMCs and IgE-Ag dependent β -HEX release was assessed. *Paf-ah2*^{-/-} BMMCs retrovirally overexpressed PAF-AH (II) or S234C were also stimulated with IgE-Ag (n=4).

(c) Structure of oxidized ω 3 fatty acids which were more abundant in wild-type BMMC-conditioned media than *pafah2*^{-/-} BMMC-conditioned media. ω 3-monoepoxides and ω 3-monohydroxides are surrounded with red and blue dot-line, respectively. sEH converts ω 3-monoepoxides to the corresponding dihydrodiols.

(d) IgE-Ag or A23187 dependent β -HEX release of *pafah2*^{-/-} (KO) BMMCs cultured for three days in the presence of 300 nM of mixture of ω 3-monohydroxides or ω 3-epoxides. Exogenous lipids addition was performed as (a) (n=4). Epoxide mix : 17,18-EpETE/19,20-EpDPE = 2/3, Monohydroxy mix : 20-HEPE/19-HEPE/18-HEPE/22HDoHE/21-HDoHE/20-HDoHE = 2/2/1/2/2/1 (mean \pm s.e.m., ****p* < 0.001).

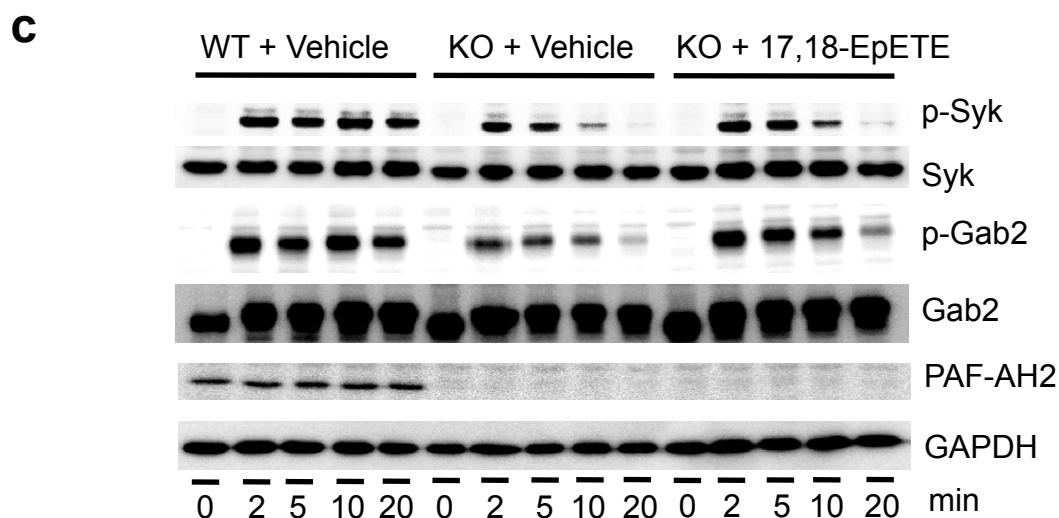
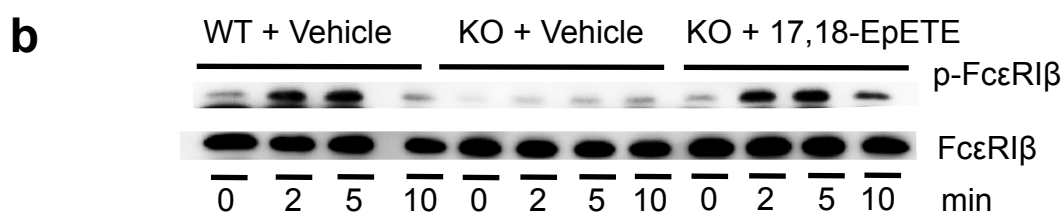
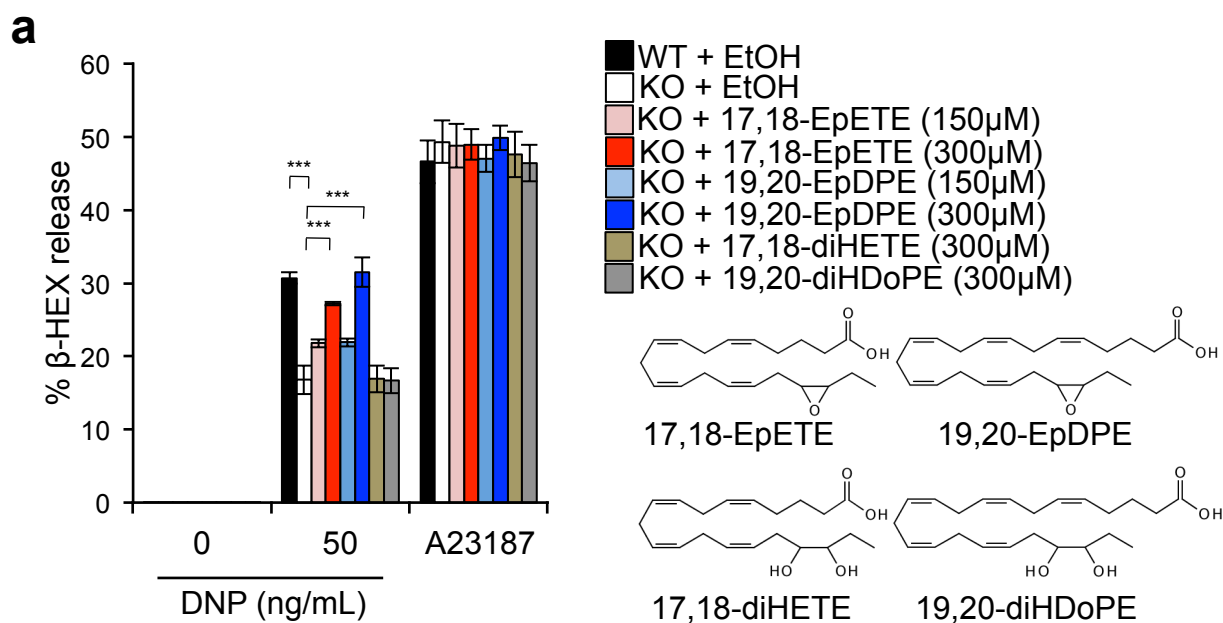


Figure 17. Impaired production of ω 3-epoxides causes defective mast cell activation obtained from PAF-AH (II) knockout mice

(a) IgE-Ag or A23187 dependent β -HEX release of *pafah2*^{-/-} (KO) BMMCs cultured for three days in the presence of 150 or 300 nM of 17,18-EpETE, 19,20-EpDPE, 17,18-diHETE and 19,20-diHDoPE. sEH converts ω 3-monoepoxides to the corresponding dihydrodiols.

(b, c) Exogenous lipids addition was performed as Fig. 16 (a) (n=4). (b) *Pafah2*^{-/-} (KO) BMMCs cultured with 300nM 17,18-EpETE as (a) were stimulated with 50ng/mL of the antigen DNP-HAS for the indicated times. Immunoprecipitates of FcεRIβ were probed with antibodies to FcεRIβ or phosphotyrosine. (c) *Pafah2*^{-/-} (KO) BMMCs cultured with 300nM 17,18-EpETE as (a) were stimulated with 50 ng/mL of the antigen DNP-HAS for the indicated times. Whole cell lysates were probed with antibodies to Syk, phospho-Syk, Gab2, phospho-Gab2, PAF-AH (II) and GAPDH.

(mean \pm s.e.m., ****p*, <0.001; n.s., not significant).

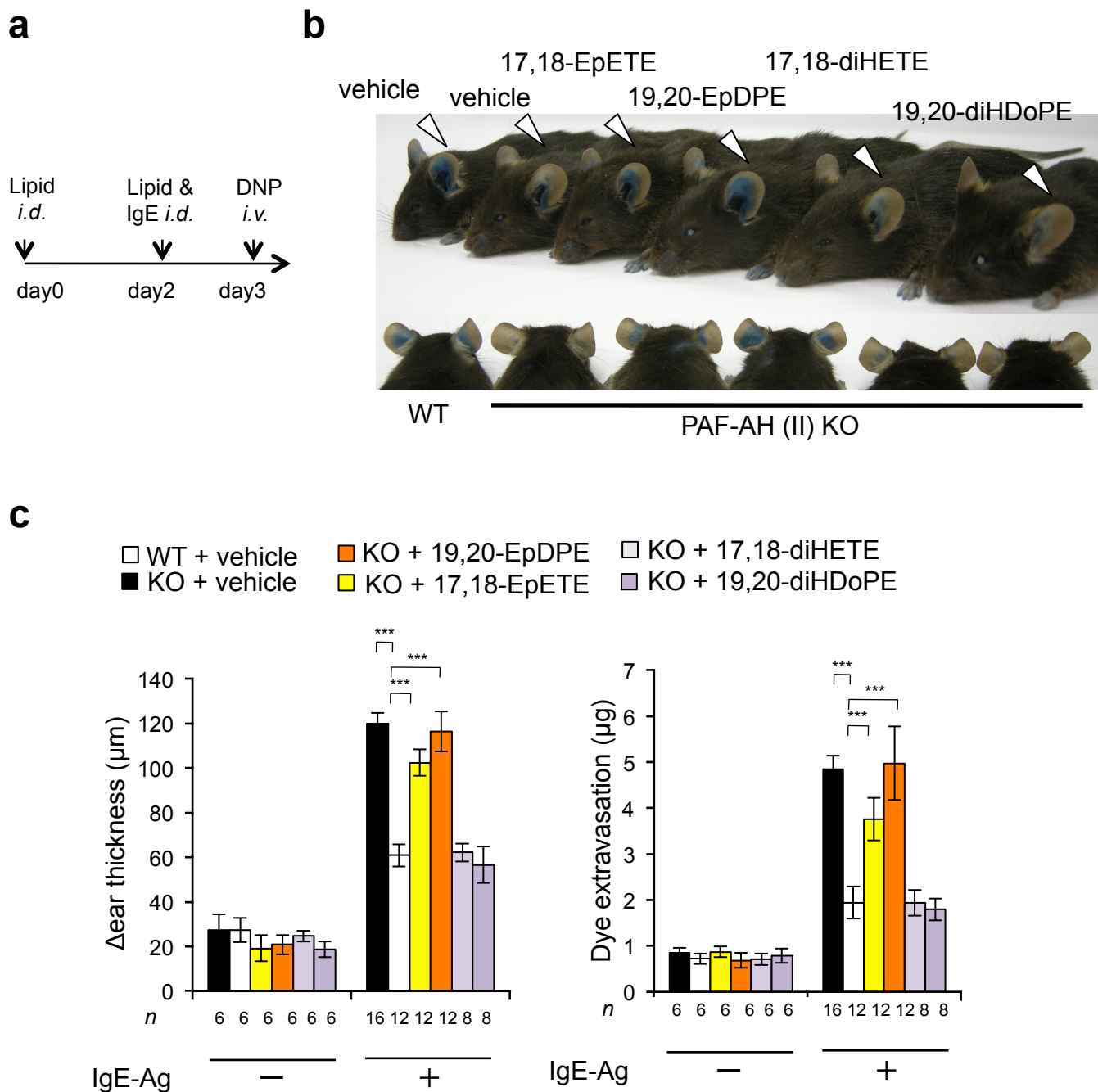


Figure 18. Impaired production of ω 3-epoxides causes defective IgE-dependent anaphylaxis of PAF-AH (II) knockout mice

(a) Schematic protocol of exogenous lipid challenge into the ear of *pafah2*^{-/-} (KO) mice. 16pmol of 17,18-EpETE, 19,20-EpDPE, 17,18-diHETE or 19,20-diHDoPE was injected into the ears of *pafah2*^{-/-} mice twice in three days and PCA assay was performed a day after last lipid treatment.

(b) Representative photo of lipid treated mice.

(c) Extravasation of Evans blue in the ears and changes in ear thickness after challenge with 500µg of antigen.

Experiments were repeated at least twice and the data were pooled.

(mean \pm s.e.m., * p <0.05; ** p <0.01; *** p <0.001; n.s., not significant).

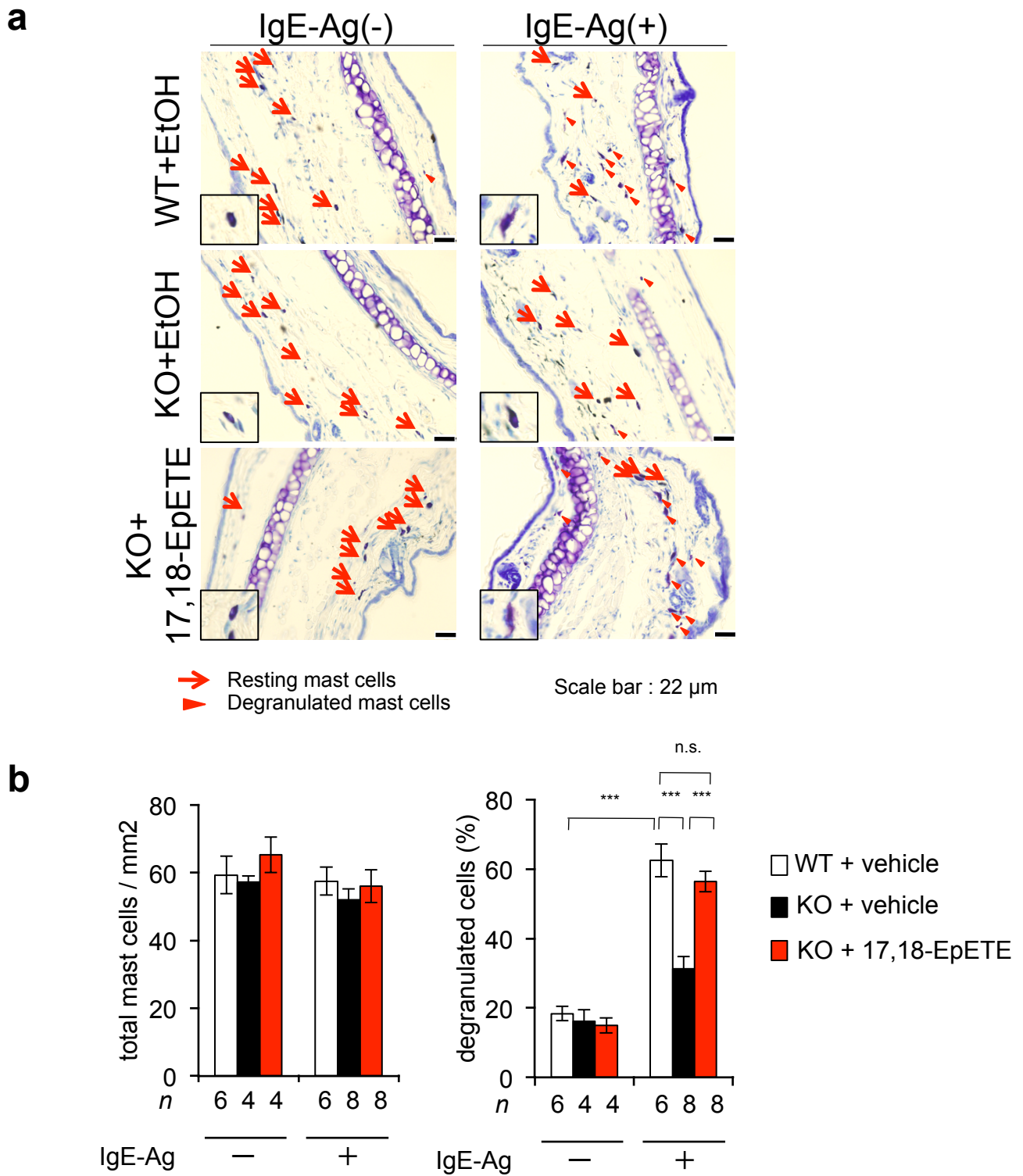


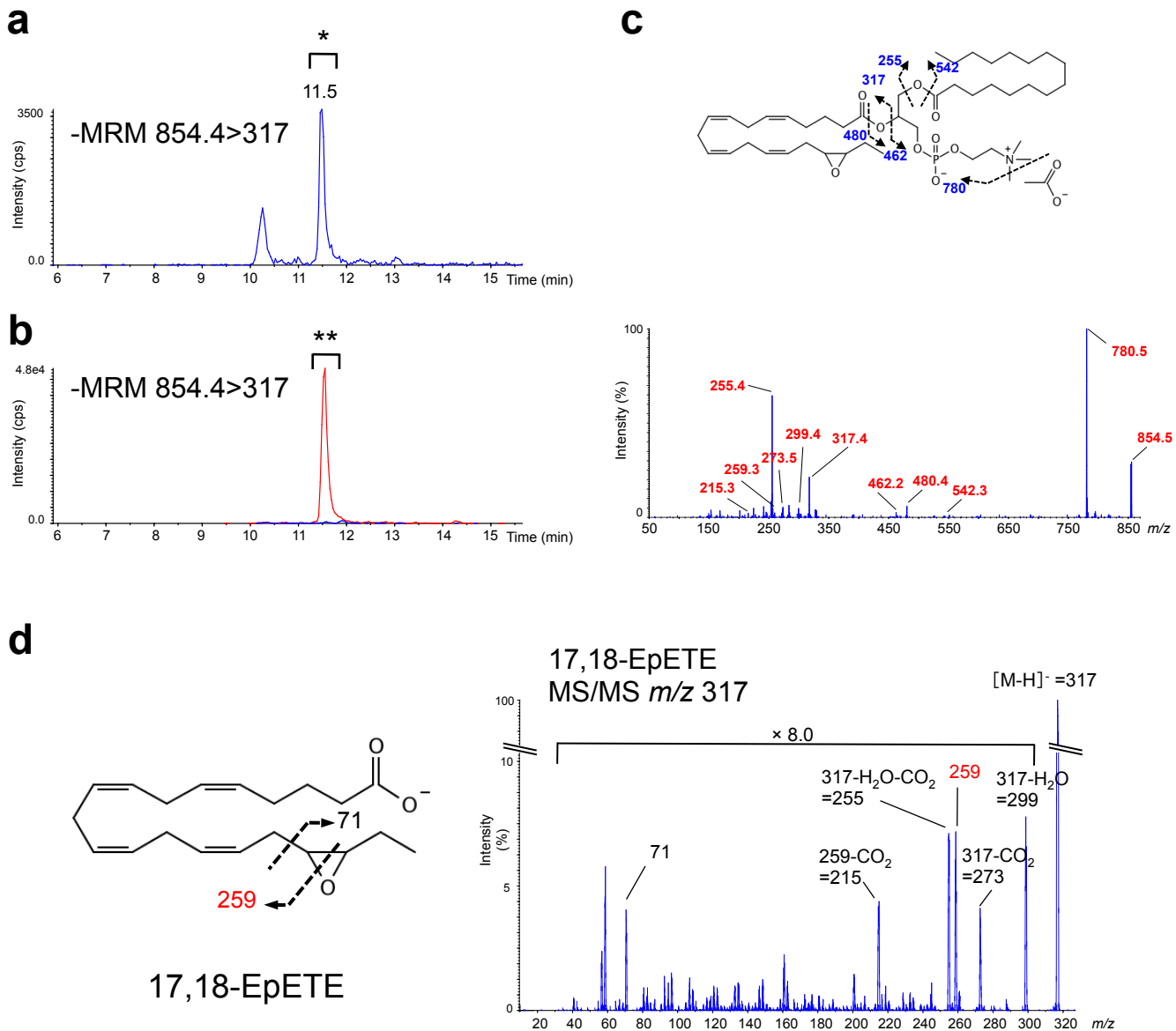
Figure 19. ω 3-epoxides restore IgE-mediated mast cell degranulation in PAF-AH (II) knockout mice

(a, b) 17,18-EpETE was injected into the ears of *pafah2*^{-/-} (KO) mice as Fig. 18 (a) and mice were subjected to IgE-mediated PCA. Before and 2 min after antigen challenge, the ear sections were stained with toluidine blue to quantify degranulated mast cells by light microscopy.

(a) Representative photographs of tissue sections of each genotypes after antigen challenge. Arrows and arrow heads indicate intact and degranulated tissue mast cells, respectively.

(b) The number of total mast cells per 1 mm² tissue section and the amount of degranulated mast cells in the tissue sections.

(mean \pm s.e.m., * p <0.05; ** p <0.01; *** p <0.001; n.s., not significant).



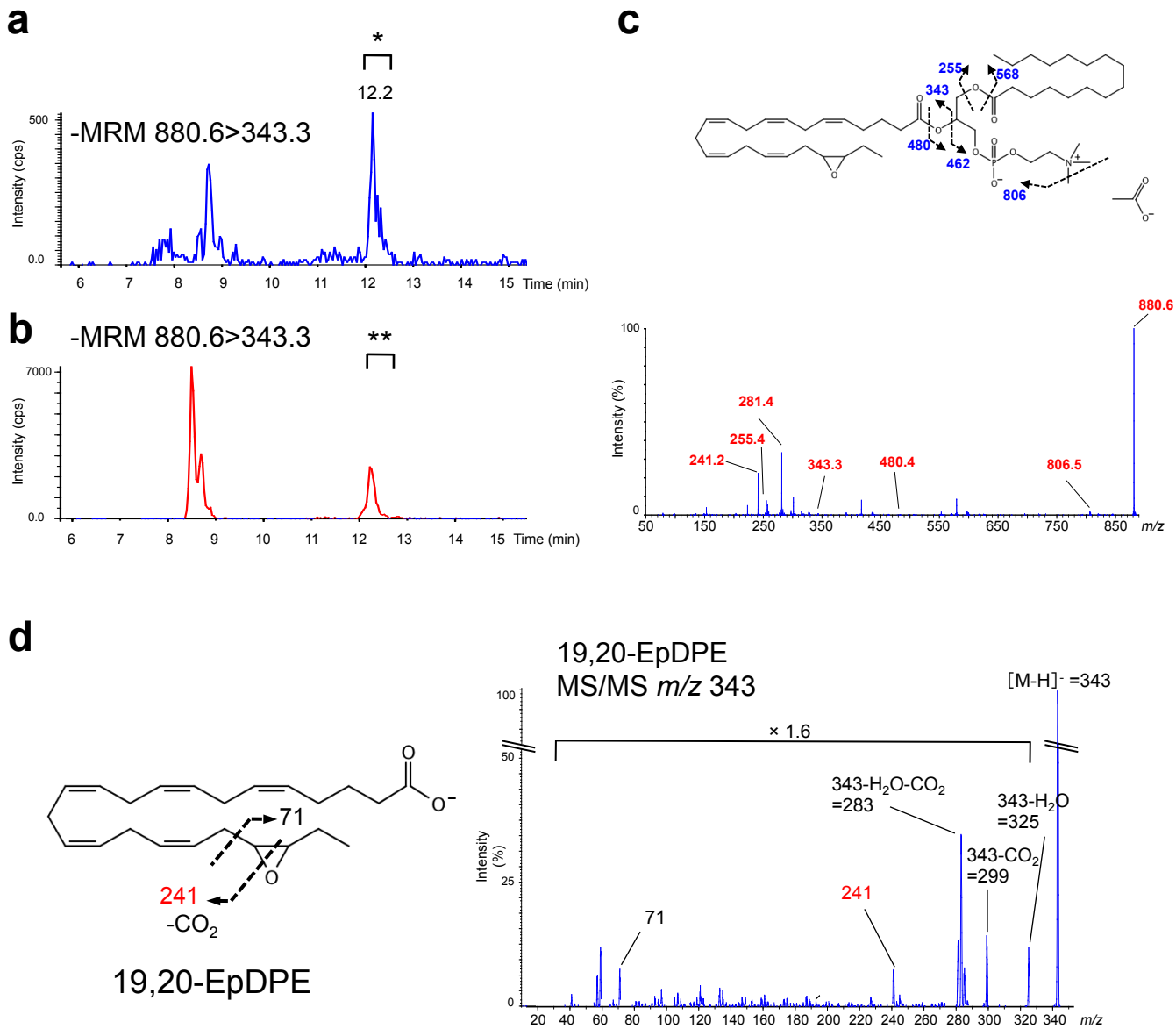


Figure 21. Detection of 19,20-EpDPE containing phosphatidylcholine in BMMCs
 (a-c) MRM chromatogram (a, b) and MS/MS spectrum (c) of 16:0/19,20-EpDPE-PC. Lipid extracts from wild-type BMMCs (a) or 19,20-EpDPE incorporated BMMCs (b, c) were separated by UPLC as Fig. 20 (a). (a, b) MRM chromatogram monitoring 880.6→343 MRM transition. (c) MS/MS spectrum of m/z 880.6.
 (d) MS/MS spectrum of 19,20-EpDPE.

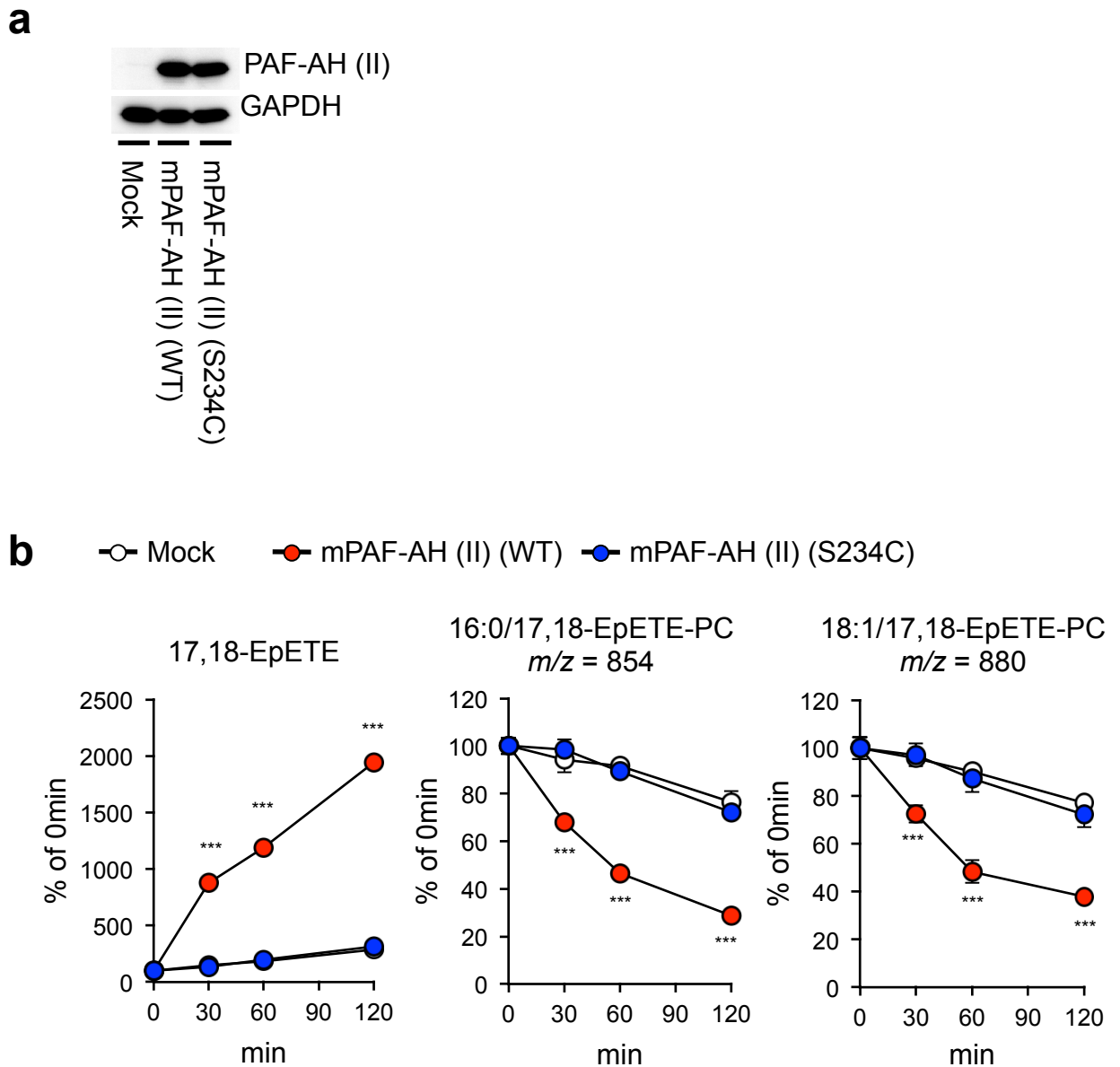
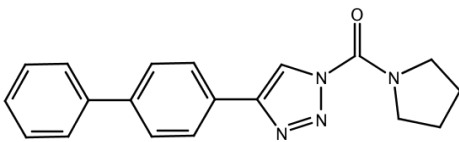


Figure 22. PAF-AH (II) hydrolyzes esterified ω 3-epoxides

(a) HEK293T cells were transiently transfected with pcDNA3 vectors carrying no insert, wild-type PAF-AH (II) or S234C mutant. Cytosolic fractions of these transfected cells were collected and PAF-AH (II) or GAPDH were detected by western blotting.

(b) Cytosolic fractions from cells transfected with pcDNA3 vectors carrying no insert, wild-type PAF-AH (II) or S234C mutant were incubated with membrane fractions of 17,18-EpETE incorporated *pafah2*^{-/-} BMMCs for the indicated times. Lipid extracts were separated by UPLC as described in experimental methods and the amount of 17,18-EpETE, 16:0/17,18-EpETE-PC and 18:1/17,18-EpETE-PC and were monitored using MRM. Fold induction of lipids normalized to the amount of each individual lipid in a given time point was determined by the relative ratio of signal intensity and compared with 0min (arbitrarily set to 100%, *n*=3). (mean \pm s.e.m., ****p*, <0.001).

a



b

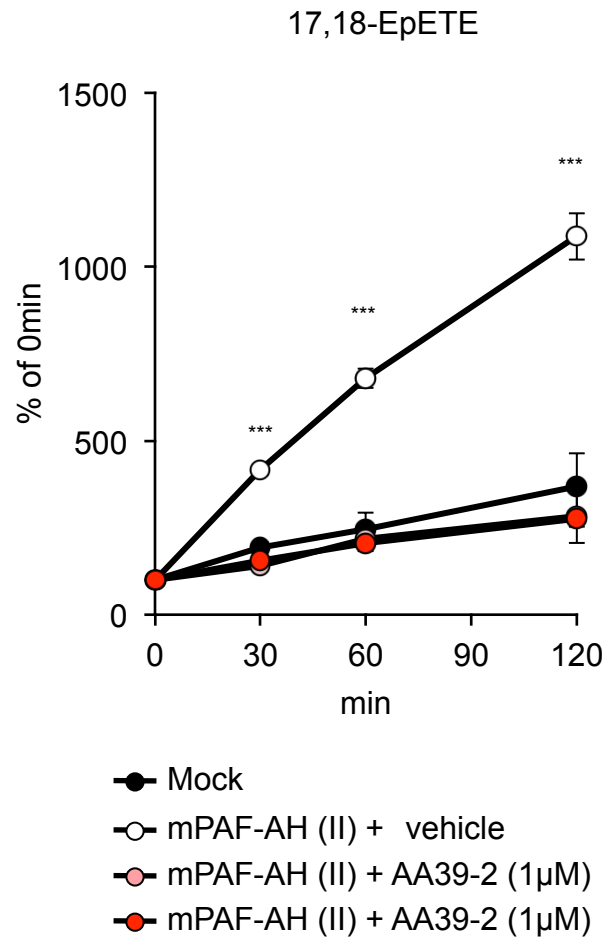


Figure 23. AA39-2 inhibits activities of PAF-AH (II) to release ω 3-epoxides from esterified precursors

(a) Structure of AA39-2.

(b) Cytosolic fractions from cells transfected with pcDNA3 vectors carrying no insert or wild-type PAF-AH (II) were incubated with membrane fractions of 17,18-EpETE incorporated *pafah2*^{-/-} BMMCs in the presence of AA39-2 for the indicated times. The amount of 17,18-EpETE were monitored as Fig 22 (b) (arbitrarily set to 100%, n=3).

(mean \pm s.e.m., *** p , <0.001).

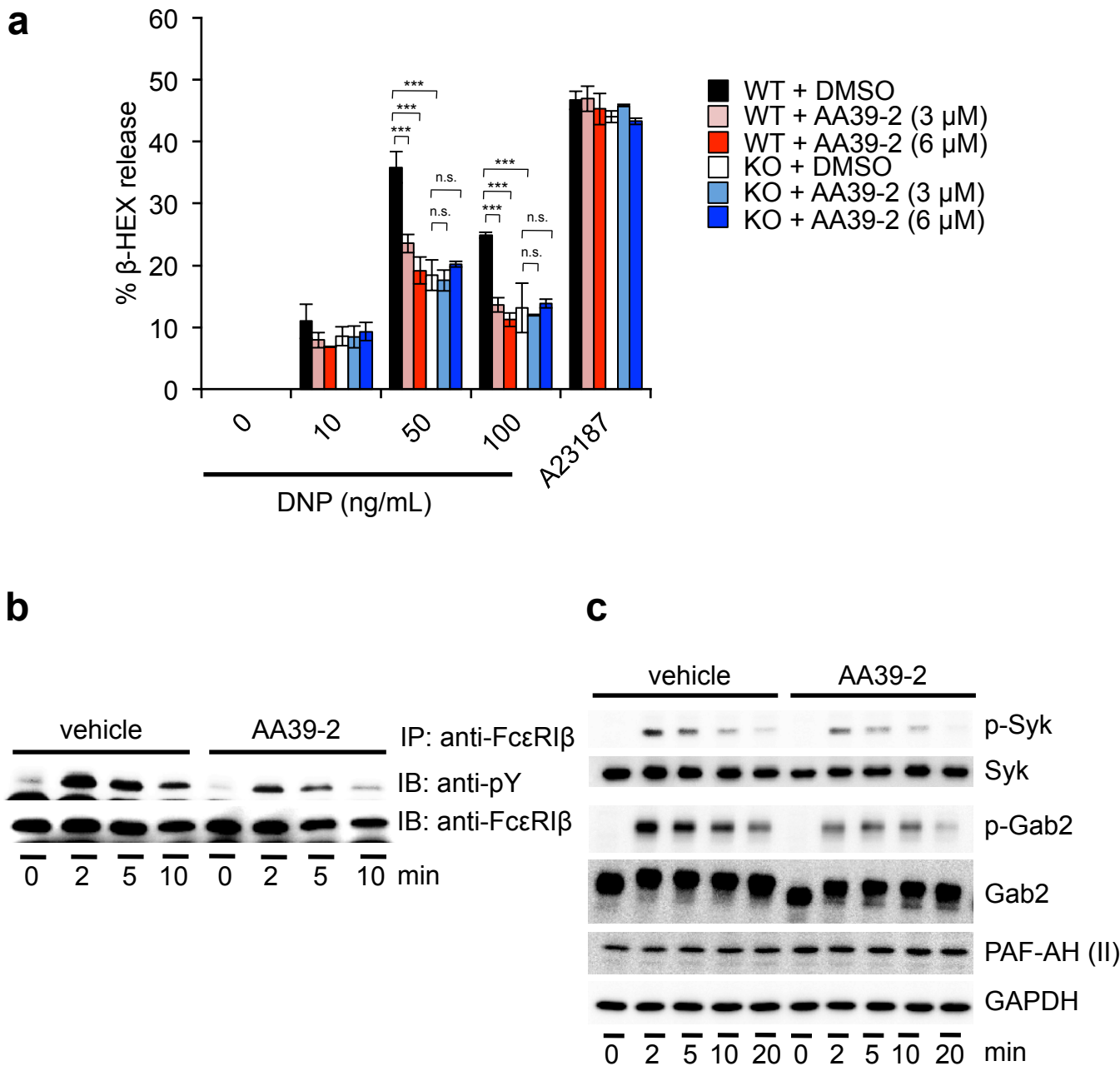


Figure 24. Selective PAF-AH (II) inhibitor reduces IgE-mediated activation of BMMCs

(a) IgE-Ag or A23187 dependent β HEX release of BMMCs cultured for three days in the presence of 3 or 6 μ M of AA39-2. AA39-2 was dissolved in DMSO and added to BMMCs twice in three days and β -HEX assay was performed a day after last AA39-2 treatment (n=4).

(b, c) Wild-type BMMCs cultured with 3 μ M AA39-2 as (a) were stimulated with 50 ng/mL of the antigen DNP-HAS for the indicated times. Immunoprecipitates of Fc ϵ RI β were probed with antibodies to Fc ϵ RI β or phosphotyrosine or whole cell lysates of stimulated BMMCs were probed with antibodies to Syk, phospho-Syk, Gab2, phospho-Gab2, PAF-AH (II) and GAPDH.

Experiments were repeated at least twice and the data were pooled.

(mean \pm s.e.m., *** p , <0.001; n.s., not significant).

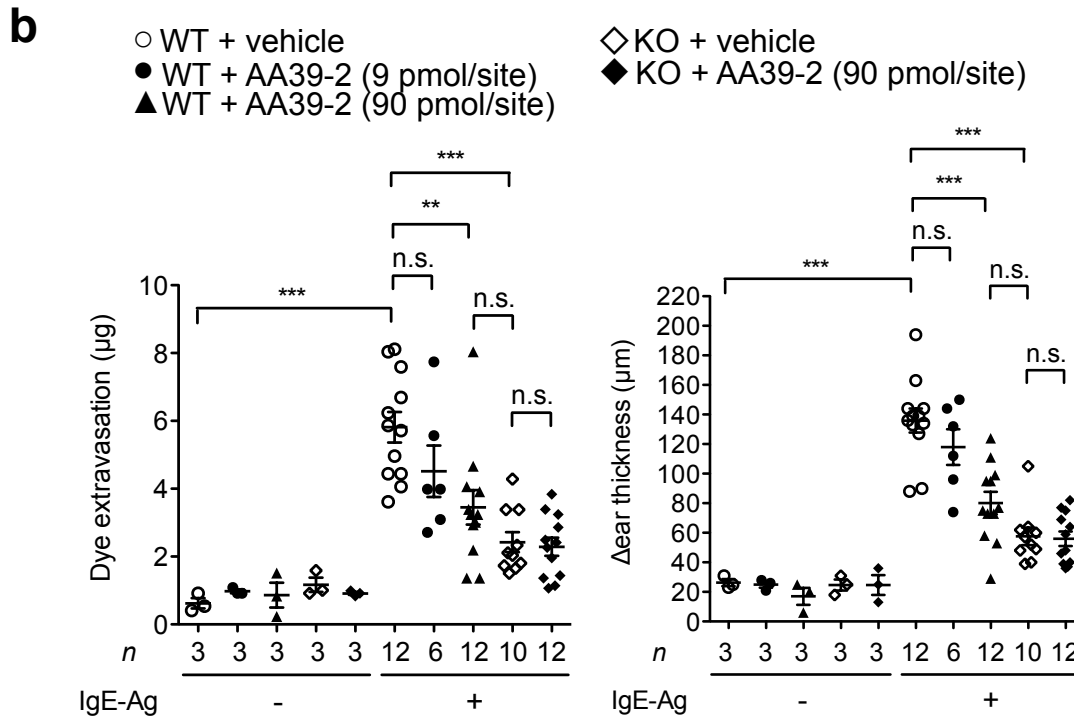
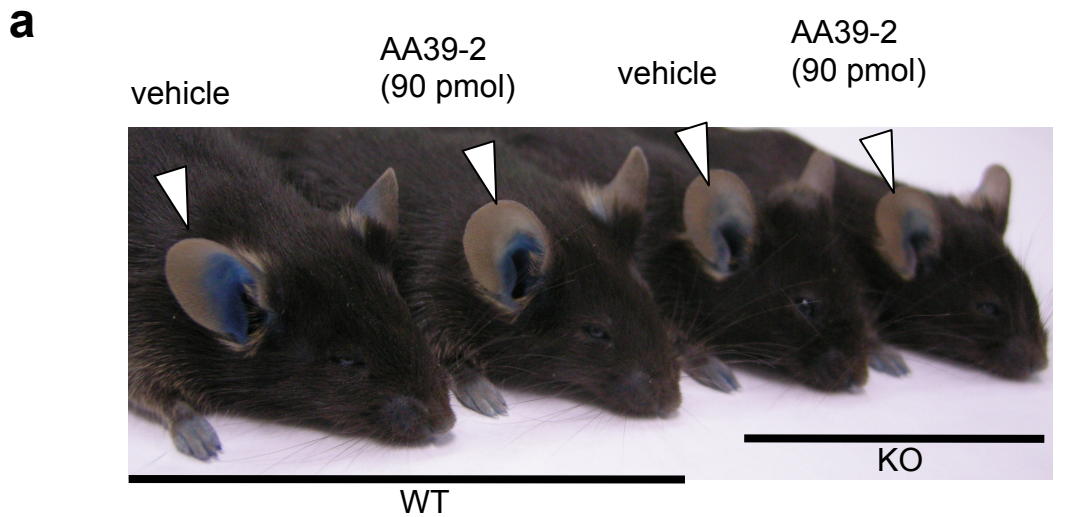


Figure 25. Selective PAF-AH (II) inhibitor reduces IgE-mediated mast cell activation *in vivo*

(a, b) 9 or 90 pmol of AA39-2 was injected into the ears of mice twice in three days and PCA assay was performed a day after last AA39-2 treatment.

(a) Representative photo of AA39-2 treated mice.

(b) Extravasation of Evans blue in the ears and changes in ear thickness after challenge with 500 μg of antigen.

Experiments were repeated at least twice and the data were pooled.

(mean \pm s.e.m., ** $p < 0.01$; *** $p < 0.001$; n.s., not significant).

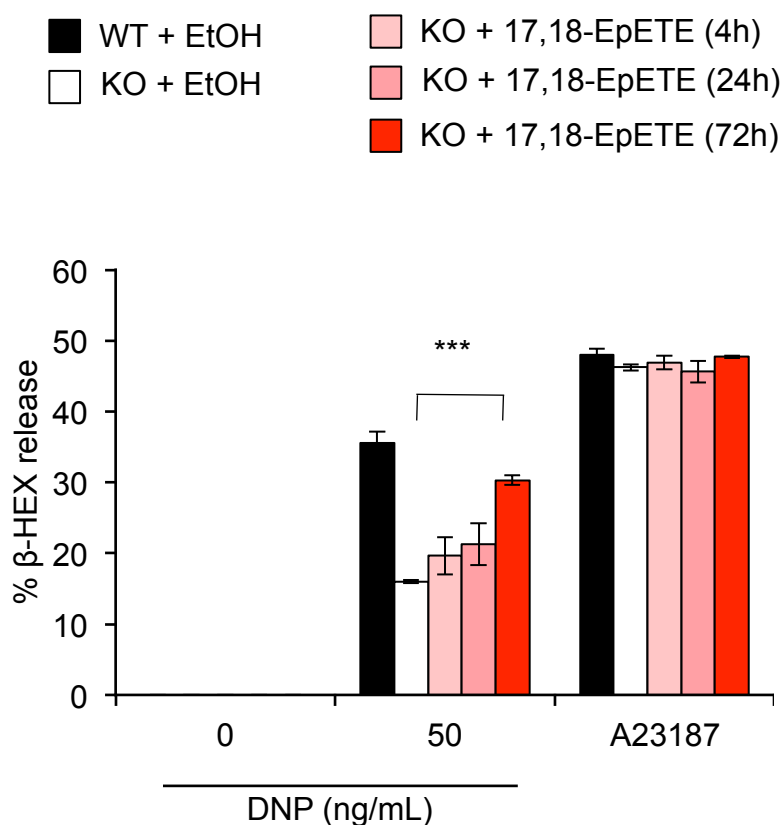


Figure 26. Long time exposure to ω 3-epoxides is needed to restore IgE-mediated degranulation of *pafah2*^{-/-} BMMCs

IgE-Ag or A23187 dependent β HEX release of BMMCs cultured for the indicated times in the presence of 300 nM of 17,18-EpETE. 17,18-EpETE was added to *pafah2*^{-/-} BMMCs once for 4 h or 24h or twice in three days and β -HEX assay was performed a day after last lipid treatment (n=4).

Experiments were repeated at least twice and the data were pooled. (mean \pm s.e.m., ****p*, <0.001).

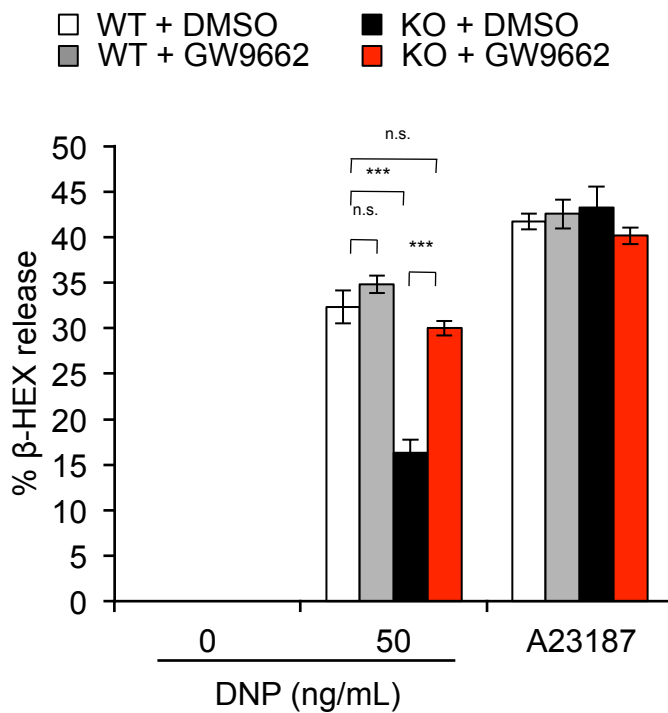


Figure 27. PPAR γ antagonist GW9662 restores IgE-mediated degranulation of *pafah2*^{-/-} BMMCs

IgE-Ag or A23187 dependent β HEX release of *pafah2*^{-/-} (KO) BMMCs cultured for three days in the presence of 0.5 μ M of GW9662. GW9662 was dissolved in DMSO and added to BMMCs twice in three days and β -HEX assay was performed a day after last GW9662 treatment (n=4).

Experiments were repeated at least twice and the data were pooled. (mean \pm s.e.m., ** p <0.01; *** p <0.001; n.s., not significant).

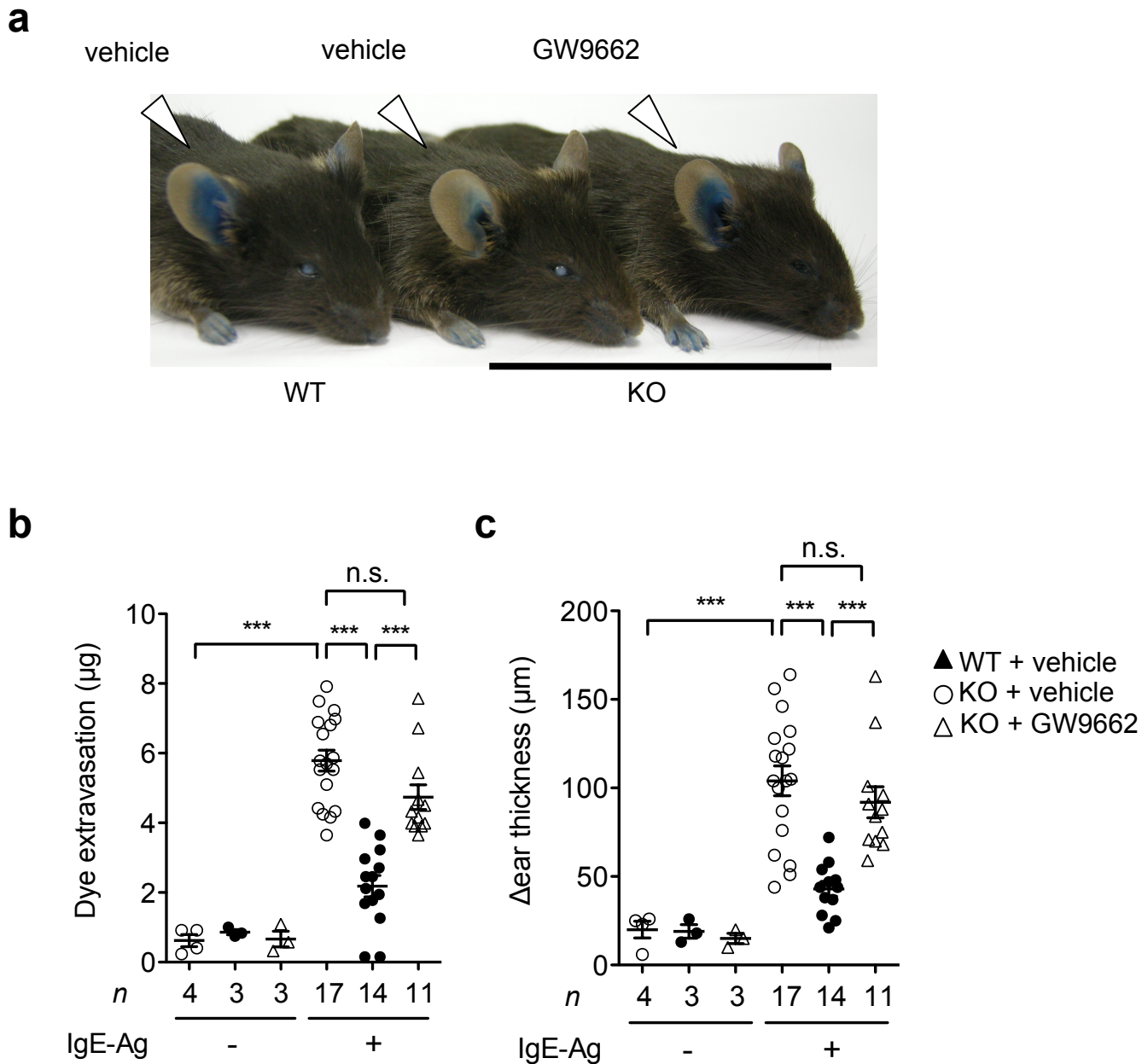


Figure 28. PPAR γ antagonist GW9662 restores IgE-mediated anaphylaxis in PAF-AH (II) knockout mice *in vivo*

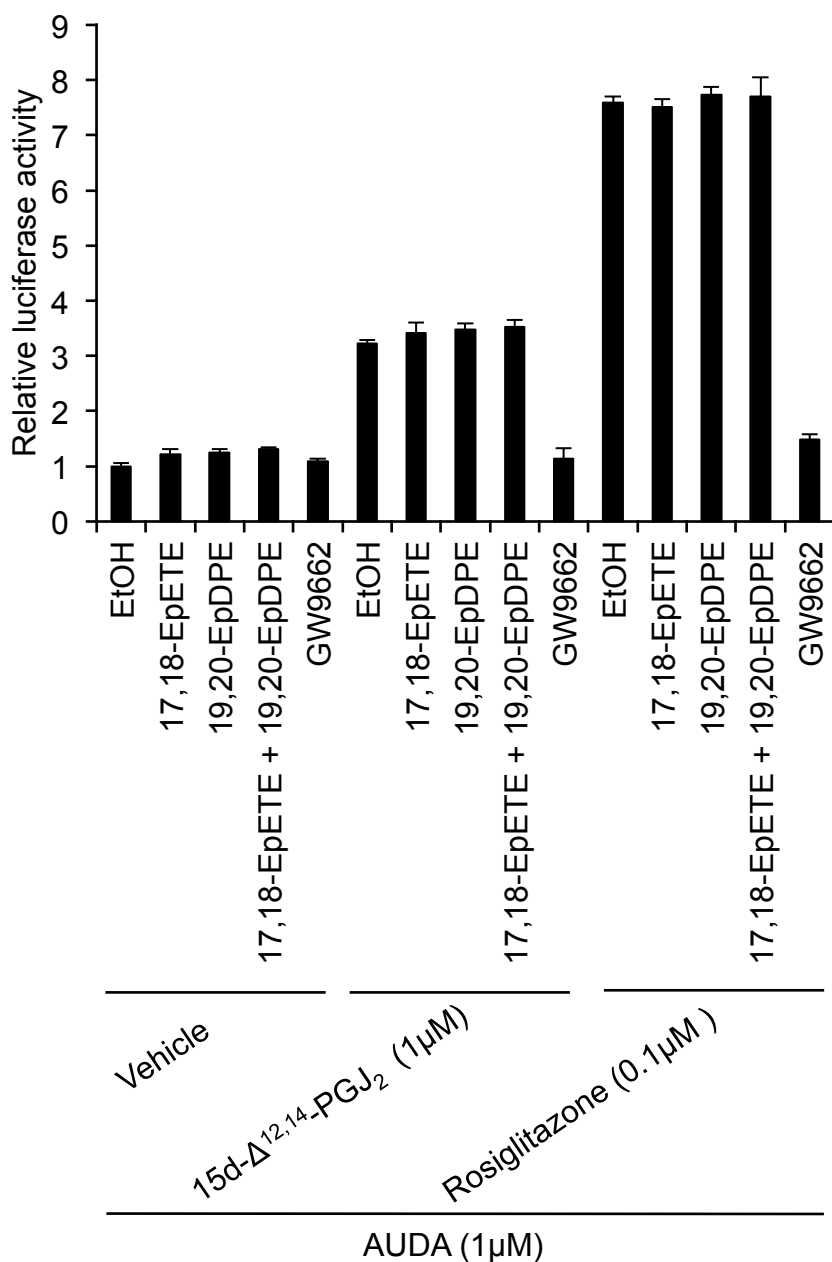
(a-c) 30 pmol of GW9662 was injected into the ears of mice twice in three days and PCA assay was performed a day after last GW9662 treatment.

(a) Representative photo of AA39-2 treated mice.

(b, c) Extravasation of Evans blue in the ears and changes in ear thickness after challenge with 500 μg of antigen.

Experiments were repeated at least twice and the data were pooled.

(mean \pm s.e.m., ** $p < 0.01$; *** $p < 0.001$; n.s., not significant).



17,18-EpETE : 5 μM
 19,20-EpDPE : 5 μM
 Mix : 17,18-EpETE (2 μM) + 19,20-EpDPE (3 μM)

Figure 29. ω3-epoxides have no effect on PPARγ reporter gene assay

Transcriptional activity of ω3-epoxides. HEK293T cells were transiently transfected with UAS×4-luciferase reporter, GAL-hPPARγ-LBD expression vector and pRL-TK. The cells were treated with 17,18-EpETE, 19,20-EpDPE or mixture of them at a concentration of 5 μM with the combination of 15d-Δ^{12,14}-PGJ₂, Rosiglitazone or GW9662. Reporter gene assay was carried out in the presence of 1 μM of AUDA.

Experiments were repeated at least twice and the data were pooled. (mean ± s.e.m., **p<0.01; ***p<0.001; n.s., not significant).

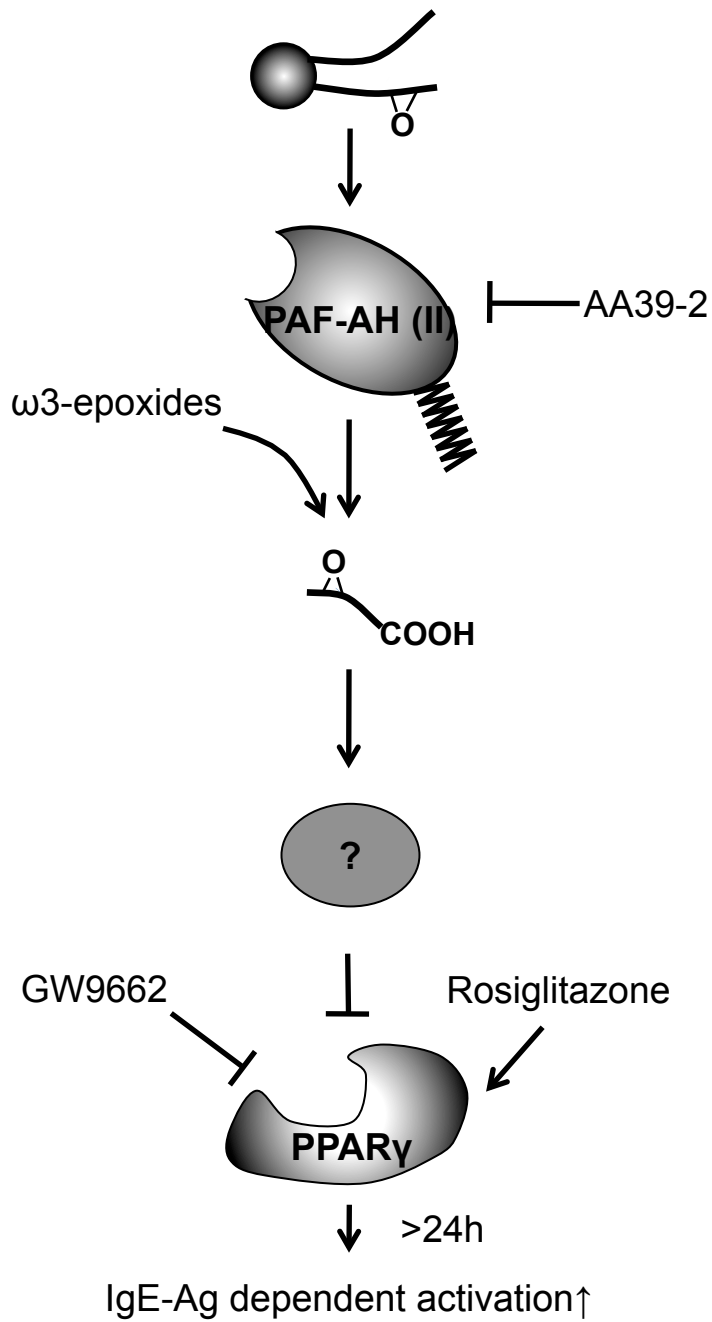


Figure 30. Summary

Schematic model of the regulatory role of PAF-AH (II) on IgE-Ag dependent mast cell activation.

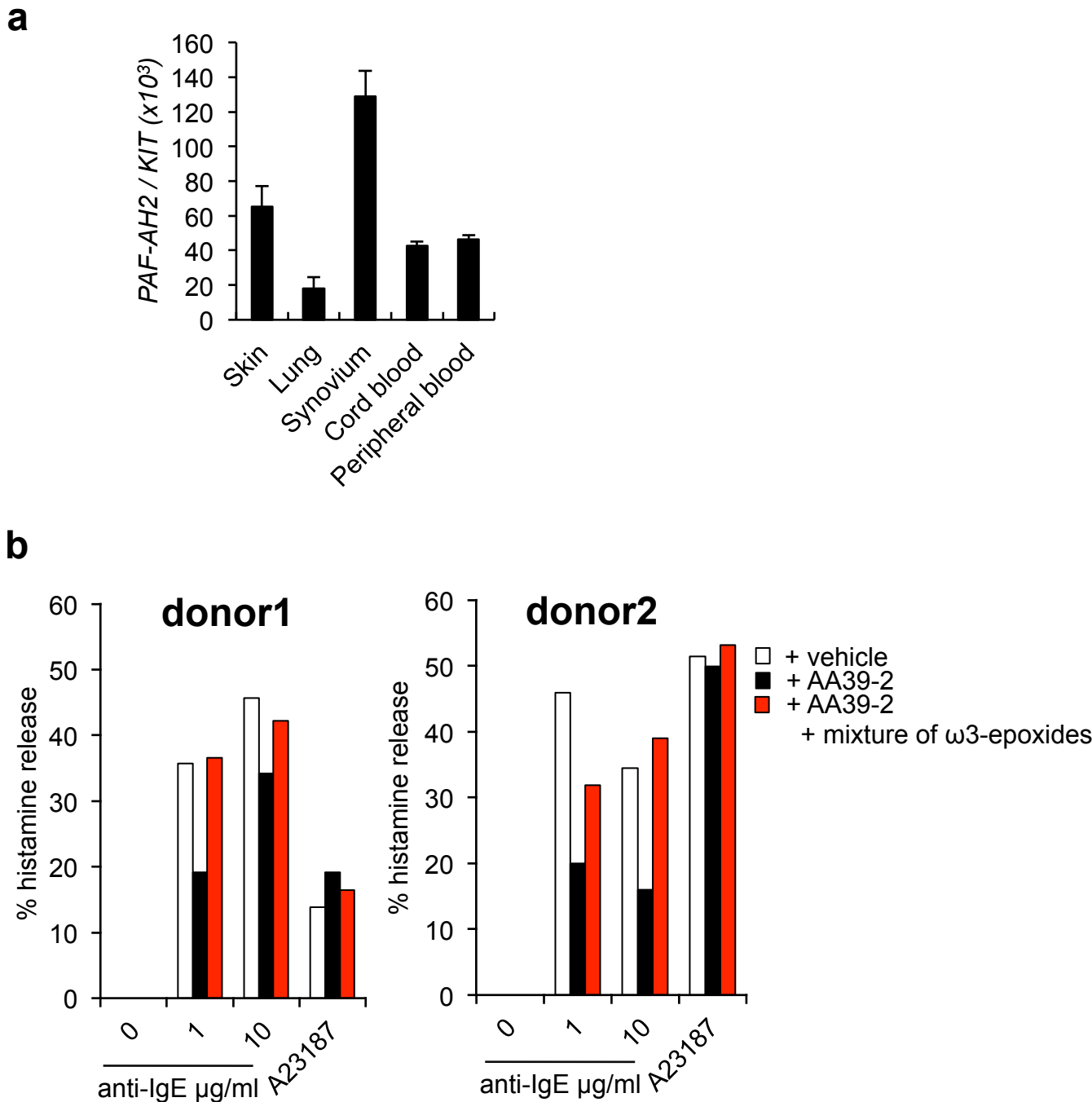


Figure 31 ω3-epoxide released by PAF-AH (II) facilitates IgE-dependent degranulation of human mast cells

(a) Real-time PCR of *PAFAH2* mRNA relative to *KIT* in indicated human mast cells (n=3~5).
 (b) Histamine release from cultured human synovium mast cells. AA39-2 and mixture of ω3-epoxides were added to cultured human synovium mast cells from two donors twice in three days and the amount of histamine released from human mast cells were measured a day after last lipid treatment. Cultured human synovium mast cells were sensitized with the human IgE and challenged with the indicated concentrations of anti-IgE or A23187. Histamine released in the supernatants was measured by ELISA (n=1).
 (mean ± s.e.m.)

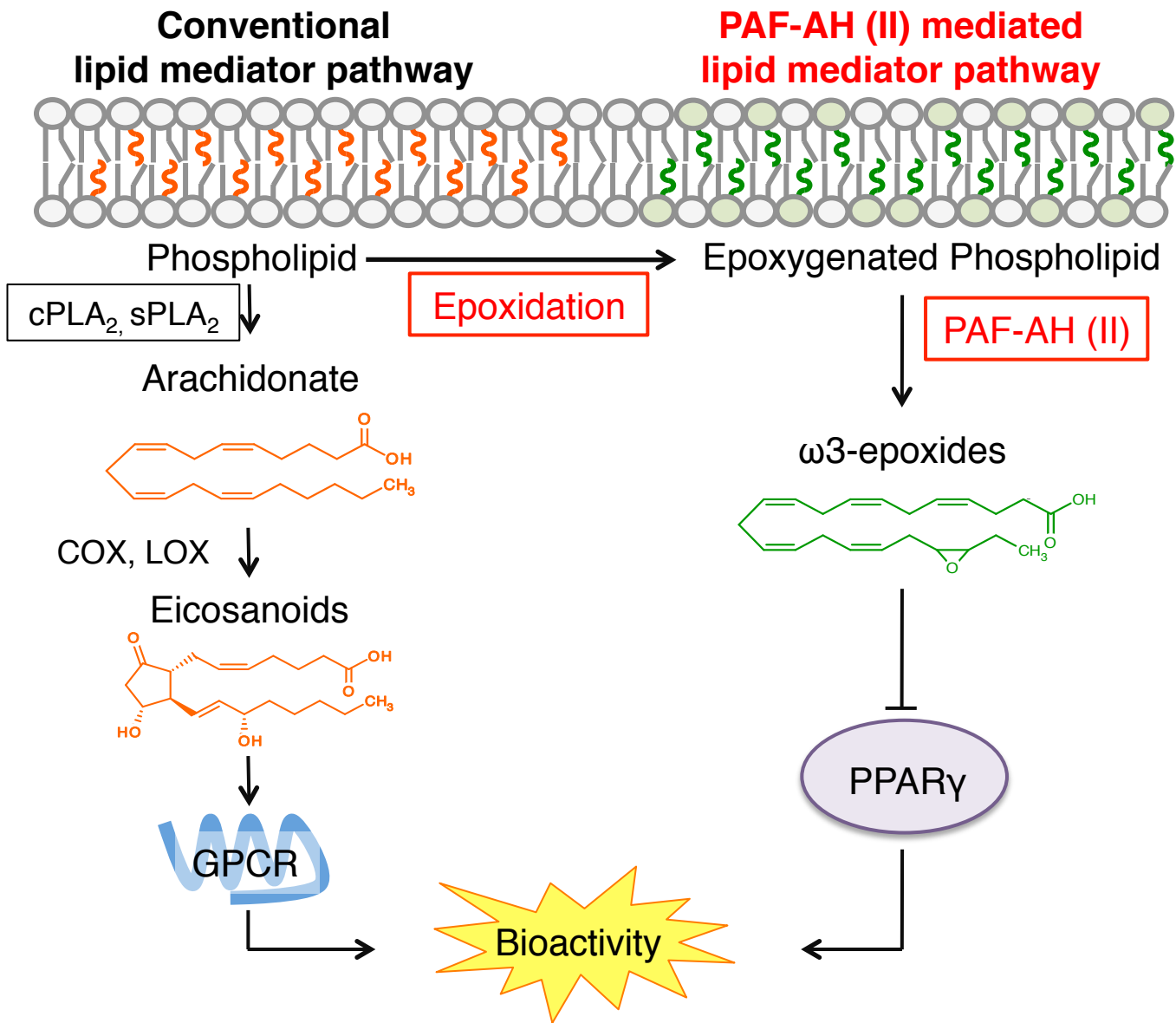


Figure 32. Schematic model of the PAF-AH (II) mediated lipid mediator pathway

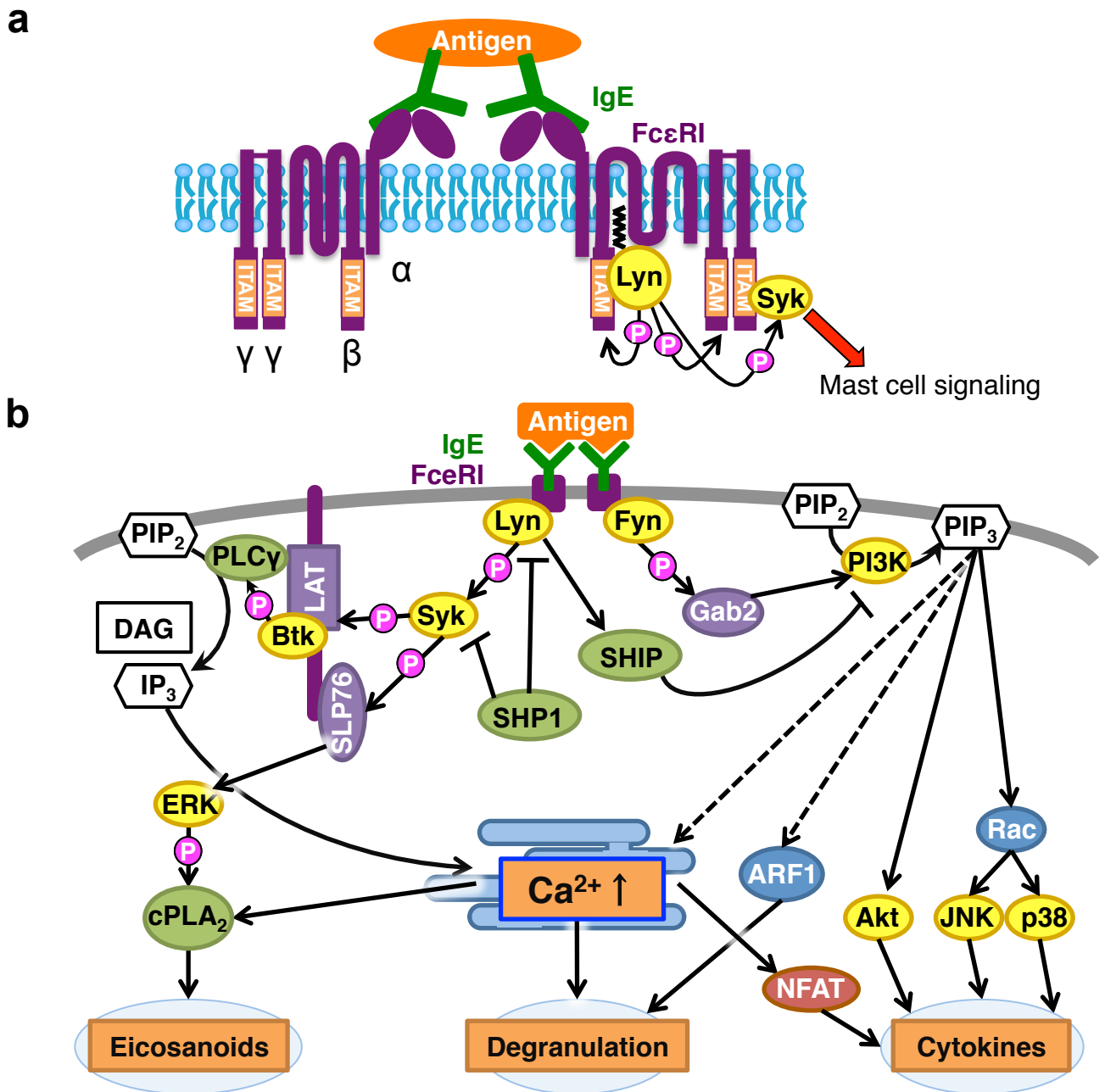


Figure 33. Simplified scheme for IgE-mediated signaling

(a) Model of FcεRI phosphorylation. FcεRI is a tetramer formed by the complex αβγ₂ chains. Binding of antigen to the IgE induces FcεRI aggregation. After FcεRI aggregation, FcεRI is translocated to “lipid rafts” where it is associated with Lyn. Lyn phosphorylates tyrosine residues within the ITAM motif of the β and γ chains, which leads to the recruitment of additional Lyn to the β chain and Syk, to the γ chains.

(b) Schematic model of IgE-mediated mast cell activation. After formation of the activated FcεRI complex, activated Syk phosphorylates linker for activation of T cells (LAT) and SH2 domain containing leukocyte protein of 76kDa (SLP76). Phospholipase C (PLC) γ recruited to phosphorylated LAT hydrolyzes phosphatidylinositol 4,5-bisphosphate (PIP₂) to yield diacylglycerol (DAG) and inositol triphosphate (IP₃). IP₃ activates IP₃ receptor on the ER which results in an influx of extracellular calcium. Phosphorylation of SLP76 activates MAPK-extracellular signal regulated kinase (ERK) signaling. Activated ERK phosphorylates cPLA₂ and leads to generation of eicosanoids in a Ca²⁺ dependent manner. Fyn also associates with activated FcεRI and phosphorylates Gab2, which results in recruitment of phosphatidylinositol 3-kinase (PI3K) to the plasma membrane and ARF1-dependent granule translocation. PIP₃ production also activates several signaling pathways which lead to cytokine transcription. SHP1 and SHIP negatively regulate these signaling pathways by inhibiting activation of Syk and Lyn and generation of PIP₃.

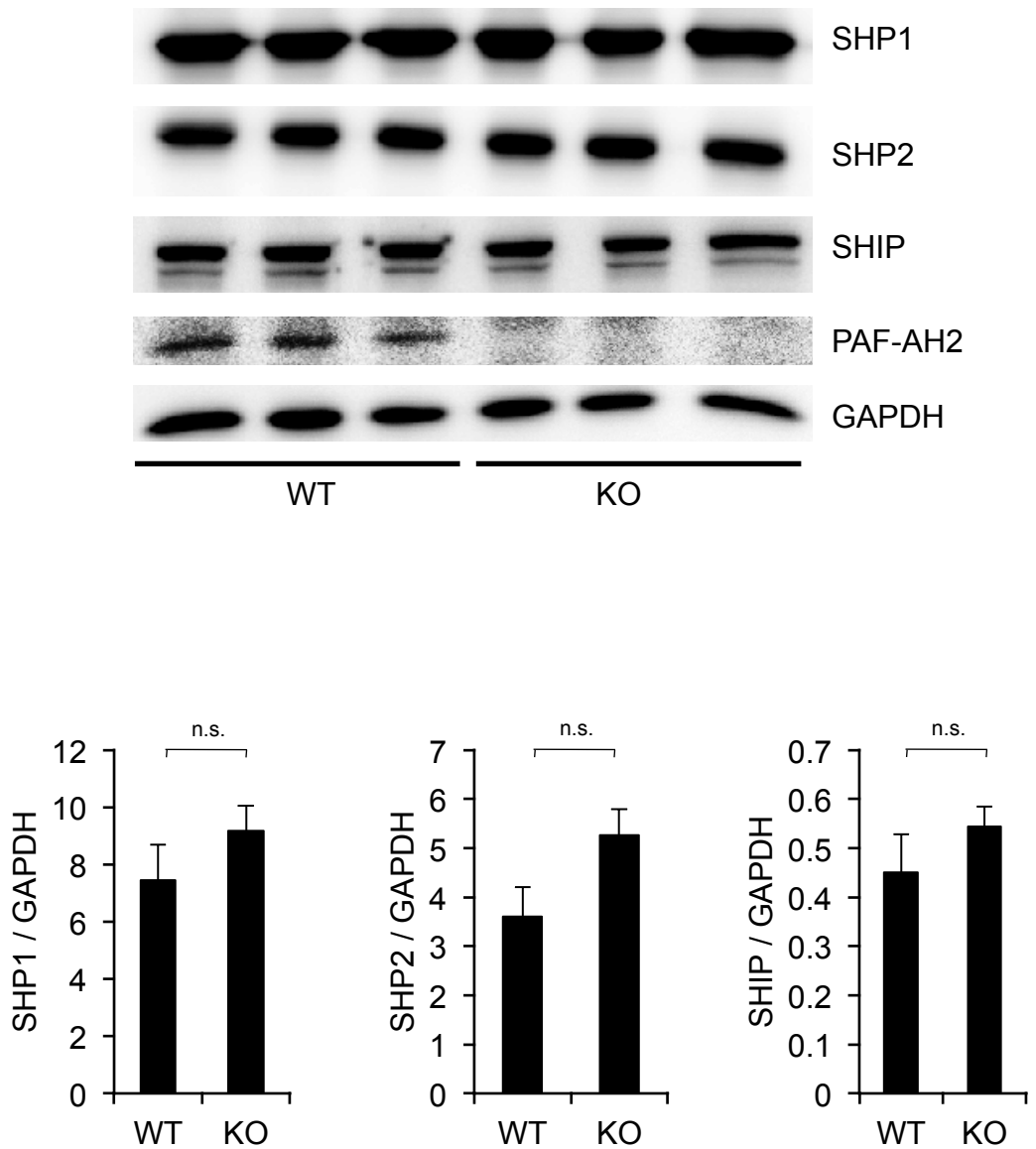
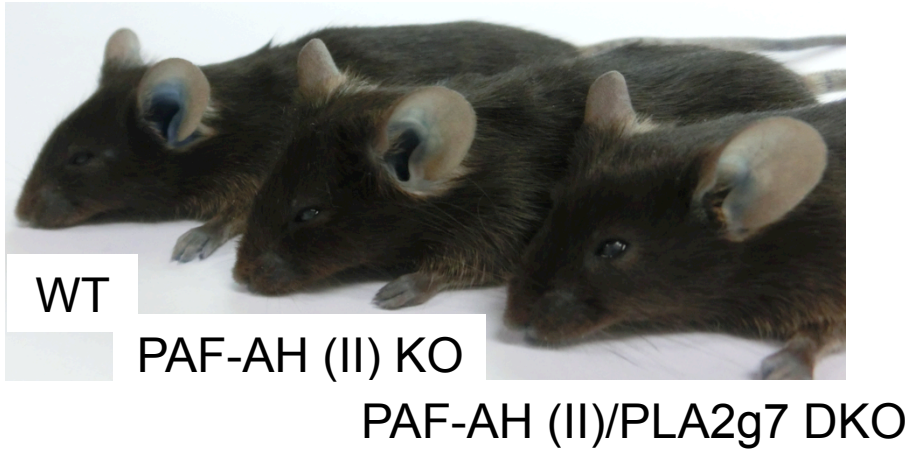


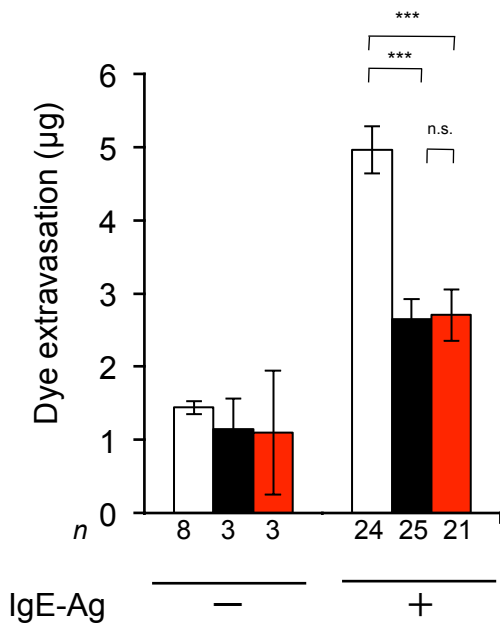
Figure 34. The expression of SHIP and SHP1 were comparable between *pafah2*^{-/-} and wild-type BMMCs

Expression of SHP1, SHP2, SHIP in BMMCs (western blotting). The ratio of SHP1/GAPDH, SHP2/GAPDH and SHIP/GAPDH were quantified by densitometric analysis (n=3).

(mean ± s.e.m., n.s., not significant).

a**b**

□ WT
■ PAF-AH (II) KO
■ PAF-AH (II)/PLA2G7 DKO

**c**

□ WT
■ PAF-AH (II) KO
■ PAF-AH (II)/PLA2G7 DKO

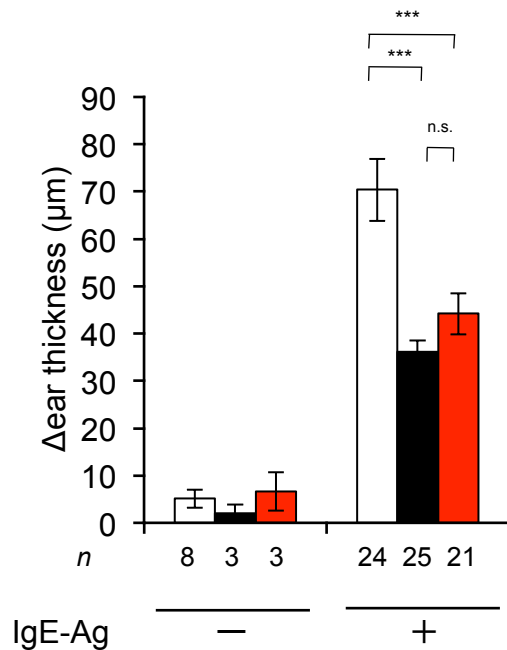


Figure 35. PLA2G7 depletion from PAF-AH (II) knockout mice did nothing on IgE-dependent passive cutaneous anaphylaxis

(a-c) Analysis of ear edema in IgE-Ag dependent PCA in wild-type (WT), *pafah2*^{-/-} (KO) and *pafah2*^{-/-}*pla2g7*^{-/-} (DKO) mice on a C57BL/6J back ground. (a) Representative photo of wild-type (WT), *pafah2*^{-/-} (KO) and *pafah2*^{-/-}*pla2g7*^{-/-} (DKO) mice after IgE-Ag mediated PCA. (b) Extravasation of Evans blue in the ears. (c) Changes in ear thickness after antigen challenge.

(mean ± s.e.m., ****p*, <0.001, , n.s., not significant).

Table 1. Optimized MRM pairs and parameters for lipids.

		Retention time (min)	m/z		DP (V)	CE (V)	CXP (V)
			Precursor	Product			
Phospholipid	16:0p/17,18-EpETE-PE	12.63	736	317	-105	-52	-11
	18:1p/17,18-EpETE-PE	12.88	762	317	-105	-52	-11
	18:0O/17,18-EpETE-PE	12.51	766	317	-105	-52	-11
	18:0/17,18-EpETE-PE	13.66	780	317	-105	-52	-11
	16:0/17,18-EpETE-PC	11.54	854	317	-105	-52	-11
	18:1/17,18-EpETE-PC	11.86	880	317	-105	-52	-11
	18:0/17,18-EpETE-PI	10.84	899	317	-105	-52	-11
	16:0p/19,20-EpDPE-PE	13.31	762.5	343	-105	-52	-11
	18:0/19,20-EpDPE-PE	14.31	806.6	343	-105	-52	-11
	16:0/19,20-EpDPE-PC	12.23	880.7	343	-105	-52	-11
	18:1/19,20-EpDPE-PC	12.48	906.6	343	-105	-52	-11
	18:0/19,20-EpDPE-PI	11.42	925.4	343	-105	-52	-11
	12:0/13:0-PC	10.25	694	620	-105	-52	-9
	Free Fatty Acid	17,18-EpETE	4.17	317	259	-100	-16
19,20-EpDPE		4.68	343	241	-75	-18	-21
17,18-diHETE		2.81	335	247	-80	-22	-9
19,20-diHDoPE		3.31	361	273	-20	-22	-9
EPA		6.45	301	257	-115	-16	-9
DHA		7.27	327	283	-75	-14	-9
AA-d8		7.50	311	267	-125	-20	-9
Neutral Lipid	14:0(2)-16:1 TG	20.81	771.5	526.3	136	39	14

Table 2. A list of primer sets for real –time PCR (related to Material and Methods).

Name	Forward primer	Reverse primer
<i>Cpa3</i>	5'-ACCAAACTCCACCTGCATTGGCAC-3'	5'-GGTCCTGGTGGTTAGGAGGCAGTTT-3'
<i>Gapdh</i>	5'-AGGTCGGTGTGAACGGATTTG-3'	5'-TGTAGACCATGTAGTTGAGGTCA-3'
<i>Hdc</i>	5'-CCCATCTACCTCCGACATGCCAA-3'	5'-CCCGAAGGACCGAATCACAAACCAC-3'
<i>Kit</i>	5'-CGATGTGGGCAAGAGTTCCGCCTT-3'	5'-ACAGAGTGTGGGCCTGGATTTGCT-3'
<i>Mcpt4</i>	5'-CTTCTCTTGCCTTCTGGGGCTGGA-3'	5'-GGCCATGTAAGGGCGAGAATGTGGT-3'
<i>Mcpt9</i>	5'-GGGCAGTTCCACAAAGGTGGCATCA-3'	5'-GGGCTTTGCATTTCCGCGTCCA-3'
<i>Mtif</i>	5'-GGGGAGGAGTTTCACGAAGAACCCA-3'	5'-GCTGGCGTAGCAAGATGCGTGA-3'
<i>Pla2g3</i>	5'-TGTGGTGCGGTGTTGGGAACTCT-3'	5'-TGCAAGGGCGAAATGGTTTGTGGG-3'

Table 3. A list of probes for Quantitative PCR by the TaqMan System (related to Material and Methods).

A. TaqMan System.

Name	Assay No.
<i>Gapdh</i>	Mouse GAPDH Endogenous Control (VIC/MGB probe, primer limited, 4352339E, Applied Biosystems)
<i>Pafah2</i>	Mm00505684_m1
<i>Pla2g1b</i>	Mm00478249_m1
<i>Pla2g10</i>	Mm01344435_m1
<i>Pla2g12a</i>	Mm00458226_m1
<i>Pla2g2d</i>	Mm00478250_m1
<i>Pla2g2e</i>	Mm00478870_m1
<i>Pla2g2f</i>	Mm00478872_m1
<i>Pla2g3</i>	Mm01191142_m1
<i>Pla2g4a</i>	Mm00447040_m1
<i>Pla2g4b</i>	Mm01271079_m1
<i>Pla2g4c</i>	Mm01195718_m1
<i>Pla2g4d</i>	Mm01279782_m1
<i>Pla2g4e</i>	Mm00625711_m1
<i>Pla2g4f</i>	Mm01338183_m1
<i>Pla2g5</i>	Mm00448162_m1
<i>Pla2g6</i>	Mm01299491_m1
<i>Pla2g7</i>	Mm00479105_m1
<i>Pnpla8</i>	Mm01295015_m1
<i>PAFAH2</i>	Hs00166476_m1
<i>Kit</i>	Hs00174029_m1

Material and Methods

Materials. All chemicals were purchased from Wako Pure Chemicals (Osaka, Japan) unless otherwise stated. 17,18-EpETE, 19,20-EpDPE, (\pm)17,18-DiHETE, (\pm)19,20-DiHDPA, (\pm)18-HEPE, (\pm)20-HDoHE, 15d- $\Delta^{12,14}$ -PGJ2, GW9662 and AUDA were purchased from Cayman Chemicals (Ann Arbor, MI). (\pm)19-HEPE, (\pm)20-HEPE, (\pm)21-HDoHE, (\pm)22-HDoHE were kindly provided by M Arita (RIKEN Center for Integrative Medical Science). AA39-2 was kindly provided by BF Cravatt (The Scripps Research Institute). Dulbecco's modified Eagle's medium was obtained from Invitrogen. Rosiglitazone and A23187 were purchased from Sigma Aldrich.

Antibodies. Antibodies to Syk, SHIP-1, SHP-1 and SHP-2 was from Santa Cruz Biotechnology (Santa Cruz, CA). Antibodies to phospho-Syk (Tyr525/526), phospho-Gab2 (Tyr452), Gab2 were purchased from Cell Signaling Technology (Beverly, MA). Antibodies to GAPDH was from Calbiochem. Anti-phosphotyrosine 4G10 mAb was from Upstate Biotechnology (Lake Placid, NY). Antibodies to PAF-AH (II) was from Sigma Aldrich. Monoclonal mouse anti-Fc ϵ RI β (clone: JRK) was kindly provided by J. Rivera (National Institutes of Health) ⁷⁴.

Mice. *Pafah2*^{-/-} mice have been described previously ²². These mice were backcrossed to C57BL/6 mice for 12 generations or to BALB/c background for 9 generations. All

experiments using knockout mice (male, 12-14-week-old) were compared with their age-matched littermate control mice or wild-type mice purchased from CLEA Japan. Mast cell-deficient *Kit* mutant mice, C57BL/6J-*Kit^{W-sh/W-sh}* were purchased from the Jackson Laboratories. *Pla2g7*^{-/-} mice were kindly provided by DM Stafforini (University of Utah)⁷⁵. All mice were housed in climate-controlled (23 °C) specific pathogen-free facilities with a 12-h light/dark cycle, with free access to standard laboratory food (CE2; CLEA) and water. All animal experiments were performed in accordance with protocols approved by the University of Tokyo Animal Committee, in accordance with the Standards Relating to the Care and Management of Experimental Animals in Japan.

Real-time PCR. Total RNA was extracted from tissues and cells using Isogen II (Nippon-gene, Japan). First-strand cDNA synthesis was performed using the High-Capacity cDNA Reverse-Transcriptase Kit (Applied Biosystems). Quantitative real-time PCRs were carried out using the TaqMan Gene Expression System (Applied Biosystems) on an ABI7700 Real-Time PCR system (Applied Biosystems) or SYBR® Green PCR Master Mix (TaKaRa) and LightCycler 480 (Roche Diagnostics). The probe-primer sets and the sequences of the oligonucleotides are listed in Table 2, 3.

Anaphylaxis. For PCA, 30 ng of monoclonal anti-DNP IgE (SPE-7; Sigma-Aldrich) was intradermally injected into both ears of mice. After 24 h, the mice were challenged by intravenous injection of 60 µg of DNP-conjugated human serum albumin (HSA;

Sigma-Aldrich) in saline containing Evans blue dye (Wako) ⁷⁶. Extravasation of blue dye in the ear was monitored for 30 min, and dissected ears were incubated at 37 °C in 3 N KOH. Then, Evans blue dye was extracted in acetone. Quantitative analysis of the extracts was performed by measuring the absorbance of blue dye at 620 nm. Ear thickness was measured 30 min after Ag challenge using a dial thickness gauge (Mitutoyo Corporation). Changes in ear thickness were determined as the difference before and after Ag challenge. For IgE-independent secretagogue compound 48/80-induced anaphylaxis, the ears were intradermally injected with 100 ng of compound 48/80 (Sigma-Aldrich) followed by *i.v.* injection of 1 mg of Evans blue ⁷⁶. After 30 min, Evans blue extravasation was measured as described above. For PSA, mice were administered 3 µg of anti-DNP IgE intravenously. After 24 h, the mice were challenged with 500 µg of DNP-HSA ⁷⁶. After Ag challenge, the rectal temperature was monitored for 120 min with an electronic thermometer (Physitemp Instruments).

Histological analysis. Ears were fixed in 10% (v/v) neutral buffered formalin and embedded in paraffin. The sections (5 µm thickness) were cut using a microtome and stained with 0.05% toluidine blue (pH 0.5) for the detection of mast cells ¹⁸. Degranulated mast cells were defined as those showing the release of cellular granules. For immunohistochemistry, dorsal skins were frozen in O.C.T. Compound (Sakura Finetek, Torrance, CA) and cut using a cryostat. The sections (10 µm thickness) were allowed to dry overnight at room temperature and reacted with a mouse monoclonal antibody to human PAF-AH (II) at dilutions of 1:50 in 3% BSA-PBS at 4 °C overnight.

An avidin-biotin-peroxidase complex method (Histofine; Nichirei Biosciences, Tokyo, Japan) was then employed followed by counterstaining with toluidine blue.

Culture of mouse BMMCs and other bone marrow-derived cells. To prepare BMMCs, total bone marrow (BM) cells from 12-wk-old male mice were cultured in IL-3-containing BMMC complete medium⁷⁶. After 4–6 weeks of culture, >95% of the floating cells were confirmed to be Kit⁺FcεRIα⁺ mast cells by flow cytometry. Other bone marrow-derived cells were obtained as described previously¹⁸.

Activation of BMMCs. Before stimulation, BMMCs were incubated with 1 μg/ml anti-DNP IgE for 3 h and then washed twice with Tyrode's buffer (20mM HEPES buffer at pH7.4, 135mM NaCl, 5mM KCl, 5.6mM glucose, 1.8mM CaCl₂, 1mM MgCl₂ and 0.5mg/mL bovine serum albumin). BMMCs (10⁶ cells) were stimulated with various concentrations (typically 50 ng/ml) of DNP-BSA (Sigma-Aldrich) or 10 μM A23187 (Sigma-Aldrich). Degranulation was assessed by the amount of released β-HEX, as described previously⁷⁶. The amount of PGD₂, LTC₄, TNF α and IL-6 were determined by ELISA in accordance with the manufacturer's instructions (Cayman Chemical).

Retrovirus-mediated gene expression and selection. pMX-puro-WT-PAF-AH (II), pMX-puro-S234C-PAF-AH (II) or pMX-puro (as a control) were transfected to a transient retrovirus packaging cell line PlatE (provided by T. Kitamura)⁷⁷ using

Lipofectamine2000 transfection reagents (invitrogen). 48 h after transfection, retrovirus was collected by centrifugation. For infection on BMMCs, cells were incubated with the retrovirus for 24h in the presence of 10 ng/ml murine IL-3, 50 ng/ml murine stem cell factor (PeproTech), and 10 μ g/ml polybrene (Sigma-Aldrich). Infected BMMCs were selected with fresh medium containing IL-3 and 1 μ g/ml of puromycin.

Adoptive transfer of BMMCs into mast cell-deficient mice. BMMCs (10^6 cells) were reconstituted by intradermal injection into 6-week-old male *Kit^{W-sh/W-sh}* mice. Forty days after reconstitution, IgE-dependent PCA was performed, as described above. The distribution and maturation of reconstituted BMMCs were evaluated by toluidine blue staining or by real-time PCR of mast cell marker genes.

Western Blot Analysis. Cells were lysed in SDS-sample buffer (62.5 mM Tris-HCl, pH 6.8, 10 % glycerol, 1 % SDS) with protease inhibitors (0.5 mM phenylmethylsulfonyl fluoride, 2 g/ml pepstatin, 2 g/ml leupeptin, 2 g/ml aprotinin) and phosphatase inhibitors (5mM NaF, 2mM sodium orthovanadate). After sonication, the lysates were used as the total protein extracts. The protein concentrations of samples were determined by the BCA assay (Pierce). For immunoprecipitation, stimulated cells were lysed in IP buffer (20 mM Tris-HCl, pH 7.4, 150 mM NaCl, 2 mM EDTA, 1 % NonidetP-40) with protease inhibitors and phosphatase inhibitors for 30 min on ice. Lysates were centrifuged for 20min (4°C) at 12000g. Cell lysates were incubated for 3 h with antibodies prebound to protein G Sepharose. Proteins were recovered with an equal

volume of 2× SDS-sample buffer (125 mM Tris-HCl, pH 6.8, 20 % glycerol, 2 % SDS, 200 mM DTT, 0.01% BPB).

Proteins was separated by SDS-PAGE and transferred to PVDF membranes. The membranes were blocked with 5% (w/v) bovine serum albumin (Sigma-Aldrich) in TTBS buffer (10 mM Tris-HCl, pH 7.4, 150 mM NaCl, 0.1% (w/v) Tween 20) and incubated with the 1st antibodies. After incubation with horseradish peroxidase-conjugated anti-mouse IgG antibody (GE Healthcare) or anti-rabbit IgG antibody (GE Healthcare), protein was detected by enhanced chemiluminescence (ECL Western blotting detection system, GE Healthcare).

Generating ω 3-epoxide-containing phospholipid. Generation of ω 3-epoxide-containing phospholipid was performed by a method as described previously ⁷⁸ with a little modification. Briefly, 1.0×10^7 cells of *Pafah2*^{-/-} BMBCs were incubated for 2 h with 9 μ M 17,18-EpETE or 19,20-EpDPE that had been dissolved in 500 μ M Tyrode's Buffer (135 mM NaCl, 5 mM KCl, 20 mM Hepes, 5.6 mM glucose, 1 mM MgCl₂, 1.8 mM CaCl₂, 0.05% BSA, pH 7.4) containing 5mg/ml essentially fatty acid free bovine serum albumin. After incubation, the suspension was centrifuged at 400g for 10min, and washed once with fresh Tyrode's Buffer. Phospholipids were extracted by the method of Bligh and Dyer ⁷⁹. The membrane fraction containing ω 3-epoxide-esterified phospholipids was obtained as follows. ω 3-epoxide treated *Pafah2*^{-/-} BMBCs were disrupted by sonication and cell lysates were centrifuged at 100,000 g for 1 h at 4 °C to separate the cytosol (supernatant) and

membrane (pellet) fractions. The membrane fractions were dissolved in assay buffer containing 50 mM Tris-HCl (pH 7.4), 5 mM EDTA and 2.0mM DTT. The suspension was homogenized by 50 strokes of a loose –fitting dounce homogenizer and sonicated.

Lipid extraction from the conditioned media of BMMCs. To get the BMMCs-conditioned media, BMMCs were cultured in IL-3-containing BMMC complete medium for 4 days. Neutral lipid, phospholipid and free fatty acid were extracted from the conditioned media by solid-phase extraction using Sep-Pak C18 cartridges (Waters). Briefly, conditioned media was added to Sep-Pak columns and neural lipids were eluted with 10mL of hexane. Free fatty acids were subsequently eluted with 10mL of methyl formate. Phospholipids were finally eluted 10mL of methanol.

Electrospray ionization mass spectrometry (ESI-MS). For the quantification of fatty acids, LC-MS/MS–based lipidomics analyses were performed using a high-performance liquid chromatography (HPLC) system (Waters UPLC) with a linear ion-trap quadrupole mass spectrometer (QTRAP5500; AB SCIEX) equipped with an Acquity UPLC BEH C₁₈ column (Waters) as described previously²³. MS/MS analyses were conducted in negative-ion mode, and fatty acid metabolites were identified and quantified by multiple reaction monitoring (MRM).

For the detection of phospholipids, LC-MS/MS–based lipidomics analyses were performed on a Shimadzu Nexera ultra high performance liquid chromatography system (Shimadzu, Kyoto, Japan) coupled with a QTRAP 4500 hybrid triple quadrupole linear

ion trap mass spectrometer (AB SCIEX, Framingham, MA, USA). Lipids extracted from BMMCs were simply injected by the autosampler; typically, 10 μ l (3 nmol phosphorous equivalent) of sample was applied. Chromatographic separation was performed on an Acquity UPLC HSS T3 column (100 mm \times 2.1 mm, 1.8 μ m; Waters) maintained at 40 °C using mobile phase A (water/methanol (50/50, v/v) containing 10 mM ammonium acetate and 0.2% acetic acid) and mobile phase B (isopropanol/acetone (50/50, v/v)) in a gradient program (0–3 min: 30% B \rightarrow 50% B; 3–24 min: 50% B \rightarrow 90% B; 24–28 min: 30% B) with a flow rate of 0.3 mL/min. The instrument parameters for negative ion mode were as follows: curtain gas, 10 psi; collision gas, 7 arb. unit; ionspray voltage, -4500 V; temperature, 700 °C; ion source gas 1, 30 psi; ion source gas 2, 70 psi. The instrument parameters for positive ion mode were as follows: curtain gas, 10 psi; collision gas, 7 arb. unit; ionspray voltage, 4500 V; temperature, 700 °C; ion source gas 1, 30 psi; ion source gas 2, 50 psi. The specific detection was performed by MRM as described in Table. 1.

The characteristic fragmentation patterns of individual molecular PC species were determined by enhanced product ion scanning (EPI). MS/MS analyses were conducted in negative-ion mode. The instrument parameters for negative ion mode were as follows: curtain gas, 10 psi; collision gas, High; ionspray voltage, -4500 V; temperature, 700 °C; ion source gas 1, 30 psi; ion source gas 2, 80 psi; declustering potential, -105 V; entrance potential, -10 V; collision energy, -52 V; collision cell exit potential, -20 V. The linear ion trap fill-time was set to “dynamic fill time”. The scan range of the instrument was set at m/z 50-900, at a scan speed of 10000 Da/s.

Chemical hydrolysis. Chemical hydrolysis of lipids was performed by a method as described previously⁸⁰ with a little modification. Briefly, lipids extracts from BMMCs were fractioned into phospholipids, free fatty acids and netral lipids by solid-phase extraction using Sep-Pak C18 cartridges as described above. The purified lipid fractions were dried under nitrogen. To the resulting residue, 1mL of 0.2N KOH/Methanol (1:5) was added and incubated for 60min at 50°C. After incubation, HCl was added to adjust the pH of the mixture to 4.0. Free fatty acid-fraction of chemically hydrolyzed lipids were obtained using Sep-Pak C18 cartridges and quantification of the specific fatty acids was performed by MRM as described in Table. 1.

Enzyme Assays. ω 3-epoxide-containing phospholipid-hydrolyzing activity was measured as follows. The standard incubation system for assay comprised 50 mM Tris-HCl (pH 7.4), 5 mM EDTA, 2.0mM DTT, the membrane fraction containing ω 3-epoxide-esterified phospholipids, and the cytosol fraction obtained from HEK293T cells transfected with empty vector, wild-type PAF-AH (II) or S234C mutant in a total volume of 0.125 ml. After incubation for indicated time at 37 °C, the reaction was stopped by adding 1.25 ml of chloroform/methanol (4:1, v/v) followed by adding 0.125 ml of water and 16.6 pmol of 1-dodecanoyl-2-tridecanoyl PC as internal standard. The lipids in the organic phase were extracted and reconstituted in 1:1 isopropanol/methanol, and the ESI-MS analysis was performed as described above.

Luciferase assay. HEK293T cells were transiently transfected with reporter construct (pG5*luc* vector), an expression plasmid encoding GAL-hPPAR γ -LBD, a fusion protein in which the DNA binding domain of GAL4 is fused to hPPAR γ -LBD³³ and pRL-TK using Lipofectamine2000 transfection reagents (Invitrogen). Six h after transfection, cells were stimulated with 15d- $\Delta^{12,14}$ -PGJ2 (Cayman), GW9662 (Cayman), 17,18-EpETE (Cayman), or 19,20-EpDPE (Cayman) at 37°C for 12h in the presence of AUDA (Cayman). Luciferase activity was measured by the dual luciferase assay system (Promega). Firefly luciferase activity of pG5*luc* was normalized by Renilla luciferase activity of pRL-TK.

Preparation and culture of human mast cells. Preparation and culture of mast cells from human synovium, cord blood, peripheral blood, skin and lung were performed as described previously^{81, 82}. Human tissue was obtained during surgery at the Nihon University Hospital under approval of the faculty ethics committee and informed consent from the patient. More than 97% of the floating cells were confirmed to be mast cells by metachromatic staining.

Activation of human mast cells. Human mast cells obtained from synovium, were sensitized with 1 mg/ mL recombinant human myeloma IgE (Calbiochem, Gibbstown, NJ) at 37°C for 24 h. After washing, the cells were challenged with rabbit anti-human IgE antibody (Dako, Glostrup, Denmark) or 1 μ M A23187 (Sigma-Aldrich) at 37°C for

30 min. After incubation, cell-free culture supernatants and cell pellets were harvested to measure histamine levels. The levels of histamine were determined by ELISA in accordance with the manufacturer's instructions (Immunotech, MBL, Nagoya, Japan).

References

1. Devereux, G. The increase in the prevalence of asthma and allergy: food for thought. *Nat Rev Immunol* **6**, 869-874 (2006).
2. Kalesnikoff, J. & Galli, S. J. New developments in mast cell biology. *Nat Immunol* **9**, 1215-1223 (2008).
3. Thurmond, R. L., Gelfand, E. W. & Dunford, P. J. The role of histamine H1 and H4 receptors in allergic inflammation: the search for new antihistamines. *Nat Rev Drug Discov* **7**, 41-53 (2008).
4. Ames, S. A., Gleeson, C. D. & Kirkpatrick, P. Omalizumab. *Nat Rev Drug Discov* **3**, 199-200 (2004).
5. Pearce, F. L., Befus, A. D., Gauldie, J. & Bienenstock, J. Mucosal mast cells. II. Effects of anti-allergic compounds on histamine secretion by isolated intestinal mast cells. *J Immunol* **128**, 2481-2486 (1982).
6. Finn, D. F. & Walsh, J. J. Twenty-first century mast cell stabilizers. *Br J Pharmacol* **170**, 23-37 (2013).
7. Clark, M. J. & Million, R. P. Allergic rhinitis: market evolution. *Nat Rev Drug Discov* **8**, 271-272 (2009).
8. Nakamura, T. et al. PGD2 deficiency exacerbates food antigen-induced mast cell hyperplasia. *Nat Commun* **6**, 7514 (2015).
9. Weller, C. L. et al. Leukotriene B4, an activation product of mast cells, is a chemoattractant for their progenitors. *J Exp Med* **201**, 1961-1971 (2005).

10. Weller, C. L. et al. Chemotactic action of prostaglandin E2 on mouse mast cells acting via the PGE2 receptor 3. *Proc Natl Acad Sci U S A* **104**, 11712-11717 (2007).
11. Arnold, C. et al. Arachidonic acid-metabolizing cytochrome P450 enzymes are targets of {omega}-3 fatty acids. *J Biol Chem* **285**, 32720-32733 (2010).
12. Hercule, H. C. et al. The vasodilator 17,18-epoxyeicosatetraenoic acid targets the pore-forming BK alpha channel subunit in rodents. *Exp Physiol* **92**, 1067-1076 (2007).
13. Morin, C., Sirois, M., Echave, V., Albadine, R. & Rousseau, E. 17,18-epoxyeicosatetraenoic acid targets PPARgamma and p38 mitogen-activated protein kinase to mediate its anti-inflammatory effects in the lung: role of soluble epoxide hydrolase. *Am J Respir Cell Mol Biol* **43**, 564-575 (2010).
14. Yanai, R. et al. Cytochrome P450-generated metabolites derived from omega-3 fatty acids attenuate neovascularization. *Proc Natl Acad Sci U S A* **111**, 9603-9608 (2014).
15. Lopez-Vicario, C. et al. Inhibition of soluble epoxide hydrolase modulates inflammation and autophagy in obese adipose tissue and liver: role for omega-3 epoxides. *Proc Natl Acad Sci U S A* **112**, 536-541 (2015).
16. Zhang, G. et al. Epoxy metabolites of docosahexaenoic acid (DHA) inhibit angiogenesis, tumor growth, and metastasis. *Proc Natl Acad Sci U S A* **110**, 6530-6535 (2013).

17. Nakatani, N. et al. Role of cytosolic phospholipase A2 in the production of lipid mediators and histamine release in mouse bone-marrow-derived mast cells. *Biochem J* **352 Pt 2**, 311-317 (2000).
18. Taketomi, Y. et al. Mast cell maturation is driven via a group III phospholipase A2-prostaglandin D2-DP1 receptor paracrine axis. *Nat Immunol* **14**, 554-563 (2013).
19. Stafforini, D. M., Prescott, S. M., Zimmerman, G. A. & McIntyre, T. M. Mammalian platelet-activating factor acetylhydrolases. *Biochim Biophys Acta* **1301**, 161-173 (1996).
20. Matsuzawa, A., Hattori, K., Aoki, J., Arai, H. & Inoue, K. Protection against oxidative stress-induced cell death by intracellular platelet-activating factor-acetylhydrolase II. *J Biol Chem* **272**, 32315-32320 (1997).
21. Karasawa, K. & Inoue, K. Overview of PAF-Degrading Enzymes. *Enzymes* **38**, 1-22 (2015).
22. Kono, N. et al. Protection against oxidative stress-induced hepatic injury by intracellular type II platelet-activating factor acetylhydrolase by metabolism of oxidized phospholipids in vivo. *J Biol Chem* **283**, 1628-1636 (2008).
23. Arita, M. Mediator lipidomics in acute inflammation and resolution. *J Biochem* **152**, 313-319 (2012).
24. Lundstrom, S. L. et al. Lipid mediator metabolic profiling demonstrates differences in eicosanoid patterns in two phenotypically distinct mast cell populations. *J Lipid Res* **54**, 116-126 (2013).

25. Costello, P. S. et al. Critical role for the tyrosine kinase Syk in signalling through the high affinity IgE receptor of mast cells. *Oncogene* **13**, 2595-2605 (1996).
26. Nishida, K. et al. Fc{epsilon}RI-mediated mast cell degranulation requires calcium-independent microtubule-dependent translocation of granules to the plasma membrane. *J Cell Biol* **170**, 115-126 (2005).
27. Shen, H. C. Soluble epoxide hydrolase inhibitors: a patent review. *Expert Opin Ther Pat* **20**, 941-956 (2010).
28. Morisseau, C. & Hammock, B. D. Impact of soluble epoxide hydrolase and epoxyeicosanoids on human health. *Annu Rev Pharmacol Toxicol* **53**, 37-58 (2013).
29. Adibekian, A. et al. Click-generated triazole ureas as ultrapotent in vivo-active serine hydrolase inhibitors. *Nat Chem Biol* **7**, 469-478 (2011).
30. Sugiyama, H. et al. Peroxisome proliferator-activated receptors are expressed in mouse bone marrow-derived mast cells. *FEBS Lett* **467**, 259-262 (2000).
31. Tachibana, M. et al. Activation of peroxisome proliferator-activated receptor gamma suppresses mast cell maturation involved in allergic diseases. *Allergy* **63**, 1136-1147 (2008).
32. Liu, Y. et al. The antiinflammatory effect of laminar flow: the role of PPARgamma, epoxyeicosatrienoic acids, and soluble epoxide hydrolase. *Proc Natl Acad Sci U S A* **102**, 16747-16752 (2005).
33. Forman, B. M. et al. 15-Deoxy-delta 12, 14-prostaglandin J2 is a ligand for the adipocyte determination factor PPAR gamma. *Cell* **83**, 803-812 (1995).

34. Nagakura, T., Matsuda, S., Shichijyo, K., Sugimoto, H. & Hata, K. Dietary supplementation with fish oil rich in omega-3 polyunsaturated fatty acids in children with bronchial asthma. *Eur Respir J* **16**, 861-865 (2000).
35. Wong, K. W. Clinical efficacy of n-3 fatty acid supplementation in patients with asthma. *J Am Diet Assoc* **105**, 98-105 (2005).
36. Devereux, G. & Seaton, A. Diet as a risk factor for atopy and asthma. *J Allergy Clin Immunol* **115**, 1109-17; quiz 1118 (2005).
37. Peat, J. K. et al. Three-year outcomes of dietary fatty acid modification and house dust mite reduction in the Childhood Asthma Prevention Study. *J Allergy Clin Immunol* **114**, 807-813 (2004).
38. Trak-Fellermeier, M. A., Brasche, S., Winkler, G., Koletzko, B. & Heinrich, J. Food and fatty acid intake and atopic disease in adults. *European Respiratory Journal* **23**, 575-582 (2004).
39. Broadfield, E. C. et al. A case-control study of dietary and erythrocyte membrane fatty acids in asthma. *Clin Exp Allergy* **34**, 1232-1236 (2004).
40. Woods, R. K., Raven, J. M., Walters, E. H., Abramson, M. J. & Thien, F. C. Fatty acid levels and risk of asthma in young adults. *Thorax* **59**, 105-110 (2004).
41. Mickleborough, T. D. & Rundell, K. W. Dietary polyunsaturated fatty acids in asthma- and exercise-induced bronchoconstriction. *Eur J Clin Nutr* **59**, 1335-1346 (2005).

42. Almqvist, C. et al. Omega-3 and omega-6 fatty acid exposure from early life does not affect atopy and asthma at age 5 years. *J Allergy Clin Immunol* **119**, 1438-1444 (2007).
43. Schwab, J. M., Chiang, N., Arita, M. & Serhan, C. N. Resolvin E1 and protectin D1 activate inflammation-resolution programmes. *Nature* **447**, 869-874 (2007).
44. Endo, J. et al. 18-HEPE, an n-3 fatty acid metabolite released by macrophages, prevents pressure overload-induced maladaptive cardiac remodeling. *J Exp Med* **211**, 1673-1687 (2014).
45. Aldrovandi, M. et al. Human platelets generate phospholipid-esterified prostaglandins via cyclooxygenase-1 that are inhibited by low dose aspirin supplementation. *J Lipid Res* **54**, 3085-3097 (2013).
46. Metcalfe, D. D., Peavy, R. D. & Gilfillan, A. M. Mechanisms of mast cell signaling in anaphylaxis. *J Allergy Clin Immunol* **124**, 639-46; quiz 647-8 (2009).
47. Kovarova, M. et al. Structure-function analysis of Lyn kinase association with lipid rafts and initiation of early signaling events after Fcepsilon receptor I aggregation. *Mol Cell Biol* **21**, 8318-8328 (2001).
48. Xiao, W. et al. Positive and negative regulation of mast cell activation by Lyn via the FcepsilonRI. *J Immunol* **175**, 6885-6892 (2005).
49. Odom, S. et al. Negative regulation of immunoglobulin E-dependent allergic responses by Lyn kinase. *J Exp Med* **199**, 1491-1502 (2004).

50. Nishizumi, H. & Yamamoto, T. Impaired tyrosine phosphorylation and Ca²⁺ mobilization, but not degranulation, in lyn-deficient bone marrow-derived mast cells. *J Immunol* **158**, 2350-2355 (1997).
51. Hibbs, M. L. et al. Multiple defects in the immune system of Lyn-deficient mice, culminating in autoimmune disease. *Cell* **83**, 301-311 (1995).
52. Kawakami, Y. et al. Redundant and opposing functions of two tyrosine kinases, Btk and Lyn, in mast cell activation. *J Immunol* **165**, 1210-1219 (2000).
53. Alvarez-Errico, D. et al. Functional analysis of Lyn kinase A and B isoforms reveals redundant and distinct roles in Fc epsilon RI-dependent mast cell activation. *J Immunol* **184**, 5000-5008 (2010).
54. Hong, H. et al. The Src family kinase Hck regulates mast cell activation by suppressing an inhibitory Src family kinase Lyn. *Blood* **110**, 2511-2519 (2007).
55. Lee, J. H. et al. The Src family kinase Fgr is critical for activation of mast cells and IgE-mediated anaphylaxis in mice. *J Immunol* **187**, 1807-1815 (2011).
56. Kim, M. S., Radinger, M. & Gilfillan, A. M. The multiple roles of phosphoinositide 3-kinase in mast cell biology. *Trends Immunol* **29**, 493-501 (2008).
57. Mertsching, E. et al. A mouse Fc gamma-Fc epsilon protein that inhibits mast cells through activation of Fc gammaRIIB, SH2 domain-containing inositol phosphatase 1, and SH2 domain-containing protein tyrosine phosphatases. *J Allergy Clin Immunol* **121**, 441-447.e5 (2008).

58. Somani, A. K. et al. The SH2 domain containing tyrosine phosphatase-1 down-regulates activation of Lyn and Lyn-induced tyrosine phosphorylation of the CD19 receptor in B cells. *J Biol Chem* **276**, 1938-1944 (2001).
59. Murakami, M. et al. Recent progress in phospholipase A(2) research: from cells to animals to humans. *Prog Lipid Res* **50**, 152-192 (2011).
60. Nakajima, K. et al. Activated mast cells release extracellular type platelet-activating factor acetylhydrolase that contributes to autocrine inactivation of platelet-activating factor. *J Biol Chem* **272**, 19708-19713 (1997).
61. Stafforini, D. M. et al. Release of free F2-isoprostanes from esterified phospholipids is catalyzed by intracellular and plasma platelet-activating factor acetylhydrolases. *J Biol Chem* **281**, 4616-4623 (2006).
62. Choi, J. H. et al. Anti-diabetic drugs inhibit obesity-linked phosphorylation of PPARgamma by Cdk5. *Nature* **466**, 451-456 (2010).
63. Choi, J. H. et al. Antidiabetic actions of a non-agonist PPARgamma ligand blocking Cdk5-mediated phosphorylation. *Nature* **477**, 477-481 (2011).
64. Ohtera, A. et al. Identification of a New Type of Covalent PPARgamma Agonist using a Ligand-Linking Strategy. *ACS Chem Biol* **10**, 2794-2804 (2015).
65. Shiraki, T. et al. Alpha,beta-unsaturated ketone is a core moiety of natural ligands for covalent binding to peroxisome proliferator-activated receptor gamma. *J Biol Chem* **280**, 14145-14153 (2005).
66. Itoh, T. et al. Structural basis for the activation of PPAR γ by oxidized fatty acids. *Nat Struct Mol Biol* **15**, 924-931 (2008).

67. Node, K. Anti-inflammatory Properties of Cytochrome P450 Epoxygenase-Derived Eicosanoids. *Science* **285**, 1276-1279 (1999).
68. Muller, D. N. et al. Mouse Cyp4a isoforms: enzymatic properties, gender- and strain-specific expression, and role in renal 20-hydroxyeicosatetraenoic acid formation. *Biochem J* **403**, 109-118 (2007).
69. Lucas, D. et al. Stereoselective epoxidation of the last double bond of polyunsaturated fatty acids by human cytochromes P450. *J Lipid Res* **51**, 1125-1133 (2010).
70. Arnold, C. et al. Arachidonic acid-metabolizing cytochrome P450 enzymes are targets of ω -3 fatty acids. *J Biol Chem* **285**, 32720-32733 (2010).
71. Westphal, C., Konkel, A. & Schunck, W. H. CYP-eicosanoids--a new link between omega-3 fatty acids and cardiac disease? *Prostaglandins Other Lipid Mediat* **96**, 99-108 (2011).
72. Serhan, C. N. Pro-resolving lipid mediators are leads for resolution physiology. *Nature* **510**, 92-101 (2014).
73. Teodosio, C. et al. Gene expression profile of highly purified bone marrow mast cells in systemic mastocytosis. *J Allergy Clin Immunol* **131**, 1213-24, 1224.e1-4 (2013).
74. Rivera, J., Kinet, J. P., Kim, J., Pucillo, C. & Metzger, H. Studies with a monoclonal antibody to the beta subunit of the receptor with high affinity for immunoglobulin E. *Mol Immunol* **25**, 647-661 (1988).

75. Lu, J. et al. Dual roles of endogenous platelet-activating factor acetylhydrolase in a murine model of necrotizing enterocolitis. *Pediatr Res* **68**, 225-230 (2010).
76. Taketomi, Y. et al. Impaired mast cell maturation and degranulation and attenuated allergic responses in *Ndr1*-deficient mice. *J Immunol* **178**, 7042-7053 (2007).
77. Morita, S., Kojima, T. & Kitamura, T. Plat-E: an efficient and stable system for transient packaging of retroviruses. *Gene Ther* **7**, 1063-1066 (2000).
78. Bernstrom, K., Kayganich, K. & Murphy, R. C. Collisionally induced dissociation of epoxyeicosatrienoic acids and epoxyeicosatrienoic acid-phospholipid molecular species. *Anal Biochem* **198**, 203-211 (1991).
79. BLIGH, E. G. & DYER, W. J. A rapid method of total lipid extraction and purification. *Can J Biochem Physiol* **37**, 911-917 (1959).
80. Karara, A., Dishman, E., Blair, I., Falck, J. R. & Capdevila, J. H. Endogenous epoxyeicosatrienoic acids. Cytochrome P-450 controlled stereoselectivity of the hepatic arachidonic acid epoxygenase. *J Biol Chem* **264**, 19822-19827 (1989).
81. Saito, H., Kato, A., Matsumoto, K. & Okayama, Y. Culture of human mast cells from peripheral blood progenitors. *Nat Protoc* **1**, 2178-2183 (2006).
82. Kajiwarra, N. et al. Activation of human mast cells through the platelet-activating factor receptor. *J Allergy Clin Immunol* **125**, 1137-1145.e6 (2010).

《謝辞》

本研究を進めるにあたり、終始 御指導して下さいました 東京大学薬学部衛生化学教室の 新井洋由 教授、田口友彦 准教授、河野望 講師、今江理恵子 助教、向井康治朗 助教、大場陽介 助教に心より感謝致します。特に、研究の方針などについて日々議論し、直接御指導下さいました 新井洋由 教授、河野望 講師に深く感謝致します。また、本研究テーマが開始した当初、共に PAF-AH(II)を研究し、日々議論して下さいました向井康治朗 助教に深く感謝致します。

マスト細胞を用いた実験系について直接指導していただき、日々議論とお酒を交わして下さいました、東京都医学総合研究所脂質代謝プロジェクトの村上誠 プロジェクトリーダー、武富芳隆 研究員に深く感謝致します。

酸化脂肪酸に対するリピッドメタボロミクスを行ってくださり、様々な助言を下さりました、理化学研究所統合生命医科学研究センターメタボローム研究チームの有田誠 チームリーダーに深く感謝いたします。

ヒトマスト細胞を用いた実験において共同研究をしてくださった、日本大学大学院医学研究科先端医学系分子細胞免疫・アレルギー学分野の岡山吉道 准教授に深く感謝いたします。

マウスの飼育にあたり、いつも支えて下さりました、牧田さんをはじめとする動物舎のスタッフの方々に感謝致します。

研究生活を共にし、本研究を様々な面で支えて下さいました衛生化学教室の皆さんに心より感謝致します。特に、同期として苦楽をともにした久保卓也 博士、李尚憲 博士には大変感謝しています。日々、あらゆる面で快適な実験生活環境を整えて下さいました高田祥恵さん、秋村貴子さん、田邊瑠美さん、大澤由季子さんに心より感謝致します。

最後にいつも応援し、暖かく見守ってくれた、父 雄二、母 真理子、妹 由理子、猫 栗子に心より感謝したいと思います。とりわけ、幼少時より私が学究生活に進むのを楽しみにしていた亡き祖父 牧野東彦に深く感謝したいと思います。

ありがとうございました。

平成28年 3月 10日